Optimised dispersion management and modulation formats for high speed optical communication systems

Tokle, Torger; Jeppesen, Palle

Publication date:
2004

Document Version
Publisher's PDF, also known as Version of record

Optimised Dispersion Management and Modulation Formats for High Speed Optical Communication Systems

Torger Tokle

September 27, 2004

Revision 1.0—2004-12-21

Research Center COM
Technical University of Denmark
Building 345V
2800 Kgs. Lyngby
DENMARK

Abstract

This thesis studies dispersion management and modulation formats for optical communication systems using per channel bit rates at and above 10 Gbit/s. Novel modulation formats—including recently proposed multi-level phase modulation—are investigated and demonstrated at bit rates up to 80 Gbit/s.

New dispersion compensating fibre (DCF) types—referred to as inverse dispersion fibres (IDFs)—allow for novel span designs by using the DCF as cabled transmission fibre. These novel fibre span designs are compared to conventional spans for 10 and 40 Gbit/s systems with 80 km span length based on single mode fibre (SMF). We find that using SMF+IDF results in improved transmission performance, compared to SMF+DCF, primarily due to lower span loss.

A systematic investigation of non return-to-zero (NRZ) and return-to-zero (RZ) line coding in 10 Gbit/s systems with 80 km fibre spans shows that for a single-channel system, the optimum pulse width is very narrow. We find that a pulse width equal to 5% of the bit slot results in optimum performance for the system studied here. These narrow RZ pulses offer good receiver sensitivity and excellent tolerance to the nonlinear effect self phase modulation (SPM). However, due to the broad spectrum associated with narrow pulses, the optimum pulse width in wavelength division multiplexing (WDM) systems will be a tradeoff between receiver sensitivity and nonlinear tolerance on one hand, and spectral efficiency requirements on the other.

Several advanced modulation formats have recently been suggested in order to mitigate effects of dispersion-induced broadening or non-linear signal degradation, including carrier suppressed return-to-zero (CS-RZ), single side band return-to-zero (SSB-RZ), duobinary, etc. A thorough

investigation of 40 Gbit/s systems with 80 km span length is carried out to compare the relative performance of six different on-off keying (OOK) modulation formats. We find that (plain-)RZ with narrow pulse width is optimum for single-channel systems. For a 100 GHz spaced WDM system, CS-RZ or SSB-RZ results in optimum performance as these formats offer both narrow spectral width and good transmission properties.

The cost of an optical communication system can be lowered by using longer span lengths to reduce the number of amplifier stations. We experimentally study optimum dispersion compensation schemes for systems with 160 km fibre spans made of non-zero dispersion shifted fibre (NZDSF) and DCF. Pre-, post- and symmetrical dispersion compensation schemes are compared in a 40 Gbit/s RZ system using both lumped erbium doped fibre amplifiers (EDFAs) and distributed Raman amplification. We show that the symmetrical scheme results in optimum system performance.

Differential phase shift keying (DPSK) has recently been showed to be a promising modulation format for optical communication. We study DPSK with focus on differential quadrature phase shift keying (DQPSK). In a 12.5 Gbit/s WDM system, we demonstrate the suitability of DQPSK for ultra-long haul optical communication systems by obtaining good performance even after transmission over 6500 km. Studying different channel spacings, we demonstrate transmission over transoceanic distances of this DQPSK system with up to 0.66 bit/s/Hz spectral efficiency.

Four-level modulation formats allow for generation of signal with bit rate twice that of binary systems. We demonstrate this in an experiment where 80 Gbit/s DQPSK is generated using 40 Gbit/s components. Using four-wave mixing (FWM) in a highly nonlinear fibre, we demonstrate for the first time wavelength conversion of such high-speed phase modulated signals.

In summary, we show that dispersion management using recently developed fibres in combination with advanced modulation formats significantly improves the transmission performance compared to traditional systems. Multi-level phase modulation is demonstrated at bit rates up to 80 Gbit/s, and we experimentally demonstrate that multi-level phase modulated signals are suitable for transoceanic spectrally efficient WDM systems.

Sammendrag

Denne avhandlingen omhandler dispersjonskompensering og modulasjonsformater for optiske kommunikasjonssystemer med bitrater på eller over 10 Gbit/s. Nye modulasjonsformater, blant annet multinivå fasemodulasjon, er undersøkt og demonstrert ved bitrater opptil 80 Gbit/s.

Nye typer dispersjonskompenserende fiber (DCF)—kalt invers dispersion fiber (IDF)—har åpnet for nye fiber span design ved bruk av DCF som kablet transmisjonsfiber. Bruk av IDF og DCF er sammenlignet for 10 og 40 Gbit/s systemer med 80 km fiber span basert på singel-mode fiber (SMF). Vi viser at bruk av SMF+IDF gir betydelig bedre signal etter transmisjon, sammenlignet med SMF+DCF, hovedsaklig på grunn av lavere samlet fibertap.

Systematiske studier av *non return-to-zero* (NRZ) og *return-to-zero* (RZ) pulsformer for 10 Gbit/s systemer med 80 km forsterkeravstand viser at den optimale pulsbredde er meget smal for énkanalsystemer. For systemer studert her, var 5% pulsbredde optimalt. Disse smale RZ pulsene gir både høy følsomhet i mottakeren og utmerket toleranse ovenfor den ulineære effekt *self phase modulation* (SPM). Men det brede optiske spektrum til signaler med smale pulser forhindrer bruk i flerkanalsystemer (WDM systemer) med liten kanalavstand. I slike systemer vil den optimale pulsbredde være en avveining mellom transmisjonsegenskaper og mottakerfølsomhet på den ene siden, og spektraleffektivitet på den andre.

Flere avanserte modulasjonsformater er i de siste årene foreslått til bruk i optiske kommunikasjonssystemer. Disse nye formater kan overkomme begrensninger tilknyttet pulsspredning på grunn av dispersjon, eller ulineær signaldegradering på grunn av *self phase modulation* (SPM). En systematisk undersøkelse av seks *on-off keying* (OOK) modulasjonsformater i et 40 Gbit/s system med 80 km span lengde viser at vanlig return-to-

zero (RZ) med smal pulsbredde er optimalt for énkanalsystemer. For et 100 GHz WDM system, fant vi at *carrier suppressed return-to-zero* (CS-RZ) og *single side band return-to-zero* (SSB-RZ) ga best resultat, da disse formater kombinerer liten spektralbredde med gode transmisjonsegenskaper.

Én metode til å redusere kostnadene ved optiske kommunikasjonssystemer er å bruke lange fiberspan for redusere antall forsterkerstasjoner. Vi sammenligner tre forskjellige strategier for dispersjonskompenserings i 40 Gbit/s systemer med 160 km fiber span basert på *non-zero dispersion shifted fibre* (NZDSF) og DCF. En kombinasjon av *erbium doped fibre amplifier* (EDFA) og distribuert Ramanforsterkning ble brukt for å kompensere for tapet i fibrene. Resultatene viser at symmetrisk dispersjonskompensering gir betydelige fordele over pre- og post-kompensering.

Differential phase shift keying (DPSK) har for nylig vist seg å være et lovende modulasjonsformat for optiske kommunikasjonssystemer. Vi studerer DPSK med fokus på *differential quadrature phase shift keying* (DQPSK). Vi demonstrerer transmisjonspotensialet til DQPSK i et eksperiment der 12.5 Gbit/s RZ-DQPSK ble sendt over 6500 km i et 64 kanalers WDM system. Fem forskjellige kanalavstander ble undersøkt, og suksessfull transmisjon over 6500 km med dette 12.5 Gbit/s systemet ble demonstrert med en spektraleffektivitet på opptil 0.66 bit/s/Hz.

Modulasjonsformater med fire symbolnivåer muliggjør generering av signaler med dobbelt bitrate av den tilgjengelige elektriske og elektrooptiske utstyr. Dette ble demonstrert ved å generere og motta 80 Gbit/s NRZ-DQPSK ved bruk av komponenter beregnet til 40 Gbit/s signaler. Ved å bruke firebølgeblanding i en meget ulineær fiber, demonstrerer vi for første gang bølgelengdekonvertering av et fasemodulert signal med så høy bitrate.

Denne avhandlingen viser at optimering av dispersjonskompensering sammen med avanserte modulasjonsformater tillater overførsel over betydelig lengre avstander sammenlignet med tradisjonelle systemer. Vi har vist at multinivå fasemodulasjon muliggjør signaler med ultrahøy 80 Gbit/s bitrate, og vi viser at multinivå fasemodulerte signaler er velegnet til transoseaniske spektraleffektive WDM systemer.

Resumé

Denne afhandling omhandler dispersionskompensering og modulationsformater for optiske kommunikationssystemer med bitrater på 10 Gbit/s og derover. Nye modulationsformater, blandt andet multiniveau fasemodulation, er undersøgt og demonstreret ved bitrater op til 80 Gbit/s.

Nye typer dispersionskompenserende fiber (DCF)—såkaldt invers dispersion fiber (IDF)—muliggør nye design af fiber span med brug af DCF som kablet transmissionsfiber. Brug af IDF og DCF er sammenlignet for 10 og 40 Gbit/s systemer med 80 km fiber span baseret på standard singlemode fiber (SMF). Vi viser at brug af SMF+IDF giver et betydeligt bedre signal efter transmission sammenlignet med SMF+DCF, hovedsagelig på grund af lavere samlet fibertab.

Systematiske studier af *non return-to-zero* (NRZ) og *return-to-zero* (RZ) kodning for 10 Gbit/s systemer med 80 km forstærkerafstand viser, at den optimale pulsbredde er meget smal for énkanalsystemer. For systemer studeret her var en pulsbredde på 5% af bitperioden optimalt. Disse smalle RZ pulser giver både høj følsomhed i modtageren og fremragende tolerance ovenfor den ulineære effekt *self phase modulation* (SPM). Men det brede optiske spektrum kendetegnende for signaler med smalle pulser forhindrer brug i flerkanalsystemer (WDM systemer) med lille kanalafstand. I sådanne systemer vil den optimale pulsbredde være en afvejning mellem transmissionsegenskaber og modtagerfølsomhed på den ene side og spektraleffektivitet på den anden.

I løbet af de sidste år er flere avancerede modulationsformater blevet foreslået til brug i optiske kommunikationssystemer. Disse nye formater kan overkomme begrænsninger i forbindelse med pulsspredning forårsaget af dispersion eller signaldegradering på grund af *self phase modulation* (SPM). En systematisk undersøgelse af seks *on-off keying* (OOK) mo-

dulationsformater i et 40 Gbit/s system med 80 km span længde viser, at almindelig RZ med smal pulsbredde er optimalt for énkanalsystemer. For et 100 GHz WDM system fandt vi at *carrier suppressed return-to-zero* (CS-RZ) og *single side band return-to-zero* (SSB-RZ) gav det bedste resultat, da disse formater kombinerer en lille spektralbredde med gode transmissionsegenskaber.

Én metode til at reducere omkostningerne ved optiske kommunikationssystemer er at bruge lange fiberspan til reduktion af antallet af forstærkerstationer. Vi sammenlignede tre forskellige strategier for dispersionskompensering for 40 Gbit/s systemer med 160 km fiber span baseret på *non-zero dispersion shifted fibre* (NZDSF) og DCF. En kombination af *erbium doped fibre amplifier* (EDFA) og distribueret Ramanforstærkning blev brugt til at kompensere for tabet i fibrene. Resultaterne viser, at symmetrisk dispersionskompensering giver betydelige fordele sammenlignet med pre- og post-kompensering.

Differential phase shift keying (DPSK) har for nylig vist sig at være et lovende modulationsformat for optiske kommunikationssystemer. Denne afhandling studerer DPSK med fokus på *differential quadrature phase shift keying* (DQPSK). Vi demonstrerer transmissionspotentialet til DQPSK i et eksperiment, hvor 12.5 Gbit/s RZ-DQPSK blev transmitteret over 6500 km i et 64 kanalers WDM system. Fem forskellige kanalafstande blev undersøgt, og succesfuld transmission over 6500 km med dette 12.5 Gbit/s system blev demonstreret med en spektraleffektivitet på op til 0.66 bit/s/Hz.

Modulationsformater med fire symbolniveauer gør det muligt at generere signaler med dobbelt bitrate af det tilgængelige elektriske og elektrooptiske udstyr. Dette blev demonstreret ved at generere og modtage 80 Gbit/s NRZ-DQPSK ved brug af komponenter beregnet til 40 Gbit/s signaler. Ved at bruge firebølgeblanding i en stærkt ulineær fiber, demonstrerede vi for første gang bølgelængdekonvertering af et fasemoduleret signal med så høj bitrate.

Denne afhandling viser, at optimering af dispersionskompensering sammen med avancerede modulationsformater tillader transmission over betydelig længere afstande sammenlignet med traditionelle systemer. Vi har vist, at multiniveau fasemodulation muliggør signaler med ultrahøj 80 Gbit/s bitrate, og vi viser at multiniveau fasemodulerede signaler er velegnede til transoceaniske spektraleffektive WDM systemer.

Acknowledgements

I am very grateful for all the support, advice and motivation I have received from my supervisors, Palle and Christophe, over the last years. Thank you for keeping your doors open and always having time for me.

The Systems Competence Area at Research Center COM have been a perfect place to perform this study, and I have really enjoyed the company and friendship of past and present fine colleagues. Late nights either in the lab or at the Friday bar have left lasting memories. Special thanks to Jorge, who have suffered from my company in the office for so many years. Also thanks to the FOM committee for my three outstanding FOM awards.

I would like to thank Tyco Telecommunication for allowing me to stay six months with them in New Jersey. Thanks to Morten, Alexei and Neal for welcoming me and for good cooperation. I am grateful for being allowed to play in Tyco's impressive laboratories. Special thanks to Carl, Jin-Xing, Dimitri and many others for all the help and late hours in the lab. I really enjoyed the company and discussions with all of you at lunch time. Morten, thanks for the hiking trips and marathon training in the weekends.

As a reader, you should appreciate the help I received from Jorge and Beáta while writing this thesis—their input and corrections has made much more understandable.

Heidi—thank you for being.

Torger Tokle
September 27, 2004

Ph.D. Publications

The following publications have resulted from this Ph.D. project.

[A] T. Tokle, B. Zsigri, C. Peucheret, and P. Jeppesen. "Generation and transmission of a 160 Gbit/s polarisation multiplexed RZ-DBPSK-ASK signal". Submitted to Electronics Letters

[B] T. Tokle, P. A. Andersen, Y. Geng, B. Zsigri, C. Peucheret, and P. Jeppesen. "Generation, transmission and wavelength conversion an 80 Gbit/s RZ-DBPSK-ASK signal". Submitted to Conference on Lasers and Electro-Optics, CLEO'05

[C] T. Tokle, Y. Geng, C. Peucheret, and P. Jeppesen. "Wavelength conversion of 80 Gbit/s optical DQPSK using FWM in a highly non-linear fibre". Submitted to Conference on Lasers and Electro-Optics, CLEO'05

[D] T. Tokle, Q. N. T. Le, C. Peucheret, and P. Jeppesen. "Optimum dispersion map for Raman amplified 160 km NZDSF + DCF fibre spans with 40 Gbit/s RZ signals", *Electronics Letters*, vol. 40, no. 22, pp. 1443–1444, October 2004. doi:10.1049/el:20040605.

[E] N. Chi, P. V. Holm-Nielsen, L. Xu, J. Zhang, T. Tokle, and P. Jeppesen. "Cascaded transmission, packet switching and all-optical wavelength conversion for a 40 Gb/s RZ payload with a 10 Gb/s serial-bit label", *Electronics Letters*, vol. 40, no. 21, pp. 1366 – 1367, October 2004. doi:10.1049/el:20045677.

[F] T. Tokle, C. R. Davidson, M. Nissov, J.-X. Cai, D. G. Foursa, and A. Pilipetskii. "Transmission of RZ-DQPSK over 6500 km with 0.66 bit/s/Hz spectral efficiency", in *IEEE/LEOS 2004 Workshop on Advanced Modulation Formats,* San Francisco, California, U.S.A, pp. 3–4, Paper ThA2, July 2004.

[G] T. Tokle, C. R. Davidson, M. Nissov, J.-X. Cai, D. G. Foursa, and A. Pilipetskii. "6500 km transmission of RZ-DQPSK WDM signals", *Electronics Letters*, vol. 40, no. 7, pp. 444–445, April 2004. doi:10.1049/el:20040274

[H] T. Tokle, C. Peucheret, and P. Jeppesen. "System optimisation of dispersion maps using new cabled dispersion compensating fibers", *Journal of Optical Communication*, vol. 25, no. 2, pp. 75–78, March 2004.

[I] T. Tokle, C. Peucheret, and P. Jeppesen. "Advanced modulation formats in 40 Gbit/s optical communication systems with 80 km fibre spans", *Optics Communications*, vol. 225, pp. 79–87, September 2003. doi:10.1016/j.optcom.2003.07.030

[J] A. Buxens, T. Tokle, C. Peucheret, and P. Jeppesen. "Influence of optical time domain demultiplexing in chromatic dispersion and PMD induced penalty measurements at 40 Gb/s", in *Proceedings European Conference on Optical Communication, ECOC'03,* Rimini, Italy, vol. 3, pp. 798–799, Paper We4.P.121, September 2003.

[K] N. Chi, L. Xu, K. S. Berg, T. Tokle, and P. Jeppesen. "All optical wavelength conversion and multichannel 2R regeneration based on highly nonlinear dispersion-imbalanced loop mirror", *IEEE Photonics Technology Letters*, vol. 14, no. 11, pp. 1581–1583, November 2002. doi:10.1109/LPT.2002.803343

[L] N. Chi, L. Xu, L. K. Oxenløwe, T. Tokle, and P. Jeppesen. "2R regenerator based on high non-linear dispersion-imbalanced loop mirror", *Optics Communication*, vol. 206, pp. 295–300, June 2002. doi:10.1016/S0030-4018(02)01258-0

[M] N. Chi, C. Peucheret, L. K. Oxenløwe, T. Tokle, and P. Jeppesen. "2R all-optical regenerator assessment at 10 Gbit/s over 94 km standard fiber using in-line dispersion-imbalanced loop mirror", in *Proceedings International Conference on Telecommunications, ICT'2002,* Beijing, China, pp. 1288–1290, Paper D-017, June 2002, Invited paper.

List of Figures

List of Tables

Contents

Chapter 1

Introduction

In today's information age, there is a large and rapidly growing demand for transporting information from one place to another. This demand is very diversified—ranging from relatively low-capacity, short-distance private home connections to ultra-high capacity transoceanic submarine connections between continents. Optical communication systems are proven to be a very suitable method for moving massive amounts of information over long distances at a low cost. Today almost all long-haul high-capacity information transport needs are fulfilled by optical communication systems [1, 2].

Internet traffic growth is the prime driver for increasing the capacity of today's fibre optic systems. Everyone agrees that the Internet traffic is increasing, but there is no strong consensus on the actual rate of increase. Most people have realised that the over-hyped statement "The internet is doubling every three months" is not true today, if it ever was (see e.g. [3]). Recent estimates on current Internet growth claim a doubling of the traffic every year [4–6]. But even if the traffic "only" doubles every couple of years, it will still be one of fastest growing markets in the world.

For an industry still struggling with the financial difficulties due to the over-optimistic investments of the past, the light at the end of the tunnel is becoming brighter. The increasing Internet data traffic will inevitably lead to future capacity upgrades. More importantly—at least for the network operators—is that the revenue from high-speed data subscriptions is also dramatically increasing, due to a massive increase in the number of subscribers. The U.S.A. is currently seeing almost 2 million new broad-

band subscribers each quarter, to a total of 29 million subscriptions by the middle of 2004 [7]. And in Denmark, the number of high-speed internet subscribers increased by more than 60% just from 2002 to 2003 [8]. This increased revenue to the telecommunication industry should allow for the future capacity upgrades.

For the next generation of optical communication systems to fulfill future capacity demands, state-of-the-art dispersion management will be required to effectively compensate for dispersion in a wide bandwidth, and minimise nonlinear signal degradation. Advanced modulation formats can be used to improve the transmission performance and to achieve high spectral efficiency. This thesis focuses on these two key aspects of optical communication systems—dispersion management and modulation formats.

The dispersion in optical fibres is a main limitation for optical communication systems with per channel bit rates above 2.5 Gbit/s. Fortunately, the dispersion induced degradations can be compensated for by using dispersion compensating fibres (DCFs). For a linear system, the dispersion can be compensated 100%, and the optimisation of the dispersion compensation would be trivial. However, due to the complex interaction of dispersion and nonlinear signal degradation, the optimisation process becomes very complicated. The introduction of novel DCFs—referred to as inverse dispersion fibres (IDFs)—has recently allowed for new span designs, where the IDF is cabled and used as transmission fibre. We study several different dispersion compensation schemes, both numerically and experimentally. Results indicate that significant improvements can be obtained by using new IDF compared to conventional DCF, primarily due to reduced span loss.

Over the last years, many "new" modulation formats—some previously known from radio communication—have been introduced as alternatives to the commonly used non return-to-zero (NRZ) and 50% return-to-zero (RZ). These include RZ with narrow pulse widths, carrier suppressed return-to-zero (CS-RZ), single side band return-to-zero (SSB-RZ), and duobinary. We study different modulation formats at per channel bit rates of 10 and 40 Gbit/s, and compare their relative performance in systems with various 80 km single mode fibre (SMF) + DCF fibre spans.

Recently, the use of phase modulation formats have also been studied, with focus on differential binary phase shift keying (DBPSK). We study the four-level differential quadrature phase shift keying (DQPSK),

describing transmitter and receiver designs, and experimental demonstration of a 12.5 Gbit/s wavelength division multiplexing (WDM) DQPSK system over 6500 km with spectral efficiency of 0.66 bit/s/Hz. Generation and detection of 80 Gbit/s DQPSK is experimentally demonstrated. Using four-wave mixing (FWM) in highly nonlinear fibre we demonstrate wavelength conversion of phase modulated signals at 40 and 80 Gbit/s.

1.1 Structure of the Thesis

Chapter 2 presents a short introduction to the dispersion management and modulation formats for optical communication systems, and introduces the terminology used in this thesis.

In Chapter 3 the optimum dispersion compensation scheme for 10 Gbit/s systems using NRZ or RZ modulation format is discussed. Three different RZ pulse widths are studied, 50, 10 and 5% of the bit slot. We study four different dispersion maps based on SMF+DCF and SMF+IDF×n, with $n = \{1, 2, 3\}$ being the SMF to IDF length ratio. We show that narrow pulse-width RZ signals offer a 3 dB transmission length up to three times longer than NRZ due to improved tolerance to self phase modulation (SPM). Spans with IDFs has lower span loss, resulting in up to 20% improved 3 dB transmission distance.

Novel on-off keying modulation formats are compared in Chapter 4, where NRZ, duobinary, RZ with 50 and 20% pulse widths, SSB-RZ and CS-RZ are compared for 40 Gbit/s systems using SMF + DCF or SMF + IDF×2. Studying a single-channel system, we show that the conclusions obtained at a bit rate of 10 Gbit/s are still valid at the higher bit rate of 40 Gbit/s. Using narrow RZ pulses results in optimum performance. However, when a WDM system with 100 GHz channel spacing is considered, the benefits of the SSB-RZ and CS-RZ are revealed. Narrow spectral width combined with good transmission performance due to the RZ waveform results in overall good performance for SSB-RZ and CS-RZ.

Chapter 5 presents an experimental investigation of three dispersion maps for 160 km span length. Using such long span lengths can significantly reduce the cost of the link, as the number of amplifier stations are significantly decreased. We compare pre-, post- and symmetrical dispersion maps for a system using 40 Gbit/s bit rate, and the results shows that the symmetrical dispersion map results in the best performance.

DQPSK is dealt with in Chapter 6. First, an introduction to DQPSK is presented, showing transmitter and receiver design, and basic properties such as receiver sensitivity and dispersion tolerance are discussed. Then, a series of DQPSK experiments is presented, starting with a demonstration of a 12.5 Gbit/s WDM system with transatlantic transmission lengths. We demonstrate the good WDM transmission properties of DQPSK by transmitting 12.5 Gbit/s RZ-DQPSK over 6500 km using a channel spacing of 15 GHz, corresponding to a spectral efficiency of 0.66 bit/s/Hz. We study ultra-high speed signal by generating a 80 Gbit/s non return-to-zero differential quadrature phase shift keying (NRZ-DQPSK) signal. Using FWM in a highly nonlinear fibre, we demonstrate the first wavelength conversion of such high speed phase modulated signals.

Finally, the thesis is concluded in Chapter 7.

References to Chapter 1

[1] P. R. Trischitta and W. C. Marra. "Global undersea communication networks", *IEEE Communication Magazine*, vol. 34, no. 2, pp. 20–21, February 1996.

[2] N. S. Bergano. *Undersea Communications Systems*, In I. Kaminow and T. Li, editors, *Optical Fiber Telecommunications IVB Components,* Chapter 4, Academic Press, March 2002. ISBN 0-12-395173-9.

[3] P. Sevcik. "The myth of Internet growth", *Business Communications Review*, pp. 12–14, January 1999. Available from `http://www.bcr.com/bcrmag/1999/01/p12.php`.

[4] P. Sevcik. "Internet bandwidth: It's time for accountability", *Business Communications Review*, pp. 10–11, January 2001. Available from `http://www.bcr.com/bcrmag/2001/01/p10.php`.

[5] A. M. Odlyzko. "Internet traffic growth: Sources and implications", in *Proceedings Optical Transmission Systems and Equipment for WDM Networking II,* Orlando, Florida, U.S.A., September 2003, available from `http://www.dtc.umn.edu/~odlyzko/`.

[6] K. G. Coffman and A. M. Odlyzko. *Growth of the Internet*, In I. Kaminow and T. Li, editors, *Optical Fiber Telecommunications*

IVB Components, Chapter 2, pp. 17–56, Academic Press, March 2002. ISBN 0-12-395173-9. Available from `http://www.dtc.umn.edu/~odlyzko/`.

[7] Leichtman Research Group, Inc. "Broadband Internet grows to 29 million in the U.S.", August 2004.

[8] IT- og Telestyrelsen. "Årsberetning 2003", May 2004. Available from `http://www.itst.dk/static/ITST-aarsberetning/index.htm`.

Chapter 2

Introduction to Dispersion and Modulation Formats

2.1 Introduction

This chapter gives a brief introduction to concepts and terminology critical to this thesis: modulation formats, dispersion, dispersion compensation and dispersion management. This is not intended as a complete introduction to these topics, rather as a quick walk-through with references to further information to set the stage for the following chapters.

2.2 Dispersion

2.2.1 Chromatic Dispersion

Dispersion[1] in optical communication systems is dominated by two parts, namely material dispersion and waveguide dispersion. The material dispersion comes from a wavelength dependence of the refractive index of silica, the material used for optical fibres [1]. The other contribution to the dispersion is the waveguide dispersion, caused by the structure of the fibre. The waveguide dispersion depends on fibre parameters like the core radius and the index difference [1].

In the wavelength area of interest for optical communication—around

[1]The term *dispersion* is used for *chromatic dispersion* throughout this thesis.

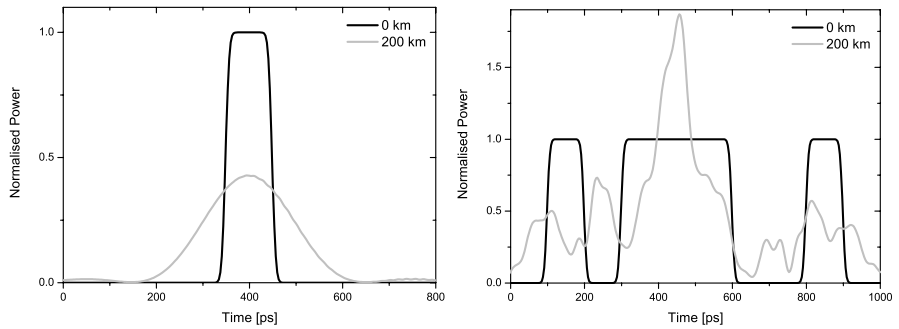

Figure 2.1: Illustration of the effect of dispersion on a 10 Gbit/s NRZ signal before and after transmission through 200 km of (loss-less and linear) SMF for a single pulse (a) and a pulse train (b).

1550 nm—the material dispersion is positive and the waveguide dispersion is negative. By careful optimisation of the fibre parameters, the amount of waveguide dispersion can be controlled such that the sum of material and waveguide dispersion can be either positive, zero or negative at the wavelength of interest. Standard single mode fibre (SMF) have a dispersion of about 17 ps/nm/km at 1550 nm.

The wavelength dependence of the refractive index causes the various spectral components of the signal to propagate at different velocities through the fibre, effectively broadening the pulse at the receiver. Figure 2.1(a) illustrates the effect of the dispersion from 200 km of standard SMF[2] on a single 10 Gbit/s non return-to-zero (NRZ) "one" bit. It is seen that the initial almost square NRZ pulse is transformed into a much wider pulse, that has energy far outside the bit slot. This leads to interference with neighbouring bits—referred to as inter-symbol interference (ISI). Figure 2.1(b) illustrates the effect ISI on the pulse train "0101110010". The ISI caused by dispersion is so severe at this point that the information is lost.

As the bit rate increases, the spectral width is increased and the bit time slot is decreased. Both the increased spectral width and decreased

[2]Assuming a linear, loss-less fibre with a dispersion of 17 ps/nm/km.

time slot increases the detrimental effect of dispersion. Therefore, the effect of dispersion scales with the *square* of the bit rate [2].

The dispersion length L_D is a rule of thumb to judge when the effect of dispersion becomes so large that the information in the signal can not be recovered. The L_D expressed in km can be written as[3]

$$L_D \simeq 0.252 \cdot \frac{T^2}{D}, \tag{2.1}$$

where T is the full width at half maximum (FWHM) pulse width of the input pulses expressed in ps and D is the dispersion expressed in ps/nm/km.

Using Eq. 2.1, we see that for a NRZ signal at 1 Gbit/s, the dispersion length is above 14 000 km for SMF.[4] Thus dispersion is not a limiting issue at such low bit rates, even for ultra-long transoceanic links. However, as the bit rate is increased the dispersion length decreases rapidly, being 2300 km for 2.5 Gbit/s and 150 km for 10 Gbit/s. For a bit rate of 40 Gbit/s, the L_D is decreased to only 9 km SMF. With non-zero dispersion shifted fibre (NZDSF), the dispersion lengths are a factor of 5–10 times longer than with SMF.

Fortunately, there are methods to compensate for the effect of dispersion, enabling transmission over distances longer than the dispersion length without expensive optical-electrical-optical conversions.

2.2.2 Dispersion Compensation

There are several different methods that can be used to compensate for dispersion, including dispersion compensating fibre (DCF) [3–6], chirped Bragg gratings [7–9], all-pass optical filters [10–13] and optical phase conjugation [14–16]. These methods restore the signal such that it can be received in a normal receiver. An alternative method is to detect the dispersed signal and perform the dispersion compensation electrically [17–19].

[3]Using $L_D = \frac{T_0^2}{|\beta_2|}$, $\beta_2 = -\frac{\lambda^2}{2\pi c} \cdot D$ and $T_{\mathrm{FWHM}} \simeq \frac{T_0}{1.763}$ at $\lambda = 1550$ nm, where c is the speed of light in vacuum and T_0 is the 1/e pulse width [2]. L_D is the length at which an unchirped first-order Gaussian pulse has broadened by a factor $\sqrt{2}$, and gives a rough estimate of when the effect of dispersion becomes significant.

[4]Using T=100% of the bit slot for the NRZ signal. This is not accurate—as Eq. 2.1 assumes Gaussian pulse width—but a useful rough approximation.

As previously mentioned, careful optimisation of the fibre parameters can make the sum of material and waveguide dispersion negative for wavelengths around 1550 nm. Dispersion compensation using negative dispersion fibre was originally proposed in 1980 [20], and DCFs have now been commercially available for more than a decade [1]. The use of DCF is now a mature technique to compensate for the dispersion of already deployed SMF, and the effectiveness of the latest generation of DCFs for wide-band compensation has already been demonstrated [3]. Due to this, and the wide-spread use of DCFs in commercial systems, this thesis deals solely with dispersion compensation using DCF.

Fortunately, dispersion is a linear effect which can be completely compensated. By placing one DCF with negative dispersion after a SMF with positive dispersion, the net dispersion will be zero if

$$D_{\mathrm{SMF}} \times L_{\mathrm{SMF}} = -D_{\mathrm{DCF}} \times L_{\mathrm{DCF}}, \tag{2.2}$$

where D and L is the dispersion and length of each fibre segment, respectively.

Traditionally, the DCF has been placed on a fibre spool in the amplifier station. In this configuration it is best to use a short DCF in order to minimise the insertion loss. Thus, the negative dispersion of the DCF needs to be large, and is normally around -100 ps/nm/km [3]. One length of DCF thus compensates for about six lengths of SMF, thus about 14 km DCF is required for an 80 km SMF span.

2.2.3 Dispersion Management

The previous section briefly introduced dispersion compensation. Here, we take the concept a little further, and introduce the term *dispersion management*. Increasing the capacity of optical communication systems relies on the effective management of dispersion and optical fibre nonlinearities. The choice of the type of fibre used for transmission as well as the dispersion management scheme are therefore of prime importance for the design of optical fibre links.

We saw in the last section that long-haul transmission of high bit rate signals such as 10 and 40 Gbit/s requires dispersion compensation. If the optical transmission path was completely linear, all of the link dispersion could have been compensated by one dispersion compensator, for example

at the receiver. Unfortunately, the phase information that is required to regenerate a dispersed signal is destroyed by nonlinear signal interaction such as self phase modulation (SPM) and cross phase modulation (XPM) in the optical path. Therefore, the dispersion should be compensated on a regular basis, and this is normally performed on a per-span basis.

From a single-channel system, one could argue that the optimum would be to produce a fibre with zero dispersion at the channel wavelength, a fibre type referred to as dispersion shifted fibre (DSF). This can be done by carefully adjusting the fibre design so that the waveguide dispersion exactly cancels out the material dispersion [1]. However, in wavelength division multiplexing (WDM) systems, fibres with zero or low dispersion suffer from enhanced nonlinear signal interaction such as four-wave mixing (FWM) [2]. A compromise between SMF and DSF was introduced in order to offer a dispersion that was lower than SMF, but high enough to avoid excessive FWM, and is referred to as NZDSF. An experimental investigation using NZDSF with a dispersion of 5.5 ps/nm/km is presented in Chapter 5.

In a linear system, it normally would be optimum to compensate for 100% of the dispersion. However, the nonlinear effect SPM creates a frequency chirp that can be partially compensated for by positive dispersion [2]. Thus, the amount of dispersion compensation needs to be optimised. Additionally, the location of the dispersion compensating fibre in the span also affects the performance. The nonlinear signal evolution is different for pre-compensated, post-compensated and symmetrically compensated spans.

Furthermore, it is not always optimum to have equal dispersion compensation ratio in each span. For long-haul submarine systems, the dispersion is often managed in a *long dispersion map* of about 10 spans (see e.g. [21–24]). Some of the spans in the map are over-compensated, and some of the maps are under-compensated so that the total accumulated dispersion in each map is close to zero. This advanced dispersion management improves performance, since as the pulse shape is different at each span input, thus avoiding build-up of the same non-linear signal degradation. Long dispersion maps are used in long-haul transmission experiments presented in Chapter 6.

This introduction on dispersion management illustrates that the optimisation of dispersion management is a difficult task. There is no “glob-

ally optimum" dispersion management scheme, as it will depend on system parameters such as fibre types used, span length, transmission distance, number of channels, modulation formats and per channel bit rate. Thus, the choice of the dispersion management scheme must be considered for each system.

The following chapters will present investigations of several dispersion management schemes. Chapters 3 and 4 presents comparisons of dispersion managed 80 km fibre spans consisting of SMF and either conventional DCF or one of three novel inverse dispersion fibres (IDFs), for bit rates of 10 and 40 Gbit/s, respectively. In Chapter 5, we compare three NZDSF + DCF dispersion maps for a 40 Gbit/s system.

2.3 Modulation Formats

When designing today's optical communication links, there is a wide variety of modulation formats to choose from. Four properties of an optical signal can be modulated—the amplitude, phase, frequency and state of polarisation (SOP). Most systems today use a binary amplitude modulation on-off keying (OOK) format with a pulse width equal to the time slot—non return-to-zero (NRZ), since very simple (and thus cheap) transmitters and receivers can be used.[5]

Over the last years, novel modulation formats with improved performance with respect to NRZ have been suggested and investigated. It has been long known that using a return-to-zero (RZ) waveform can improve the receiver sensitivity and nonlinear tolerance (see e.g. [25–28]), but at the extra cost of one additional modulator and drive circuitry in the transmitter. Recently, many OOK formats with additional phase modulation have been shown to perform very well under certain circumstances, for example chirped-RZ [29, 30]. This however, adds further complexity to the transmitter.

Recently, phase modulation have been "rediscovered" in the optical communication field [31]. Phase modulation combined with a balanced receiver offers a very attractive 3 dB improved receiver sensitivity compared to OOK. However, this improvement comes at the cost of a more complic-

[5]Only digital modulation is considered in this thesis.

ated receiver design. Four-level phase modulation—differential quadrature phase shift keying (DQPSK)—has also been studied recently [32–37].

Advanced modulation formats can offer significantly better performance compared to NRZ. However, these formats require significantly increased complexity in transmitter and receiver designs, leading to increased cost. For commercial systems, advanced modulation formats will therefore only be used when NRZ is not sufficient, or the extra cost of the modulation format lead to larger cost reductions in other parts of the system.

The various modulation formats can be classified into the following four categories, depending on which of the four properties of the carrier is modulated—amplitude, phase, frequency and SOP:

- Amplitude shift keying (OOK)[6] [28, 38–49]
- Phase shift keying [31–37, 50–54]
- Frequency shift keying [55–59]
- Polarisation shift keying [60–65]

In this work, modulation formats from the first and second group listed above have been investigated. Frequency modulation and polarisation modulation formats were not considered in this work. Chapter 3 presents an investigation on optimum pulse width of 10 Gbit/s NRZ and RZ signals. Advanced OOK modulation formats are introduced and compared in Chapter 4. Finally, phase modulated signals are discussed in Chapter 6, where DQPSK is studied at bit rates of 12.5 and 80 Gbit/s.

2.4 Summary

This chapter has briefly introduced two aspects of optical communication systems critical to this study—management of dispersion and modulation of optical signals. The detrimental effects of dispersion on high-speed

[6] Apart from NRZ and RZ, this category also includes e.g. duobinary, carrier suppressed return-to-zero (CS-RZ) and single side band return-to-zero (SSB-RZ). These formats are all OOK signals with additional phase modulation or to improve transmission performance or spectral properties.

optical signals have been illustrated, and the concept of dispersion compensation and dispersion management have been discussed. Modulation methods used in optical communication were discussed, and references to the most well-known formats were given.

References to Chapter 2

[1] G. P. Agrawal. *Fiber-Optic Communciation Systems.* Wiley, Second edition, 1997. ISBN 0-471-17540-4.

[2] G. P. Agrawal. *Nonlinear Fiber Optics.* Academic Press, Second edition, 1995. ISBN 0-12-045142-5.

[3] L. Grüner-Nielsen, S. N. Knudsen, B. Edvold, T. Veng, D. Magnussen, C. C. Larsen, and H. Damsgaard. "Dispersion compensating fibers", *Optical Fiber Technology*, vol. 6, no. 2, pp. 164–180, April 2000. doi:10.1006/ofte.1999.0324.

[4] S. N. Knudsen and T. Veng. "Large effective area dispersion compensating fiber for cabled compensation of standard single mode fiber", in *Technical Digest Optical Fiber Communication Conference, OFC'00,* Baltimore, Maryland, U.S.A., vol. 1, pp. 98–100, Paper TuG5, March 2000.

[5] S. N. Knudsen. "Design and manufacture of dispersion compensating fibers and their performance in systems", in *Technical Digest Optical Fiber Communication Conference, OFC'02,* Anaheim, California, U.S.A., pp. 330–332, Paper WU3, March 2002.

[6] Q. N. T. Le, T. Veng, and L. Grüner-Nielsen. "New dispersion compensating module for compensation of dispersion and dispersion slope of non-zero dispersion fibres in the C-band", in *Technical Digest Optical Fiber Communication Conference, OFC'01,* Anaheim, California, U.S.A., Paper TuH5, March 2001.

[7] J. A. R. Williams, I. Bennion, K. Sugden, and N. J. Doran. "Fibre dispersion compensation using a chirped in-fibre Bragg grating", *Electronics Letters*, vol. 30, no. 12, pp. 985–987, June 1994. doi:10.1049/el:19940661.

[8] M. J. N. Lima, A. L. J. Teixeira, and J. R. F. da Rocha. "Simultaneous filtering and dispersion compensation in WDM systems using apodised fibre gratings", *Electronics Letters*, vol. 36, no. 16, pp. 1412–1414, August 2000. doi:10.1049/el:20000959.

[9] M. Morin, M. Poulin, A. Mailloux, F. Trépanier, and Y. Painchaud. "Full C-band slope-matched dispersion compensation based on a phase sampled Bragg grating", in *Technical Digest Optical Fiber Communication Conference, OFC'04,* Los Angeles, California, U.S.A., Paper WK1, February 2004.

[10] G. Lenz and C. K. Madsen. "General optical all-pass filter structures for dispersion control in WDM systems", *Journal of Lightwave Technology*, vol. 17, no. 7, pp. 1248–1254, July 1999.

[11] C. K. Madsen, J. A. Walker, J. E. Ford, K. W. Goossen, T. N. Nielsen, and G. Lenz. "A tunable dispersion compensating MEMS all-pass filter", *IEEE Photonics Technology Letters*, vol. 12, no. 6, pp. 651–653, June 2000.

[12] K. Suzuki, I. Nakamatsu, T. Shimoda, S. Takaesu, J. Ushioda, E. Mizuki, M. Horie, Y. Urino, and H. Yamazaki. "WDM tuneable dispersion compensator with PLC ring resonators", in *Technical Digest Optical Fiber Communication Conference, OFC'04,* Los Angeles, California, U.S.A., Paper WK3, February 2004.

[13] M. Bohn, W. Rosenkranz, P. M. Krummrich, F. Horst, B. J. Offrein, and G. L. Bona. "Experimental verification of combined adaptive PMD and GVD compensation in a 40 Gb/s transmission using integrated optical FIR-filters and spectrum monitoring", in *Technical Digest Optical Fiber Communication Conference, OFC'04,* Los Angeles, California, U.S.A., Paper TuG3, February 2004.

[14] A. Yariv, D. Fekete, and D. M. Pepper. "Compensation for channel dispersion by nonlinear optical phase conjugation", *Optics Letters*, vol. 4, no. 2, pp. 52–54, February 1979.

[15] A. H. Gnauck, R. M. Jopson, P. P. Iannone, and R. Derosier. "Transmission of two wavelength-multiplexed 10 Gbit/s channels over

560 km of dispersive fibre", *Electronics Letters*, vol. 30, no. 9, pp. 727–728, April 1994. doi:10.1049/el:19940482.

[16] G. S. He. "Optical phase conjugation: principles, techniques, and applications", *Progress in Quantum Electronics*, vol. 26, no. 3, pp. 131–191, May 2002. doi:10.1016/S0079-6727(02)00004-6.

[17] F. Buchali, H. Bülow, W. Baumert, R. Ballentin, and T. Wehren. "Reduction of the chromatic dispersion penalty at 10 Gbit/s by integrated electronic equalisers", in *Technical Digest Optical Fiber Communication Conference, OFC'00,* Baltimore, Maryland, U.S.A., pp. 268–270, Paper ThS1, March 2000.

[18] S. Woodward, S.-Y. Huang, M. Feuer, and M. Boroditsky. "Demonstration of an electronic dispersion compensator in a 100 km 10 Gb/s ring network", *IEEE Photonics Technology Letters*, vol. 15, no. 6, pp. 867–869, June 2003. doi:10.1109/LPT.2003.811145.

[19] V. Curri, R. Gaudino, A. Napoli, and P. Poggiolini. "Electronic equalization for advanced modulation formats in dispersion-limited systems", *IEEE Photonics Technology Letters*, vol. 16, no. 11, pp. 2556–2558, November 2004. doi:10.1109/LPT.2004.835192.

[20] C. Lin, H. Kogelnik, and L. G. Cohen. "Optical-pulse equalization of low-dispersion transmission in single-mode fibers in the 1.3–1.7 μm spectral region", *Optics Letters*, vol. 5, no. 11, pp. 476–478, November 1980.

[21] G. Vareille, O. A. Sab, G. Bassier, J. P. Collet, B. Julien, D. Dufournet, F. Pitel, and J. F. Marcerou. "1.5 Terabit/s submarine 4000 km system validation over a deployed line with industrial margins using 25 GHz channel spacing and NRZ format over NZDSF", in *Technical Digest Optical Fiber Communication Conference, OFC'02,* Anaheim, California, U.S.A., pp. 293–295, Paper WP5, March 2002.

[22] R. Gleason, M. Kordahi, M. Sanders, and S. Shapiro. "Cable and joint design for high capacity systems", in *Techincal Digest SubOptic 2001 Internation Convention,* Kyoto, Japan, Paper T4.1.1, May 2001.

[23] G. Vareille, O. Ait Sab, F. Pitel, and J. F. Marcerou. "Terabit transoceanic system assessment with industrial margins using 25 GHz

channel spacing and NRZ format", in *Technical Digest Optical Fiber Communication Conference, OFC'02,* Anaheim, California, U.S.A., pp. 295–296, Paper WP5, March 2002.

[24] B. Bakhshi, M. Vaa, E. A. Golovehenko, W. W. Patterson, R. L. Maybach, and N. S. Bergano. "Comparison of CRZ, RZ and NRZ modulation formats in a 64×12.3 Gb/s WDM transmission experiment over 9000 km", in *Technical Digest Optical Fiber Communication Conference, OFC'01,* Anaheim, California, U.S.A., vol. 3, Paper WF4, March 2001.

[25] P. J. Winzer and A. Kalmar. "Sensitivity enhancement of optical receivers by impulsive coding", *Journal of Lightwave Technology*, vol. 17, no. 2, pp. 171–177, February 1999.

[26] M. Hayee and A. Willner. "NRZ versus RZ in 10–40 Gb/s dispersion-managed WDM transmission systems", *IEEE Photonics Technology Letters*, vol. 11, no. 8, pp. 991–993, August 1999.

[27] C. Caspar, H.-M. Foisel, A. Gladisch, N. Hanik, F. Küppers, R. Ludwig, A. Mattheus, W. Pieper, B. Strebel, and H. G. Weber. "RZ versus NRZ modulation format for dispersion compensated SMF-based 10 Gb/s transmission with more than 100 km amplifier spacing", *IEEE Photonics Technology Letters*, vol. 11, no. 4, pp. 481–483, April 1999.

[28] T. Tokle, C. Peucheret, and P. Jeppesen. "Transmission of 1.8 and 4.8 ps RZ signals at 10 Gbit/s over more than 2700 km of a dispersion managed link made of standard and inverse dispersion fibre", in *Proceedings OptoElectronics and Communications Conference, OECC'01,* Sydney, Australia, pp. 266–267, Paper WA4, July 2001.

[29] E. A. Golovchenko, A. N. Pilipetskii, and N. S. Bergano. "Transmission properties of chirped return-to-zero pulses and nonlinear intersymbol interference in 10 Gb/s WDM transmission", in *Technical Digest Optical Fiber Communication Conference, OFC'00,* Baltimore, Maryland, U.S.A., vol. 3, pp. 38–40, Paper FC3, March 2000.

[30] N. S. Bergano, M. Nissov, A. Pilipetskii, J.-X. Cai, C. Davidson, and B. Bakhshi. "Chirped return-to-zero formats for ultra long-haul fiber communications", in *IEEE/LEOS 2004 Workshop on Advanced Modulation Formats,* San Francisco, California, U.S.A, pp. 1–2, Paper ThA1, July 2004.

[31] M. Rohde, C. Caspar, N. Heimes, M. Konitzer, E.-J. Bachus, and N. Hanik. "Robustness of DPSK direct detection transmission format in standard fibre WDM systems", *Electronics Letters*, vol. 36, no. 17, pp. 1483–1484, August 2000. doi:10.1049/el:20000981.

[32] R. Griffin and A. Carter. "Optical differential quadrature phase-shift key (oDQPSK) for high capacity optical transmission", in *Technical Digest Optical Fiber Communication Conference, OFC'02,* Anaheim, California, U.S.A., pp. 367–368, Paper WX6, March 2002.

[33] C. Wree, J. Leibrich, J. Eick, and W. Rosenkranz. "Experimental investigation of receiver sensitivity of RZ-DQPSK modulation format using balanced detection", in *Technical Digest Optical Fiber Communication Conference, OFC'03,* Atlanta, Georgia, U.S.A., Paper ThE5, 2003.

[34] T. Tokle, C. R. Davidson, M. Nissov, J.-X. Cai, D. G. Foursa, and A. Pilipetskii. "Transmission of RZ-DQPSK over 6500 km with 0.66 bit/s/Hz spectral efficiency", in *IEEE/LEOS 2004 Workshop on Advanced Modulation Formats,* San Francisco, California, U.S.A, pp. 3–4, Paper ThA2, July 2004.

[35] T. Tokle, C. R. Davidson, M. Nissov, J.-X. Cai, D. G. Foursa, and A. Pilipetskii. "6500 km transmission of RZ-DQPSK WDM signals", *Electronics Letters*, vol. 40, no. 7, pp. 444–445, April 2004. doi:10.1049/el:20040274.

[36] P. Boffi, L. Marazzi, L. Paradiso, P. Parolari, A. Righetti, D. Setti, R. Siano, R. Cigliutti, D. Mottarella, P. Franco, and M. Martinelli. "20 Gb/s differential quadrature phase-shift keying transmission over 2000 km in a 64-channel WDM system", *Optics Communication*, vol. 237, pp. 319–323, July 2004. doi:10.1016/j.optcom.2004.04.008.

[37] P. S. Cho, G. Harston, C. J. Kerr, A. S. Greenblatt, A. Kaplan, Y. Achiam, G. Levy-Yurista, M. Margalit, Y. Gross, and J. B. Khurgin. "Investigation of 2 b/s/Hz 40 Gb/s DWDM transmission over 4×100 km SMF-28 fiber using RZ-DQPSK and polarization multiplexing", *IEEE Photonics Technology Letters*, vol. 16, no. 2, pp. 656–658, February 2004. doi:10.1109/LPT.2002.807934.

[38] K. Ennser and K. Petermann. "Performance of RZ- versus NRZ-transmission on standard single-mode fibers", *IEEE Photonics Technology Letters*, vol. 8, no. 3, pp. 443–445, March 1996.

[39] D. Breuer and K. Petermann. "Comparison of NRZ- and RZ-modulation format for 40 Gb/s TDM standard-fiber systems", *IEEE Photonics Technology Letters*, vol. 9, no. 3, pp. 398–400, March 1997.

[40] F. Forghieri, P. R. Prucnal, R. W. Tkach, and A. R. Chraplyvy. "RZ versus NRZ in nonlinear WDM systems", *IEEE Photonics Technology Letters*, vol. 9, no. 7, pp. 1035–1037, July 1997.

[41] P. J. Winzer, A. H. Gnauck, G. Raybon, S. Chandrasekhar, Y. Su, and J. Leuthold. "40 Gb/s return-to-zero alternate-mark-inversion (RZ-AMI) transmission over 2000 km", *IEEE Photonics Technology Letters*, vol. 15, no. 5, pp. 766–768, May 2003. doi:10.1109/LPT.2003.809982.

[42] Y. Miyamoto, K. Yonenaga, and S. Kuwahara. "Dispersion-tolerant RZ signal transmission using baseband differential code and carrier suppressed modulation", in *Proceedings European Conference on Optical Communication, ECOC'98,* Madrid, Spain, vol. 1, pp. 351–352, September 1998.

[43] Y. Miyamoto, T. Kataoka, K. Yonenaga, M. Tomizawa, A. Hirano, S. Kuwahara, and Y. Tada. "WDM field trials of 43 Gb/s/channel transport system for optical transport network", *Journal of Lightwave Technology*, vol. 20, no. 12, pp. 2115–2128, December 2002. doi:10.1109/JLT.2002.806775.

[44] M. Wichers, W. Kaiser, T. Wuth, and W. Rosenkranz. "Experimental demonstration of chirped duobinary transmission", *Elec-*

tronics Letters, vol. 38, no. 4, pp. 191–193, February 2002. doi:10.1049/el:20020118.

[45] Y. Miyamoto, K. Yonenaga, A. Hirano, H. Toba, K. Murata, and H. Miyazawa. "Duobinary carrier-suppressed return-to-zero format and its application to 100 GHz-spaced 8×43 Gbit/s DWDM unrepeatered transmission over 163 km", in *Technical Digest Optical Fiber Communication Conference, OFC'01,* Anaheim, California, U.S.A., Paper TuU4, March 2001.

[46] W. Idler, G. Charlet, R. Dischler, Y. Frignac, and S. Bigo. "0.8 bit/s/Hz of information spectral density by vestigal sideband filtering of 24.66 Gb/s NRZ", in *Proceedings European Conference on Optical Communication, ECOC'02,* Copenhagen, Denmark, vol. 3, Paper 8.1.5, September 2002.

[47] T. Tokle, C. Peucheret, and P. Jeppesen. "Advanced modulation formats in 40 Gbit/s optical communication systems with 80 km fibre spans", *Optics Communications*, vol. 225, pp. 79–87, September 2003. doi:10.1016/j.optcom.2003.07.030.

[48] A. Hodžić, B. Konrad, and K. Petermann. "Alternative modulation formats in N×40 Gb/s WDM standard fiber RZ-transmission systems", *Journal of Lightwave Technology*, vol. 20, no. 4, pp. 598–607, April 2002.

[49] Y. Kobayashi, K. Kinjo, K. Ishida, T. Sugihara, S. Kajiya, N. Suzuki, and K. Shimizu. "A comparison among pure-RZ, CS-RZ, and SSB-RZ format, in 1 Tbit/s (50×20 Gbit/s, 0.4 nm spacing) WDM transmission over 4,000 km", in *Proceedings European Conference on Optical Communication, ECOC'00,* Munich, Germany, Paper PD1.7, September 2000.

[50] J.-X. Cai, D. G. Foursa, C. R. Davidson, Y. Cai, G. Domagala, H. Li, L. Liu, W. W. Patterson, A. N. Pilipetskii, M. Nissov, and N. S. Bergano. "A DWDM Demonstration of 3.73 Tb/s over 11,000 km using 373 RZ-DPSK Channels at 10 Gb/s", in *Technical Digest Optical Fiber Communication Conference, OFC'03,* Atlanta, Georgia, U.S.A., Paper PD22, March 2003.

[51] L. Becouarn, G. Vareille, P. Pecci, and J. F. Marcerou. "3 Tbit/s transmission (301 DPSK channels at 10.709 Gb/s) over 10270 km with a record efficiency of 0.65 (bit/s)/Hz", in *Proceedings European Conference on Optical Communication, ECOC'03,* Rimini, Italy, Paper PD45, September 2003.

[52] C. Rasmussen, T. Fjelde, J. Bennike, F. Liu, S. Dey, B. Mikkelsen, P. Mamyshev, P. Serbe, P. van der Wagt, Y. Akasaka, D. Harris, D. Gapontsev, V. Ivshin, and P. Reeves-Hall. "DWDM 40G transmission over trans-pacific distance (10000 km) using CSRZ-DPSK, enhanced FEC, and all-Raman-amplified 100 km UltraWave fiber spans", *Journal of Lightwave Technology*, vol. 22, no. 1, pp. 203–207, January 2004. doi:10.1109/JLT.2004.824187.

[53] A. H. Gnauck, J. Leuthold, C. Xie, I. Kang, S. Chandrasekhar, P. Bernasconi, C. Doerr, L. Buhl, J. D. Bull, N. A. F. Jaeger, H. Kato, and A. Guest. "6×42.7 Gb/s transmission over ten 200 km EDFA-amplified SSMF spans using polarization-alternating RZ-DPSK", in *Technical Digest Optical Fiber Communication Conference, OFC'04,* Los Angeles, California, U.S.A., Paper PDP35, February 2004.

[54] J.-X. Cai, D. G. Foursa, L. Liu, C. R. Davidson, Y. Cai, W. W. Patterson, A. J. Lucero, B. Bakhshi, G. Mohs, P. C. Corbett, V. Gupta, W. Anderson, M. Vaa, G. Domagala, M. Mazurczyk, H. Li, M. Nissov, A. N. Pilipetskii, and N. S. Bergano. "RZ-DPSK field trial over 13,100 km of installed non slope-matched submarine fibers", in *Technical Digest Optical Fiber Communication Conference, OFC'04,* Los Angeles, California, U.S.A., Paper PDP34, February 2004.

[55] R. Vodhanel, A. Elrefaie, R. Wagner, M. Iqbal, J. Gimlett, and S. Tsuji. "Ten-to-twenty gigabit-per-second modulation performance of 1.5 μm distributed feedback lasers for frequency-shift-keying systems", *Journal of Lightwave Technology*, vol. 7, no. 10, pp. 1454–1460, November 1989.

[56] S. Yoshida and K. Iwashita. "Influence of intensity modulation produced by LD direct modulation on transmission characteristics of CPFSK differential detection system", *Journal of Lightwave Technology*, vol. 10, no. 2, pp. 255–264, February 1992.

[57] U. Fischer. "10 Gbit/s transmission over 69 km of non-dispersion-shifted singlemode fibre with CPFSK direct modulation of 1.55 μm BH DFB laser", *Electronics Letters*, vol. 28, no. 14, pp. 1305–1306, July 1992.

[58] B. Wedding, R. Jung, C. Haslach, and H. Söhnle. "10.7 Gbit/s FSK transmission with 61 dB power budget", in *Proceedings European Conference on Optical Communication, ECOC'03,* Rimini, Italy, vol. 4, pp. 916–917, Paper Th1.5.5, September 2003.

[59] W. Idler, A. Klekamp, R. Dischler, and B. Wedding. "Advantages of frequency shift keying in 10 Gb/s systems", in *IEEE/LEOS 2004 Workshop on Advanced Modulation Formats,* San Francisco, California, U.S.A, pp. 51–52, Paper ThFD3, July 2004.

[60] S. Benedetto and P. Poggiolini. "Performance evaluation of polarisation shift keying modualtion schemes", *Electronics Letters*, vol. 26, no. 4, pp. 256–258, February 1990.

[61] S. Benedetto, R. Gaudino, and P. Poggiolini. "Direct detection of optical digital transmission based on polarization shift keying modulation", *IEEE Journal on Selected Areas in Communications*, vol. 13, no. 3, pp. 531–542, April 1995.

[62] S. Benedetto, R. Gaudino, and P. Poggiolini. "Polarization recovery in optical polarization shift-keying systems", *IEEE Transactions on Communications*, vol. 45, no. 10, pp. 1269–1279, October 1997.

[63] A. Carena, V. Curri, R. Gaudino, N. Greco, P. Poggiolini, and S. Benedetto. "Polarization modulation in ultra-long haul transmission systems: a promising alternative to intensity modulation", in *Proceedings European Conference on Optical Communication, ECOC'98,* Madrid, Spain, pp. 429–430, Paper WdA24, September 1998.

[64] A. S. Siddiqui, S. G. Edirisinghe, J. J. Lepley, J. G. Ellison, and S. D. Walker. "Dispersion-tolerant transmission using a duobinary polarization-shift keying transmission scheme", *IEEE Photonics Technology Letters*, vol. 14, no. 2, pp. 158–160, February 2002.

[65] S. G. Edirisinghe, J. J. Lepley, and A. S. Siddiqui. "Polarization shaped duobinary transmission scheme", *IEEE Photonics Technology Letters*, vol. 13, no. 11, pp. 1245–1247, November 2001.

Chapter 3

Dispersion Management and Pulse Width Optimisation for 10 Gbit/s OOK Systems

3.1 Introduction

In Chapter 2 we saw that chromatic dispersion could be compensated for by using e.g. dispersion compensating fibre (DCF). In a completely linear system, dispersion compensation could be achieved by only compensating at the receiver. However, in a system with non-negligible nonlinearities and in-line erbium doped fibre amplifiers (EDFAs), the dispersion compensation is more complicated. The dispersion is normally compensated on a span-by-span basis, and the optimum dispersion compensation might deviate from 100% under certain conditions [1, 2].

Traditionally, DCFs have been placed on a fibre spool in the amplifier station. Recently, new DCF designs have been introduced—inverse dispersion fibre (IDF) [3] or reverse dispersion fibre (RDF) [4]—which enable cabled compensation of the dispersion and dispersion slope of single mode fibre (SMF) with various SMF to DCF length ratios. Such IDFs have been used several recent high capacity wavelength division multiplexing (WDM) [5–7] and optical time division multiplexing (OTDM) [8, 9] experiments. The value of dispersion ranges from about -100 ps/nm/km for conventional DCF to -17 to -55 ps/nm/km for IDF [10].

These new fibre types introduce new possibilities in system design, as the DCF now can be used as transmission fibre. This reduces the overall span loss. Furthermore, valuable space is freed up at the amplifier station since there is no longer need for bulky fibre spools. However, when the dispersion compensating fibre design is changed from conventional DCF to IDF, the intrinsic properties of the fibre (attenuation and nonlinear coefficient) as well as its position with respect to the optical amplifiers in the link will be changed. A consequence is that, due to nonlinear effects, it is not intuitively clear which type of dispersion compensating fibre performs the best for a given system.

Since the mid 1990's, there has been a strong debate on whether return-to-zero (RZ) or non return-to-zero (NRZ) waveform is the optimum for on-off keying (OOK) modulation formats (see e.g. [11–23]). Various bit rates, dispersion compensation schemes, span lengths, power levels and transmission distances have been investigated, with varying conclusions. There seems to be no clear answer that one is better than the other—a careful investigation based on the actual system design might be necessary. It is, however, clear that the use of RZ signalling results in an improved receiver sensitivity [24]. Normally about 2 dB improvement is obtained for optical communication systems, compared to NRZ [25].

This chapter presents a systematic investigation of optimum dispersion management and NRZ/RZ pulse widths for single-channel 10 Gbit/s optical communication systems using both conventional and novel dispersion compensating fibres [26]. By combining the study of dispersion management and modulation format, the results are more general than previous work varying *either* of the two. We study 10 Gbit/s NRZ and RZ OOK modulation with pulse widths of 100% (NRZ), 50%, 10% and 5% of the bit slot. Four different dispersion management strategies are studied, with fibre spans made of SMF + either DCF or one of three IDFs. The results allow us to find the optimum combination of dispersion management and OOK pulse widths. Optimising the signal input power, we find the maximum transmission distance that can be bridged using this system, and thus finding the optimum combination of dispersion management and pulse width.

3.2 Dispersion Management

When the DCF is placed on a fibre spool in the amplifier station, it does not contribute to the transmission length. When using a DCF this way, the ratio between the dispersion and the attenuation, referred to as figure of merit (FOM), should be as high as possible to minimise the fibre length and thus the loss.[1] The highest FOMs are obtained by having a large negative dispersion, and conventional DCF normally have dispersion of around -100 ps/nm/km [27].

However, with recent progress in fibre manufacturing, dispersion compensating fibres can now be cabled with good performance, and thus be used as transmission fibre [10, 28]. This opens up the door to novel dispersion compensation design, and reduces the span loss as the total fibre length is reduced. However, this does of course make the optimisation process more complicated, as the DCFs with high FOM is not necessary optimum.

Here, we consider a dispersion management scheme where the dispersion is fully compensated after each span. Standard single mode fibre with dispersion of 17 ps/nm/km at a wavelength of 1550 nm is used as the main transmission fibre, and is followed by a length of negative dispersion fibre—DCF or IDF—to compensate the dispersion. The fibre lengths are chosen such that the sum of the length of the SMF and DCF/IDF equal the span length of 80 km and the dispersion is fully compensated. As the dispersion compensating fibre is placed after the main transmission fibre and fully compensates for the dispersion in each span, these spans are referred to as 100% post-compensated spans.

We study four different dispersion compensation schemes, conventional DCF and three IDFs, with dispersion values of -100, -54, -40 and -17 ps/nm/km at 1550 nm, respectively. The IDFs are referred to as IDF$\times n$ where $n = \{1, 2, 3\}$ is the SMF to IDF length ratio. For the remainder of this chapter, DCF with a dispersion of -100 ps/nm/km at 1550 nm will be referred to as *conventional DCF*. When speaking about *dispersion compensating fibres* in general, the term *DCF* will be used.

Plotting the attenuation and nonlinear coefficient versus dispersion as in Figure 3.1, it can be seen that when the absolute value of the dispersion is reduced from conventional DCF to IDF values, both attenuation and

[1] The figure of merit is defined as FOM $= -\frac{D_{DCF}}{\alpha_{DCF}}$ [27].

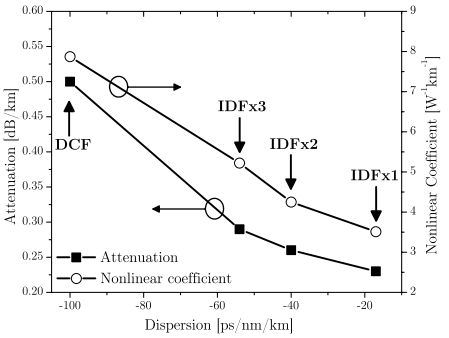

Figure 3.1: Attenuation and nonlinear coefficient as a function of dispersion parameter for conventional DCF and IDF×n. Fibre parameters are also listed in Table 3.1.

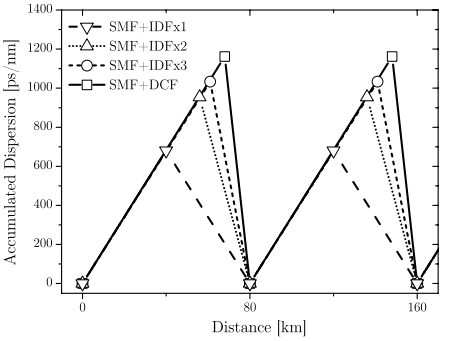

Figure 3.2: Illustration of the studied dispersion compensation schemes using conventional DCF or IDF×n, showing accumulated dispersion versus distance.

nonlinear coefficient[2] are significantly reduced. This is beneficiary in terms of reduced span loss and nonlinear signal degradation.

The accumulated dispersion versus distance is plotted in Figure 3.2 to illustrate the differences between the schemes. One length of conventional DCF compensates for about 6 lengths of SMF. IDF×1, on the other hand, compensates for only one length of SMF. We see from Figure 3.2 that when going from conventional DCF towards IDF×1, the maximum accumulated dispersion is reduced and the length of SMF is reduced.

When the length of SMF before the DCF is decreased, the power level at the output of the SMF will increase. Additionally, the pulses will be less dispersed, resulting in even higher peak power. So even though the nonlinear coefficient of the IDFs is decreased, it is not intuitively clear how the effect is on the system performance. A trade-off has to be found between increased input power and decreased nonlinear coefficient, resulting in an optimal dispersion map. This optimisation requires a full study taking nonlinear signal propagation into account.

[2]The nonlinear coefficient is defined as $\gamma = \frac{2\pi}{\lambda}\frac{n_2}{A_{\text{eff}}}$ where n_2 is the nonlinear refractive index, A_{eff} is the effective area of the fibre and λ is the wavelength [29].

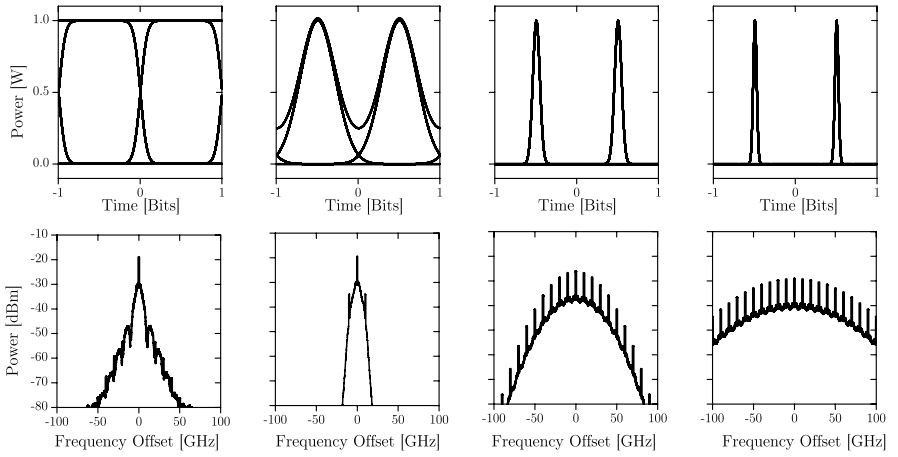

(a) NRZ (b) RZ 50% (c) RZ 10% (d) RZ 5%

Figure 3.3: Optical eye diagrams of 10 Gbit/s NRZ and RZ signals having the same peak power (top), and optical power spectrum (resolution bandwidth of 1.0 GHz) having the same average power (bottom).

3.3 Modulation Format Pulse Width

Four pulse widths are studied here, ranging from 100% to 5% of the time slot. The case of 100% pulse width corresponds to NRZ. The three RZ pulse widths studied here—50%, 10%, and 5%— are referred to as RZ 50%, RZ 10% and RZ 5%, respectively.

The eye diagrams and power spectra of the studied signals are compared in Figure 3.3, clearly illustrating that as the pulse width is decreased, the spectral width is increased. It is apparent that for the case of 5 and 10% pulse widths there is no inter-symbol interference (ISI), whereas the pulse shape of RZ 50% and NRZ clearly depends on the previous and next bit.

These differences in pulse width and spectral width dramatically affect the propagation properties. This is illustrated in Figure 3.4, where the waveforms of a 10 Gbit/s NRZ and RZ 5% have been plotted after transmission over various lengths of SMF. Self phase modulation (SPM) and noise were not included to pinpoint the effect of dispersion. We see that NRZ waveform is well maintained even after transmission over 60 km. Whereas for the RZ 5%, the pulses are completely dispersed, and the peak

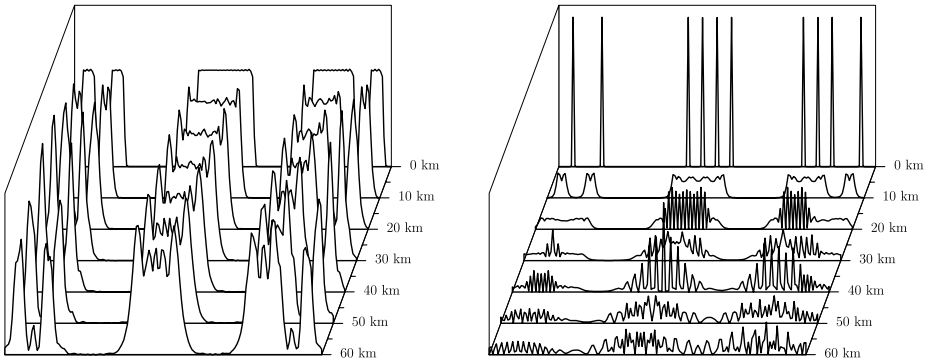

(a) NRZ (b) RZ 5%

Figure 3.4: Propagation of 10 Gbit/s NRZ and RZ 5% signals over SMF. SPM and noise not included to pinpoint the effect of dispersion.

power is lower. The waveform of the narrow RZ pulses is dominated by beating between neighbouring dispersed pulses and is rapidly changing, thus effectively reducing the nonlinear signal degradation.

3.4 Systems Under Investigation

We study a single-channel optical communication system with 100% post-compensated spans, i.e. the DCF is placed after the SMF and perfectly compensate the dispersion of the SMF. It has been shown that using a dispersion compensation ratio slightly lower than 100% can lead to an improved performance due to partial compensation of SPM [1, 2]. However, the exact value of the optimum dispersion compensating ratio depends on many variables such as power level, modulation format and fibre type. Also, since it is often not desirable for practical systems to rely on nonlinear effects, we here only investigate 100% dispersion compensation ratio. It should be noted that the dispersion compensating fibres studied here provide simultaneous 100% dispersion and dispersion slope compensation (i.e. the ratio of the dispersion slope S to the dispersion D is equal for SMF and dispersion compensating fibre [27]).

The simulated systems are shown in Figure 3.5. The signal was generated by modulating light from a continuous wave (CW) laser (for

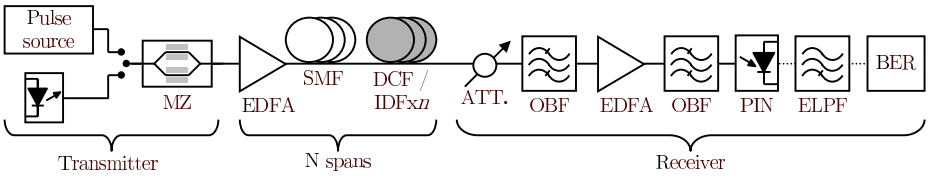

Figure 3.5: System under investigation. A CW or pulsed signal is modulated by a MZ and then transmitted through N spans of SMF + IDF or DCF.
ATT: Optical attenuator, OBF: Optical band-pass filter, PD: Photodiode, ELPF: Electrical low-pass filter, BER: Bit error rate estimation.

NRZ) or a pulse source (for RZ) with a $2^{10} - 1$ bit pseudo random bit sequence (PRBS) at a bit rate of 10 Gbit/s using a chirp-free Mach-Zehnder (MZ) modulator with 30 dB extinction ratio. The electrical data drive signal had a rise-time of 20% of the time slot. The pulse source produced a train of first-order unchirped Gaussian pulses with full width at half maximum (FWHM) of 50, 10 and 5 ps for the RZ 50%, RZ 10% and RZ 5% formats, respectively.

The modulated 10 Gbit/s signals were then transmitted through a number of fibre spans each consisting of an EDFA with 5 dB noise figure and SMF + conventional DCF/IDF$\times n$ as described in Section 3.2. The loss of the fibres in each span was fully compensated by the gain of the EDFA, so that the signal power was kept constant at the input of each span. A splicing loss of 0.25 dB was assumed for each SMF to DCF splice (two per span).

For this study, actual production average values were used for the fibre parameters [10], as presented in Table 3.1. The total fibre span loss is also shown. It is seen that the span loss varies from 18.6 to 16.8 dB for conventional DCF and IDF$\times$2, respectively. This 1.8 dB difference in span loss will have a significant impact on the optical signal to noise ratio (OSNR) after transmission over long distances.

After propagation through the desired number of spans, the signal was fed to a pre-amplified receiver where an EDFA with noise figure equal to 5 dB was positioned between two second order Gaussian optical band-pass filters with 100 GHz FWHM bandwidth. After detection, the electrical signal was filtered with a fourth-order Bessel low-pass filter with 7.5 GHz cut-off frequency. The receiver sensitivity was calculated at the input of the pre-amplifier based on calculation of the bit error rate (BER) using

	D [ps/(nm.km)]	S [ps/(nm^2.km)]	Att. [dB/km]	γ [1/(W.km)]	Span loss [dB]
SMF	17	0.0578	0.180	1.03	–
IDF×1	-17	-0.0578	0.233	3.51	17.0
IDF×2	-40	-0.1360	0.258	4.25	16.8
IDF×3	-54	-0.1836	0.293	5.22	17.1
DCF	-100	-0.3400	0.500	7.87	18.6

Table 3.1: Fibre parameters used in the simulations, and the resulting span loss for SMF+DCF/IDF×n spans.

a Gaussian approximation taking ISI into account [30]. The back-to-back sensitivity at a BER of 1.0×10^{-9} was found to be -37.0 dBm for NRZ, -38.2 dBm with RZ 50%, -39.8 dBm with RZ 10% and -39.3 dBm with RZ 5%. As expected the sensitivity for RZ is around 2 dB better than for NRZ [25]. The sensitivity for RZ 5% is 0.5 dB worse than for RZ 10% due to excessive optical and electrical filtering in the receiver.

The calculation of the field propagation in the fibre was performed using the split-step method [31]. Impairments arising from group-velocity dispersion, nonlinear Kerr effect, amplifier noise and their interactions were considered. The quality of the system was quantified by the 3 dB power penalty limit, i.e. the distance after which the sensitivity at a BER of 1.0×10^{-9} is 3 dB worse than in the back-to-back case. The relative performance of the different dispersion maps was investigated as a function of the modulation format, span length and span input power.

3.5 Transmission Performance

Using the system described in the previous sections, a thorough numerical investigation of the transmission performance of a 10 Gbit/s single-channel system with the studied pulse widths and dispersion compensation schemes was undertaken. SMF input power ranging from -6 to $+5$ dBm were investigated for each modulation format over both the SMF + conventional DCF and SMF + IDF links. We quantified the quality of the signal as the power penalty after transmission, i.e. the difference in receiver sensitivity compared to the back-to-back case.

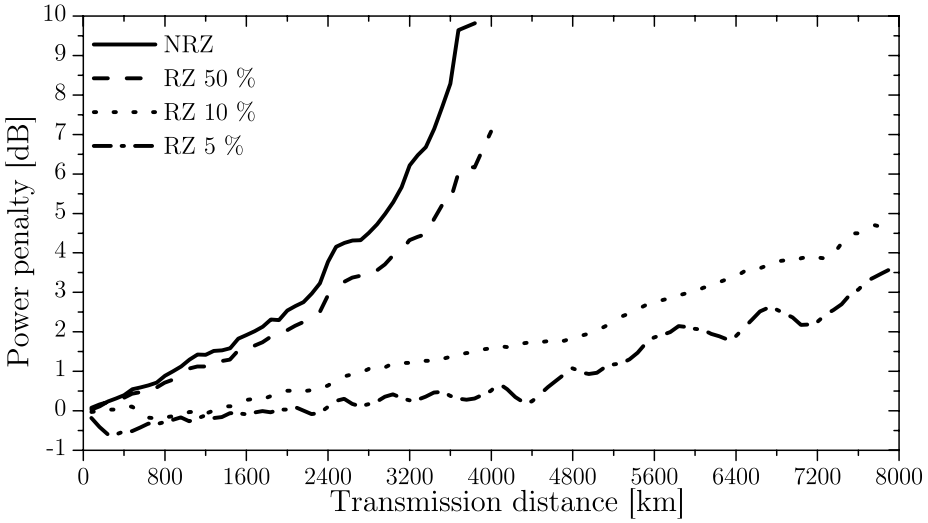

Figure 3.6: Penalty versus distance of 10 Gbit/s NRZ, RZ 50%, RZ 10% and RZ 5% signals after transmission over 80 km SMF+IDF×2 spans. Each point corresponds to the power penalty for the optimum power level at that distance.

In order to simplify the interpretation of the results, it was decided to only show the processed results here.[3] Figure 3.6 shows the power penalty versus distance *at optimum power level at each distance* for the SMF+IDF×2 dispersion map. We see a very clear trend that decreasing the pulse width improves the performance, and that transmission over more than 8000 km is feasible using RZ 10% or RZ 5%. The corresponding curve for the other dispersion maps are included as Figures A.2, A.4, A.6 and A.8 in Appendix A.

The best way to compare the results from this investigation is to look at the 3 dB power penalty limit at different power levels. This gives information about tolerance to low OSNR, nonlinear tolerance, optimum power level and maximum transmission distance. This is illustrated in Figures 3.7 and 3.8, presenting the 3 dB power penalty limit versus signal average input power for the four different types of dispersion compensating fibre, for NRZ and RZ transmission at 10 Gbit/s. The same inform-

[3]For the interested reader, the raw data is included in Figures A.1, A.3, A.5 and A.7 in Appendix A, showing the power penalty versus signal input power for different transmission distances.

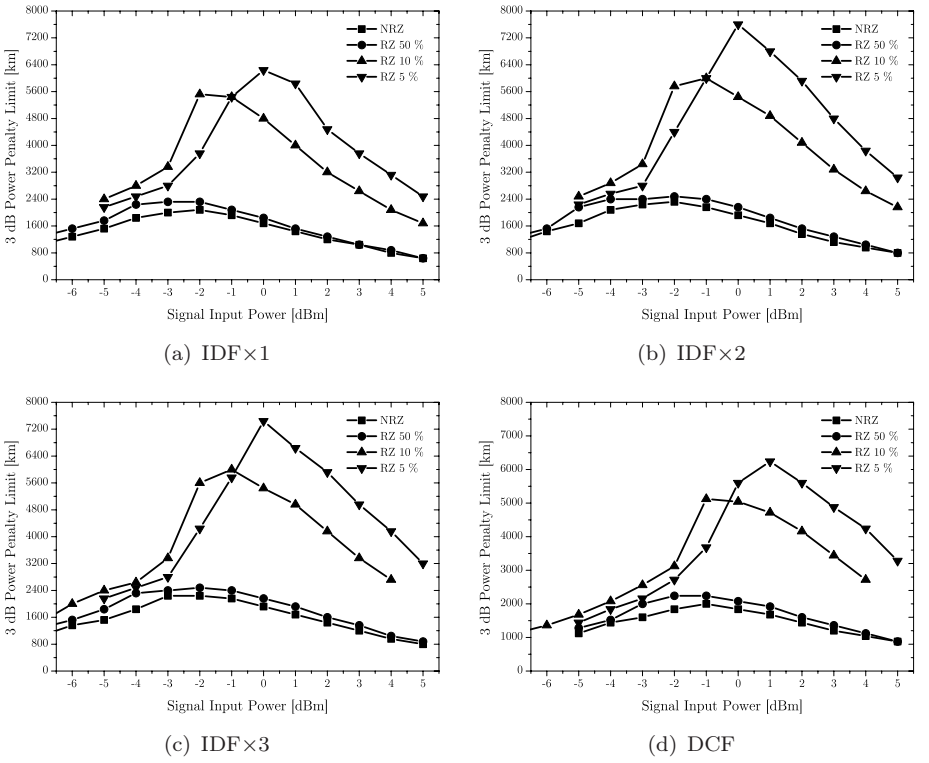

(a) IDF×1 (b) IDF×2

(c) IDF×3 (d) DCF

Figure 3.7: 3 dB power penalty limit as a function of span average input power for single-channel transmission at 10 Gbit/s over 80 km spans made of SMF + IDF×1, IDF×2, IDF×3 or conventional DCF, and using NRZ, RZ 50%, RZ 10% or RZ 5%.

ation is included in both figures, in Figure 3.7 the results are grouped by modulation format to allow easy comparison of the studied fibre spans. Likewise, in Figure 3.8 the results are grouped by fibre types to allow for easy comparison of the studied pulse widths. Finally, the 3 dB power penalty limit at the optimum power level are summarised in Table 3.2 for all the considered pulse widths and dispersion management schemes.

At low powers, the transmission distance is limited by low OSNR and by SPM at higher powers. Thus there exists an optimum power level. However, as the accumulation of degradations from amplified spontaneous emission (ASE) and SPM is quite different, the optimum signal power is not constant with distance.

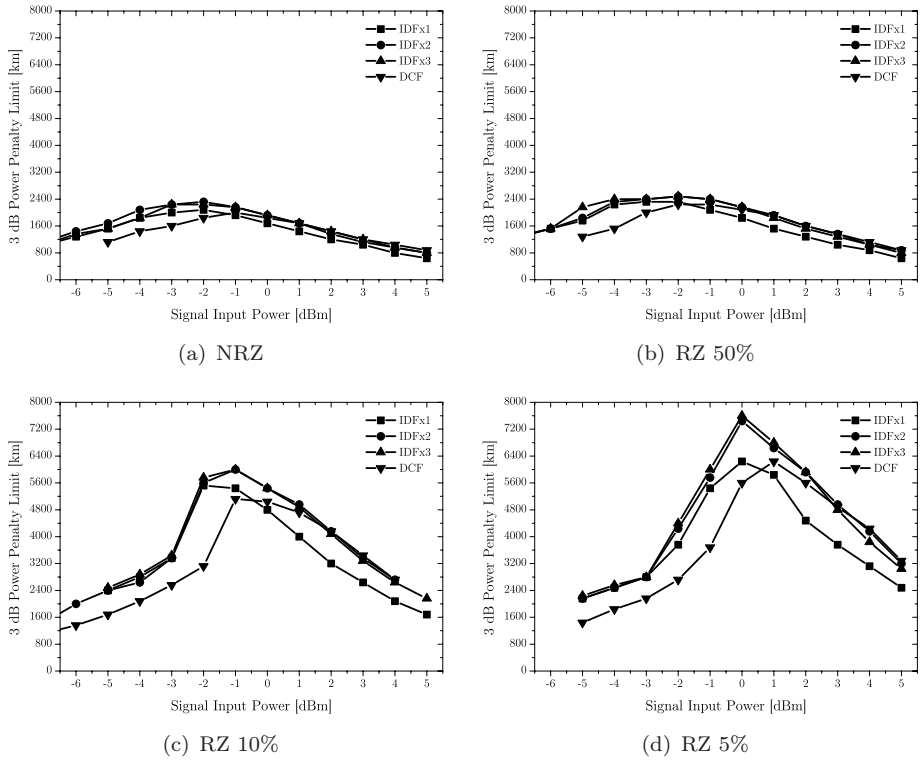

(a) NRZ (b) RZ 50%

(c) RZ 10% (d) RZ 5%

Figure 3.8: 3 dB power penalty limit as a function of span average input power for single-channel transmission at 10 Gbit/s over 80 km spans made of SMF + IDF×1, IDF×2, IDF×3 or conventional DCF, and using NRZ, RZ 50%, RZ 10% or RZ 5%.

At low power, the higher span loss of the SMF + conventional DCF map (18.6 dB, compared to 16.8 dB for SMF + IDF×2) is responsible for a reduced 3 dB transmission distance due to excess noise. For high powers on the other hand, nonlinear degradation results in almost the same distances for all fibres, except for IDF×1, which results in a significantly shorter 3 dB power penalty limit. Due to a shorter SMF length and therefore reduced attenuation and dispersion-induced pulse broadening before the IDF×1, the peak power is significantly higher at the IDF×1 input. Although the IDFs are less nonlinear than the conventional DCF, their closer proximity to the amplifiers make them more vulnerable to

	IDF×1	IDF×2	IDF×3	DCF
NRZ	2080	2320	2240	2000
RZ 50%	2320	2480	2480	2240
RZ 10%	5520	6000	6000	5120
RZ 5%	6240	7600	7440	6240

Table 3.2: Maximum transmission distance in km for 3 dB power penalty at optimum power level.

SPM. We see that IDF×2 or IDF×3 have good—and almost identical—performance for all pulse widths and power levels.

It is seen that the RZ 50% modulation format performs slightly better than NRZ, and that the shorter pulses of RZ 5% allow three times longer 3 dB transmission distance than NRZ. The reason for the improved performance for the short RZ pulses is that, even though they initially have a very high peak power, they will disperse very rapidly due to their broad spectrum. Thus, at the input of the dispersion compensating fibre the pulses are highly dispersed and their peak power is low, reducing the nonlinear degradation [32]. This also explains why the optimum span input power is larger for the RZ 5% than for NRZ and RZ 50%. The power of the shorter pulses can be increased while their nonlinear tolerance remains high. This is in turn beneficial in terms of OSNR, therefore shifting the optimum span input power to higher values.

Figure 3.9 presents the eye diagrams of the signal after transmission over 4000 km using SMF + IDF×2 with −1 dBm span input power. Both electrical and optical signals are shown, and for the optical signal, the noise was disregarded for clarity. The optical signals can be compared to the back-to-back case shown in Figure 3.3. Very strong ISI is apparent for NRZ and RZ 50% resulting from SPM-induced pulse broadening. Both these formats have a power penalty above 10 dB in this case. Significant improvement is seen with the RZ 10% and RZ 5% formats, which pulse shapes are very well maintained. Only slight amplitude and timing jitter is visible.

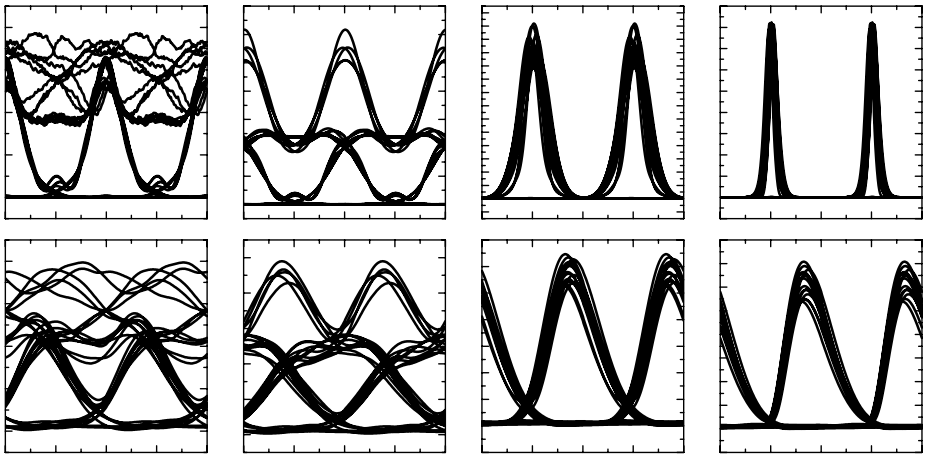

(a) NRZ (b) RZ 50% (c) RZ 10% (d) RZ 5%

Figure 3.9: Eye diagrams of 10 Gbit/s signals after transmission over 4000 km of SMF+IDF×2 using an average span input power of −1 dBm. Top row shows optical eye diagram where the noise has been disregarded, and the bottom row shows the electrical received signal. Vertical scale varies.

3.6 Summary

This chapter has discussed optimum pulse width for NRZ and RZ signals in 10 Gbit/s optical communication systems. We presented a systematic comparison of single-channel transmission performance through dispersion managed 80 km fibre spans based on SMF and conventional DCF or IDF×n.

Dispersion compensation using IDF×2 or IDF×3 provided the longest transmission distance for our system irrespective of the modulation format (RZ or NRZ) or pulse width (5%, 10% or 50%). These fibres offers a good compromise between low loss and low nonlinear signal degradation, resulting in good performance for all power levels. For NRZ and RZ 50% there were only small differences in the performance for the studied dispersion maps. The choice of dispersion map is more critical when using narrow pulse width—the maximum 3 dB power penalty limit is 20% longer when using IDF×2 compared to conventional DCF for RZ 5%.

For the modulation formats, using RZ pulses resulted in significantly improved transmission distances compared to NRZ modulation format.

Short RZ pulses were found to be optimum, and RZ 5% offers three times longer transmission distance than NRZ. Nonlinear effects in the dispersion compensating fibre were significantly reduced when using RZ 5%, due to highly dispersed pulses at the SMF output.

In conclusion, narrow pulse width RZ modulation leads to greatly increased transmission limit for single-channel 10 Gbit/s systems, compared to the traditional NRZ format. Using novel dispersion compensating fibres that can be cabled and used as transmission fibres improves the transmission performance by effectively lowering the span loss. Optimising the dispersion map is especially important when using narrow pulse widths.

References to Chapter 3

[1] C. Peucheret, N. Hanik, R. Freund, L. Molle, and P. Jeppesen. "Optimization of pre- and post-dispersion compensation schemes for 10 Gbits/s NRZ links using standard and dispersion compensating fibers", *IEEE Photonics Technology Letters*, vol. 12, no. 8, pp. 992–994, August 2000.

[2] N. Hanik, A. Ehrhardt, A. Gladisch, C. Peucheret, P. Jeppesen, L. Molle, R. Freund, and C. Caspar. "Extension of all-optical network-transparent domains based on normalized transmission sections", *Journal of Lightwave Technology*, vol. 22, no. 6, pp. 1439–1453, June 2004. doi:10.1109/JLT.2004.830288.

[3] S. N. Knudsen and T. Veng. "Large effective area dispersion compensating fiber for cabled compensation of standard single mode fiber", in *Technical Digest Optical Fiber Communication Conference, OFC'00,* Baltimore, Maryland, U.S.A., vol. 1, pp. 98–100, Paper TuG5, March 2000.

[4] K. Mukasa, Y. Akasaka, Y. Suzuki, and T. Kamiya. "Novel network fiber to manage dispersion at 1.55 μm with combination of 1.3 μm zero dispersion single mode fiber", in *Proceedings European Conference on Optical Communication, ECOC'97,* Edinburgh, Scotland, U.K., vol. 1, pp. 127–130, Paper MO3C.4, September 1997.

[5] J.-X. Cai, M. Nissov, A. N. Pilipetskii, A. J. Lucero, C. R. Davidson, D. Foursa, H. Kidorf, M. A. Mills, R. Menges, P. C. Corbett, D. Sut-

ton, and N. S. Bergano. "2.4 Tb/s (120×20 Gb/s) transmission over transoceanic distance using optimum FEC overhead and 48% spectral efficiency", in *Technical Digest Optical Fiber Communication Conference, OFC'01,* Anaheim, California, U.S.A., Paper PD20, March 2001.

[6] G. Vareille, O. Ait Sab, F. Pitel, and J. F. Marcerou. "Terabit transoceanic system assessment with industrial margins using 25 GHz channel spacing and NRZ format", in *Technical Digest Optical Fiber Communication Conference, OFC'02,* Anaheim, California, U.S.A., pp. 295–296, Paper WP5, March 2002.

[7] J.-X. Cai, D. G. Foursa, C. R. Davidson, Y. Cai, G. Domagala, H. Li, L. Liu, W. W. Patterson, A. N. Pilipetskii, M. Nissov, and N. S. Bergano. "A DWDM Demonstration of 3.73 Tb/s over 11,000 km using 373 RZ-DPSK Channels at 10 Gb/s", in *Technical Digest Optical Fiber Communication Conference, OFC'03,* Atlanta, Georgia, U.S.A., Paper PD22, March 2003.

[8] T. Yamamoto, E. Yoshida, K. R. Tamura, K. Yonenaga, and M. Nakazawa. "640 Gbit/s optical TDM transmission over 92 km through a dispersion-managed fiber consisting of single-mode fiber and "reverse dispersion fiber"", *IEEE Photonics Technology Letters*, vol. 12, no. 3, pp. 353–355, March 2000.

[9] M. Nakazawa, T. Yamamoto, and K. R. Tamura. "1.28 Tbit/s 70 km OTDM transmission using third- and fourth-order simultaneous dispersion compensation with a phase modulator", *Electronics Letters*, vol. 36, no. 24, pp. 2027–2029, November 2000. doi:10.1049/el:20001391.

[10] S. N. Knudsen, M. Ø. Pedersen, and L. Grüner-Nielsen. "Optimisation of dispersion compensating fibres for cabled long-haul applications", *Electronics Letters*, vol. 36, no. 25, pp. 2067–2068, December 2000. doi:10.1049/el:20001445.

[11] D. Breuer, K. Ennser, and K. Petermann. "Comparison of NRZ- and RZ-modulation format for 40 Gbit/s TDM standard-fibre systems", in *Proceedings European Conference on Optical Communica-*

tion, ECOC'96, Oslo, Norway, vol. 2, pp. 199–202, Paper TuD.3.3, September 1996.

[12] K. Ennser and K. Petermann. "Performance of RZ- versus NRZ-transmission on standard single-mode fibers", *IEEE Photonics Technology Letters*, vol. 8, no. 3, pp. 443–445, March 1996.

[13] D. Breuer, K. Petermann, A. Mattheus, and S. K. Turitsyn. "Combatting fibre nonlinearity in symmetrical compensation schemes using RZ-modulation format at 120 km amplifier spacing over standard fibre", in *Proceedings European Conference on Optical Communication, ECOC'97,* Edinburgh, Scotland, U.K., vol. 2, pp. 261–264, September 1997.

[14] D. Breuer and K. Petermann. "Comparison of NRZ- and RZ-modulation format for 40 Gb/s TDM standard-fiber systems", *IEEE Photonics Technology Letters*, vol. 9, no. 3, pp. 398–400, March 1997.

[15] F. Forghieri, P. R. Prucnal, R. W. Tkach, and A. R. Chraplyvy. "RZ versus NRZ in nonlinear WDM systems", *IEEE Photonics Technology Letters*, vol. 9, no. 7, pp. 1035–1037, July 1997.

[16] T. Matsuda, A. Naka, and S. Saito. "Comparison between NRZ and RZ signal formats for in-line amplifier transmission in the zero-dispersion regime", *Journal of Lightwave Technology*, vol. 16, no. 3, pp. 340–348, March 1998.

[17] N. Hanik, A. Gladisch, H.-M. Foisel, C. Caspar, U. Hilbk, F. Schmidt, and E. Schulze. "NRZ/RZ data format transparency of dispersion managed fibre links", in *Proceedings European Conference on Optical Communication, ECOC'99,* Nice, France, vol. 1, pp. 40–41, September 1999.

[18] R. Ludwig, U. Feiste, E. Dietrich, H. G. Weber, D. Breuer, M. Martin, and F. Küppers. "Experimental comparison of 40 Gbit/s RZ and NRZ transmission over standard singlemode fibre", *Electronics Letters*, vol. 35, no. 25, pp. 2216–2218, December 1999. doi:10.1049/el:19991504.

[19] C. Caspar, H.-M. Foisel, A. Gladisch, N. Hanik, F. Küppers, R. Ludwig, A. Mattheus, W. Pieper, B. Strebel, and H. G. Weber. "RZ

versus NRZ modulation format for dispersion compensated SMF-based 10 Gb/s transmission with more than 100 km amplifier spacing", *IEEE Photonics Technology Letters*, vol. 11, no. 4, pp. 481–483, April 1999.

[20] M. Hayee and A. Willner. "NRZ versus RZ in 10–40 Gb/s dispersion-managed WDM transmission systems", *IEEE Photonics Technology Letters*, vol. 11, no. 8, pp. 991–993, August 1999.

[21] C. Fürst, G. Mohs, H. Geiger, and G. Fischer. "Performance limits of nonlinear RZ and NRZ coded transmission at 10 and 40 Gb/s on different fibers", in *Technical Digest Optical Fiber Communication Conference, OFC'00,* Baltimore, Maryland, U.S.A., vol. 2, pp. 302–304, Paper WM31, March 2000.

[22] G. Mohs, C. Fürst, H. Geiger, and G. Fischer. "Advantages of nonlinear RZ over NRZ on 10 Gb/s single-span links", in *Technical Digest Optical Fiber Communication Conference, OFC'00,* Baltimore, Maryland, U.S.A., vol. 4, pp. 35–37, Paper FC2, March 2000.

[23] T. Tokle, C. Peucheret, and P. Jeppesen. "Transmission of 1.8 and 4.8 ps RZ signals at 10 Gbit/s over more than 2700 km of a dispersion managed link made of standard and inverse dispersion fibre", in *Proceedings OptoElectronics and Communications Conference, OECC'01,* Sydney, Australia, pp. 266–267, Paper WA4, July 2001.

[24] S. D. Personick. "Receiver design for optical fiber systems", *Proceedings of the IEEE*, vol. 65, no. 12, pp. 1670–1678, December 1977.

[25] P. J. Winzer and A. Kalmar. "Sensitivity enhancement of optical receivers by impulsive coding", *Journal of Lightwave Technology*, vol. 17, no. 2, pp. 171–177, February 1999.

[26] T. Tokle, C. Peucheret, and P. Jeppesen. "System optimisation of dispersion maps using new cabled dispersion compensating fibers", *Journal of Optical Communication*, vol. 25, no. 2, pp. 75–78, March 2004.

[27] L. Grüner-Nielsen, S. N. Knudsen, B. Edvold, T. Veng, D. Magnussen, C. C. Larsen, and H. Damsgaard. "Dispersion compensating

fibers", *Optical Fiber Technology*, vol. 6, no. 2, pp. 164–180, April 2000. doi:10.1006/ofte.1999.0324.

[28] L. Grüner-Nielsen and S. N. Knudsen. "Cabling of dispersion compensating fibres", in *Proceedings International Wire & Cable Symposium,* Atlantic City, New Jersey, U.S.A., pp. 483–487, November 1999.

[29] G. P. Agrawal. *Fiber-Optic Communciation Systems.* Wiley, Second edition, 1997. ISBN 0-471-17540-4.

[30] C. J. Anderson and J. A. Lyle. "Technique for evaluating system performance using Q in numerical simulations exhibiting intersymbol interference", *Electronics Letters*, vol. 30, no. 1, pp. 71–72, January 1994. doi:10.1049/el:19940045.

[31] G. P. Agrawal. *Nonlinear Fiber Optics.* Academic Press, Second edition, 1995. ISBN 0-12-045142-5.

[32] S.-G. Park, A. H. Gnauck, J. M. Wiesenfeld, and L. D. Garrett. "40 Gb/s transmission over multiple 120 km spans of conventional single-mode fiber using highly dispersed pulses", *IEEE Photonics Technology Letters*, vol. 12, no. 8, pp. 1085–1087, August 2000.

Chapter 4

Novel Modulation Formats for 40 Gbit/s Systems

4.1 Introduction

In recent years several novel modulation formats have been suggested as alternatives to the commonly used non return-to-zero (NRZ) and return-to-zero (RZ). The new formats include carrier suppressed return-to-zero (CS-RZ) [1], single side band return-to-zero (SSB-RZ) [2] and duobinary [3]. These new formats offer various improvements over NRZ or RZ. Due to their narrower spectra, duobinary and SSB-RZ are expected to provide improvements in terms of tolerance to group-velocity dispersion (GVD) and could allow increased spectral efficiency in dense wavelength division multiplexing (WDM) systems, whereas CS-RZ was initially proposed for its resilience to self phase modulation (SPM).

In this chapter, six different modulation formats are compared for single-channel and WDM systems operating at a per channel bit rate of 40 Gbit/s. We compare the transmission performance over a link consisting of single mode fibre (SMF)-based dispersion maps with 80 km fibre spans, with dispersion compensation using either conventional dispersion compensating fibre (DCF) or novel inverse dispersion fibre (IDF×2).

4.2 Modulation Formats

Six different on-off keying (OOK) modulation formats—NRZ, duobinary, RZ 50%, RZ 20%, SSB-RZ and CS-RZ—were studied at a bit rate of 40 Gbit/s. Figure 4.1 shows the schematic of the transmitters for these modulation formats, with the resulting optical eye diagram and power spectrum of the generated signal. Data and clock signal drive levels and Mach-Zehnder (MZ) modulator bias settings are included.

All the modulation formats studied in this chapter are OOK or varieties of OOK. In the simplest form of OOK, the data signal drives the laser directly, such that the laser is on for a logical one, and off for a logical zero (hence the name on-off keying). However, this operation method—known as *direct modulation*—results in a chirped signal, which reduces dispersion tolerance [4]. Additionally, as of today there are no commercially available directly modulated lasers for bit rates above 10 Gbit/s.[1]

The alternative to direct modulation is to use the laser to generate a continuous wave (CW) signal that is modulated using an external modulator—thus referred to as *external modulation*. The most frequently used external modulator is the MZ modulator [4], and all the modulation formats studied in this chapter are generated using one or more MZ modulators.

The basic OOK signal is referred to as non return-to-zero (NRZ), as the power of the signal does not drop to zero between consecutive bits. Many varieties of OOK signals exist, using different pulse widths or additional phase modulation in order to improve the receiver sensitivity, transmission performance or the spectral efficiency. When using a pulse width less than the bit slot, the modulation format is referred to as return-to-zero (RZ), as the intensity returns to zero in every bit. By modifying the phase of the signal, various advantages can be obtained. Both duobinary, CS-RZ and SSB-RZ are OOK modulation formats with additional phase modulation.[2]

However, it is important to remember that the information in *all* OOK signals is still encoded in the same way—the presence of a light pulse

[1] However, in 2003 a 40 Gbit/s NRZ signal generated with a directly modulated laser was experimentally demonstrated [5].

[2] The phase modulation required for these formats can be applied using either a phase modulator, or driving a MZ modulator in a special way, as discussed later in this chapter.

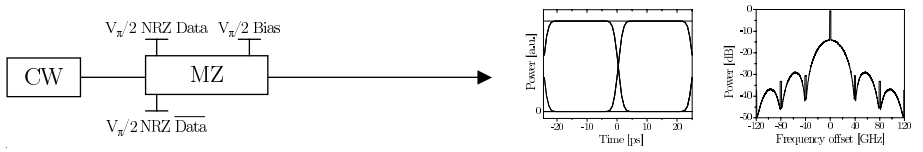

(a) NRZ

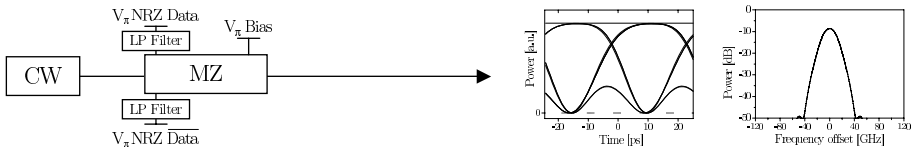

(b) Duobinary

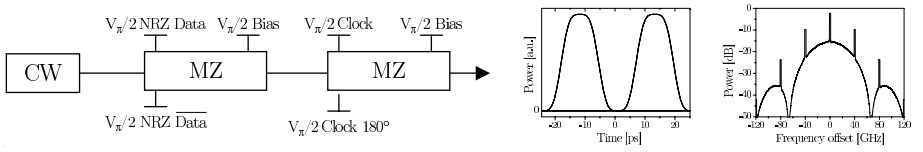

(c) RZ 50%

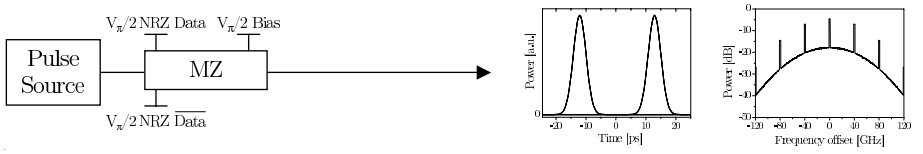

(d) RZ 20%

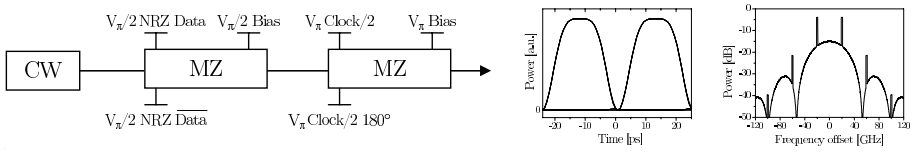

(e) CS-RZ

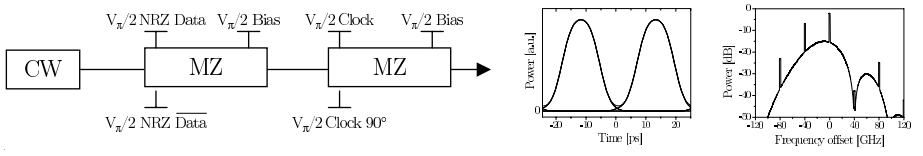

(f) SSB-RZ

Figure 4.1: Details of the transmitter setups of the studied modulation formats, indicating drive voltage and bias setting for the MZ modulators in push-pull configuration. The eye diagrams and optical power spectra (2 GHz resolution bandwidth) of the generated signals are also shown.

represents a logical one, and the absence of a light pulse represents a logical zero.

To illustrate how the information is coded onto the optical carrier for the studied modulation formats, the real part of the electric field of the generated signals versus time is plotted in Figure 4.2. Note that a pulse with amplitude $+1$ and -1 have the same power, but with π relative phase offset.

The following paragraphs introduce the six studied modulation formats.

NRZ

NRZ is the modulation format used in most commercial systems. A NRZ signal is a pure OOK modulation format; zero power is transmitted for a logical zero, and a pulse filling the entire bit slot is transmitted for a logical one.[3]

To generate the NRZ signals studied in this chapter, a CW signal is modulated by a MZ modulator biased at quadrature, as illustrated in Figure 4.1(a). The modulator is assumed to have infinite extinction ratio. An electrical 40 Gbit/s NRZ shaped data signal with a rise/fall time of 5 ps drives the MZ modulator, which is operated in push-pull mode so that a chirp-free optical NRZ signal is obtained. A data signal and an inverted data signal—both with a voltage equal to half the modulator switching voltage V_π—are applied to the two modulator arms. The waveform of the generated NRZ signal is shown in Figure 4.2(a), illustrating the simple coding.

Duobinary

Duobinary modulation [3, 6–9] was initially suggested to increase the tolerance to dispersion. In a duobinary signal, a logical one is coded as a light pulse with either 0 or π phase, and zeros are coded as either absence of a pulse, or a pulse with low intensity depending on the generation method. The phase of the ones is chosen such that there is a π phase-change between strings of ones separated by an odd number of zeros. This phase change helps to reduce the spectral width, and causes the dispersed

[3] Of course in real systems there is always *some* power in the zeros.

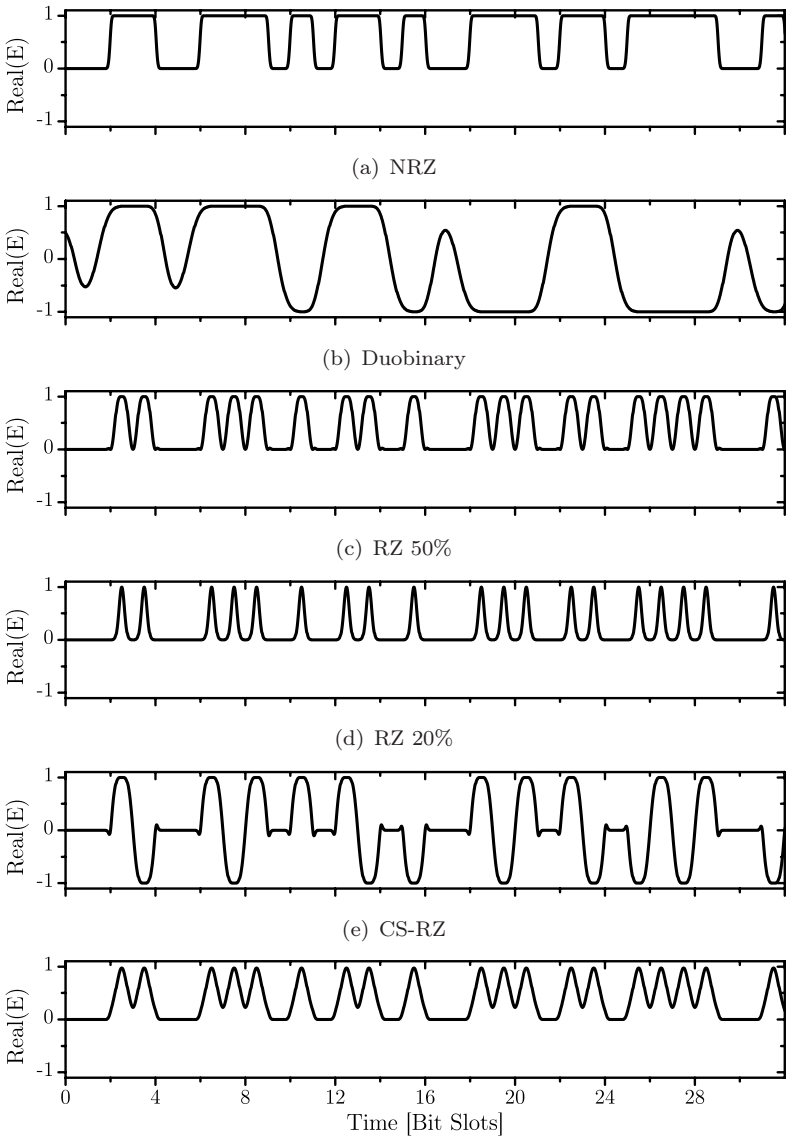

Figure 4.2: Waveforms of the six studied modulation formats, showing the real part of the electric field versus time. The data pattern used for this figure was [0011001110101101001110110111001].

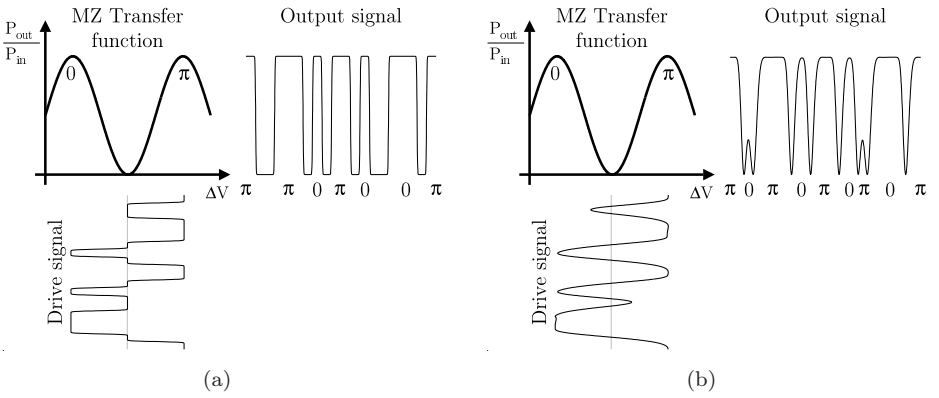

Figure 4.3: Illustration of MZ driving for duobinary generation using a drive signal generated by digital encoding (a) and low-pass filtering (b) for the bit pattern [10011101011010011101].

energy from the blocks of opposite phase to interfere destructively—thus reducing the effect of dispersion.

In order to generate a duobinary signal, a MZ modulator is normally driven with a multi-level data signal. The multilevel signal can either be generated using digital encoding with a dalay and addition circuit, or using a narrow-band electrical low-pass filter [10]. With the digital encoding, the current and the previous bit is added to form a three-level signal. The low-pass filtering relies on the inter-symbol interference (ISI) caused by the narrow filtering to generate a multi-level electrical signal. With this method a logical zero is coded as a pulse with non-zero intensity, and a phase of either 0 or π. Thus, a *four-level* signal is generated with the low-pass filtering method. For both methods, two drive signals each having an amplitude of V_π are used to drive a MZ modulator in the push-pull mode and biased at a null point as illustrated in Figures 4.1(b) and 4.3.

Both these generation methods change the information of the signal, and precoding of data signal at the transmitter is required in order for the received data signal to be equal to the transmitted. The precoding formula for duobinary can be written as [9]

$$p_k = \overline{b_k} \oplus p_{k-1}, \tag{4.1}$$

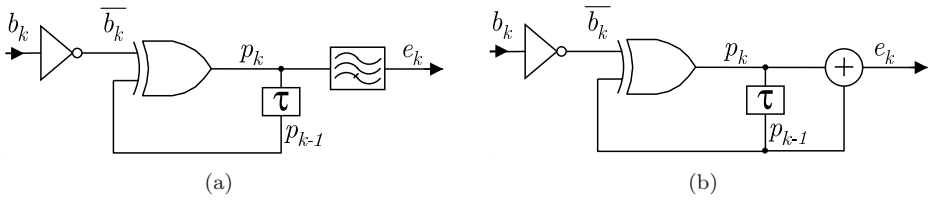

Figure 4.4: Precoding and encoding of a duobinary signal using low-pass filtering (a) and feed-back and addition circuit (b). The delay τ is equal to one bit duration.

where p is the precoded signal, $\overline{b}$ the inverted data signal[4] for bit number k and $\oplus$ represent logical XOR operation. In the case of digital encoding, the encoded signal e can be written as

$$e_k = p_k + p_{k-1} - 1, \tag{4.2}$$

which has values in {-1 0 1}. The -1 term in Eq. 4.2 is normally implemented by simply blocking the DC component of the signal. Figure 4.4 illustrates schematics of duobinary pre- and en-coders for both the digital encoding and low-pass filtering generation methods.

The data signal r after the photodiode in the receiver will simply be

$$r_k = |d_k|, \tag{4.3}$$

and is identical to the transmitted signal b. Table 4.1 illustrates the different digital signals in a duobinary system, for an example bit pattern. It is seen that the received data r is identical to the original data b.

The pre- and en-coder use digital logics that operates at the bit rate, and can be very expensive for high bit rates. By using the low-pass filter method, as illustrated in Figure 4.4(a), the encoder is significantly simplified. As suggested in [11], the pre-coder can be built using *AND* and *Flip-Flop* logics only, simplifying the design from the feed-back implementation illustrated in Figure 4.4. An implementation of this precoding for 40 Gbit/s differential binary phase shift keying (DBPSK) was recently demonstrated in [12].[5]

[4]Here, we assume that the data signal is inverted before pre- and encoding. Alternatively, the received data could be inverted instead, e.g. by using an inverting amplifier in the receiver.

[5]The same precoding is used for duobinary and DBPSK.

b_k	1	0	0	1	1	1	0	1	0	1	1	0
$\overline{b_k}$	0	1	1	0	0	0	1	0	1	0	0	1
p_k	0	1	0	0	0	0	1	1	0	0	0	1
e_k	–	0	0	−1	−1	−1	0	1	0	−1	−1	0
r_k	–	0	0	1	1	1	0	1	0	1	1	0

Table 4.1: Data, pre-coded data and received data at time $t = t_k$ in a duobinary system.

A special case of interest for laboratory experiments is that a differentially precoded pseudo random bit sequence (PRBS) results in a time-shifted version of the same PRBS [9, 13–15]. Thus, the information is maintained, and precoding is not necessary. However, the pattern is inverted, so to receive a non-inverted PRBS at the receiver, an inverted PRBS must be transmitted.

For this work, we used the low-pass filtering generation method. The electrical data signals were filtered with a 5^{th} order Bessel low-pass filter with a 3 dB bandwidth of 11.2 GHz, corresponding to 28% of the bit rate, as illustrated in Figure 4.1(b). The MZ modulator was operated in push-pull mode, biased at a null point and driving signals with a voltage swing equal to V_π applied to each arm.

Plain-RZ

Already in 1977, Personick noted that the receiver sensitivity could be increased by using a pulse width less than the bit period [16]. Normally, a 2 dB advantage is obtained by using RZ, compared to NRZ [17]. The RZ waveform is also known to improve the transmission properties by suppressing non-linear degradation [18–20]. In this chapter, we study two (plain-)RZ modulation formats, with pulse widths of 50 and 20% of the bit slot.[6]

The (plain-)RZ transmitter with 50% pulse width consists of a NRZ transmitter plus a pulse carver, as illustrated in Figure 4.1(c). A MZ modulator driven with a clock signal was used to carve the RZ pulses.

[6]The term (plain-)RZ is used as a general term for RZ signals without phase modulation, in order to distinguish these from CS-RZ and SSB-RZ.

The MZ modulator was biased at quadrature and operated in the push-pull mode with a clock signal having a voltage swing of $V_\pi/2$ to each arm and a frequency equal to the bit rate. Thus, pulses with a full width at half maximum (FWHM) of 50% of the bit slot—12.5 ps for 40 Gbit/s—are generated. This modulation format is thus referred to as RZ 50%.

Another (plain-)RZ modulation format was studied, in which narrower pulse width than RZ 50% was used. As shown in Figure 4.1(d), a pulse source creating a 40 GHz pulse train consisting of first-order Gaussian pulses with a FWHM of 5 ps was used as the input to a NRZ modulation stage. Thus, at the output we get a RZ signal with 5 ps pulse width. The 5 ps corresponds to 20% of the bit slot at 40 Gbit/s, and thus this modulation format is referred to as RZ 20%.

CS-RZ

With the carrier suppressed return-to-zero (CS-RZ) modulation format, suggested by Miyamoto [21], the phase of every other bit is reversed, resulting in a suppression of the carrier frequency. This can be beneficial as the carrier frequency is the component that has the highest power in plain-RZ. By suppressing this carrier, the tolerance to nonlinear effects is expected to improve [1]. At the same time, the spectral width is slightly reduced compared to that of plain-RZ.

Advantages of CS-RZ include the aforementioned increased nonlinear tolerance, and slightly increased dispersion tolerance (compared to plain-RZ). Another advantage is that the optimum value of dispersion compensation is almost constant with increasing fibre power, significantly simplifying link design [22].

A carrier suppressed signal is normally generated by driving a MZ modulator from one peak in the transfer function to another, as illustrated in Figure 4.5. As there is a π phase change associated with crossing the zero point of the MZ transfer function, every other pulse has opposite phase. When driving with a sinusoidal wave, an optical pulse train is generated with twice the frequency of the driving signal. Thus the drive signal should be at a frequency half that of the bit rate. This leads to cost reductions in the MZ modulator and the drive electronics, compared

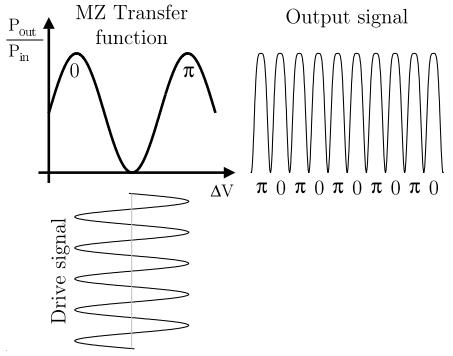

Figure 4.5: Illustration of CS-RZ pulse train generation using a MZ modulator. The drive signal has a frequency equal to half the bit rate, and the generated pulse train has a frequency at the bit rate. There is a π phase change between every consecutive pulse in the generated signal.

to plain-RZ with 50% pulse width.[7] To generate a CS-RZ signal, a NRZ modulator followed by a carrier suppressed modulator is used.

In Miyamoto's original article [21], an electrical generation method was used, where a three-level electrical drive signal was generated from the rising and falling edge of the NRZ data signal. The three levels of the drive signal are then 0 for a logical zero and $\pm V$ for a logical one. This signal is then used to modulate a MZ modulator, converting the levels $\pm V$ into symbols with equal intensity, but with opposite phase. This generation method requires only a single MZ modulator and does not require alignment of the data signal and a clock signal. However, it suffers from signal distortion in the generation of the electrical drive signal and the requirement of electrical pre-coding.

Recently, an alternative CS-RZ generation method using only one MZ modulator was suggested [23]. A three-level drive signal is generated by mixing the NRZ data signal with a clock signal with a frequency equal to half the bit rate. It is also shown in [23] that the dispersion tolerance of such a CS-RZ signal can be improved by narrow low-pass filtering of the three-level electrical drive signal.

[7] However, a plain-RZ signal with 33% pulse width can also be generated with a clock signal at half the bit rate by using the same drive signal as with CS-RZ, and biasing at a maximum transmission point.

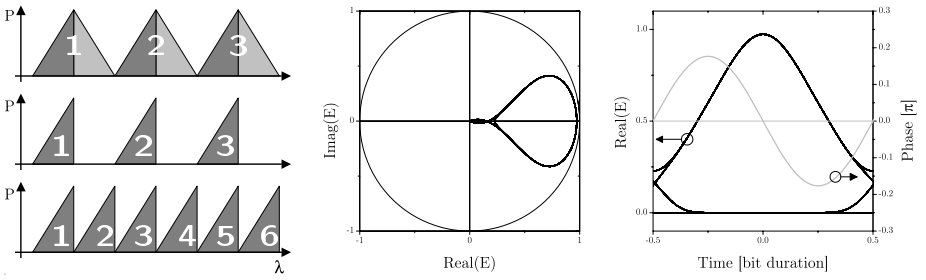

(a) (b) (c)

Figure 4.6: Illustration of how SSB can allow a doubling of the spectral efficiency (a) and illustration of the phase properties, showing the phasar representation (b) and the phase illustrated in the time domain (c).

The investigations in this work were based on the generation method using two MZ modulators. As shown in Figure 4.1(e), an optical 40 Gbit/s NRZ signal is modulated with a second MZ modulator biased at a null point, driven with 20 GHz clock signals and a voltage swing of V_π to each MZ arm.

SSB-RZ

Intensity modulated signals have double side-band spectra that carry the same information in both side-bands. Thus, one of the side-bands can be suppressed, while maintaining the information in the other. Single side band (SSB) signals [24–26] could therefore in theory double the spectral efficiency by allowing closer channel spacing in WDM systems, or increasing the per-channel bit rate for the same spacing. The principle of using SSB to increase the spectral efficiency in a WDM system is illustrated in Figure 4.6(a), where it is seen that removing one of the sidebands allows for doubling the number of channels in the same bandwidth.

There are several different methods to generate SSB signals [26–37]. Details on and comparison of the different generation methods are beyond the scope of this thesis, and the interested reader is referred to e.g. [36,37].

In this work we study single side band return-to-zero (SSB-RZ), and a simple transmitter almost identical to a plain RZ transmitter was used, as described in [35]. As seen in the schematic in Figure 4.1(f), a NRZ signal modulated by a MZ modulator driven with a sinusoidal signal at

a frequency equal to the bit rate and voltage swing equal to $V_\pi/2$ to each modulator arm was used to generate the SSB-RZ signal. The only difference between the SSB-RZ modulator and a plain RZ modulator is that there is a $\pi/2$ phase shift instead of π between the two drive signals, as shown in Figure 4.1. Depending on the sign of the $\pi/2$ phase shift, either the upper or lower side-band signal will be generated.

The output field of the SSB-RZ signal is illustrated in Figure 4.6(b), where the values of the real and imaginary parts of the field are shown. The phase in the time domain is illustrated in Figure 4.6(c), where it is seen that the leading edge of the pulse has a positive chirp, whereas the trailing edge has a negative chirp. The chirp in Figure 4.6(c) is for a SSB-RZ signal where the upper (frequency) side band has been suppressed. If the lower side band was suppressed instead, the chirp would be inverted.

Other modulation formats

On the previous pages the modulation formats studied in this chapter have been presented. The six modulation formats selected for this study are among the most well-known OOK formats. However, many more varieties of other OOK formats have been suggested and investigated, including:

- Chirped RZ [38–40]
- Chirped duobinary [41, 42]
- Duobinary return-to-zero [43]
- Duobinary carrier suppressed return-to-zero [44–46]
- Modified duobinary / alternate mark inversion (AMI) [14, 43, 46–51]

4.3 Receiver Sensitivity

We compare the receiver sensitivity of the studied 40 Gbit/s modulation formats. In the receiver, the signal is first amplified by a pre-amplifier positioned between two 100 GHz first-order Gaussian optical bandpass filters (OBPFs) and, after detection, filtered by a 30 GHz, 4^{th} order Bessel electrical low-pass filter (ELPF). The bit error rate (BER) was estimated assuming Gaussian noise distribution and taking inter-symbol interference

into account [52]. A PRBS with a length of $2^{10} - 1$ bits was used as the data pattern. Detailed simulation parameters are included in Appendix B.

The back-to-back receiver sensitivities at a BER of 1.0×10^{-9} was found to be −29.5 dBm for duobinary, −33.0 dBm for NRZ, −33.8 dBm for SSB-RZ, −34.2 dBm for RZ 50%, −34.3 dBm for CS-RZ and −34.5 dBm for RZ 20%. As expected, the RZ waveforms have a 1–2 dB better sensitivities compared to NRZ, and the best sensitivity is obtained with the narrowest pulses [17]. The sensitivities are summarised in Table 4.2, where also the receiver sensitivities resulting from a non pre-amplified receiver are shown.

For SSB-RZ, the centre frequency of the optical bandpass filter in the receiver must be tuned away from the laser frequency, since the spectrum after suppression of one of the side bands is no longer symmetrical around the carrier frequency. As shown in Figure 4.7, the receiver sensitivity of the SSB-RZ signal is best when the signal and the filter are shifted 14 GHz such that the non suppressed sideband is aligned to the centre of the band-pass filter. However, the sensitivity improvement is small, only 0.12 dB. As discussed in [31, 53], optimising the offset between the centre frequency of the band-pass filter and the laser can enable higher spectral efficiency in SSB-RZ WDM systems.

4.4 Dispersion and SPM Tolerance

We first assessed the dispersion tolerance of the different modulation formats. This was realised by applying a loss-less and linear dispersive element between the transmitter and receiver. A full fibre model was not used, to ensure that other signal degradation mechanisms such as those due to SPM and amplified spontaneous emission (ASE) noise are omitted in the dispersion tolerance evaluation. The resulting plot of receiver sensitivity and power penalty versus accumulated dispersion is shown in Figure 4.8. Duobinary offers the highest dispersion tolerance, with a 1 dB power penalty limit of 440 ps/nm, compared to 65 ps/nm for NRZ, 61 ps/nm for RZ 50%, 50 ps/nm for RZ 20%, 71 ps/nm for CS-RZ and 73 ps/nm for SSB-RZ. These values and those for a receiver without the pre-amplifier are summarised Table 4.2. These results clearly show that the wider spectra of RZ modulated signals result in a reduced dispersion tolerance.

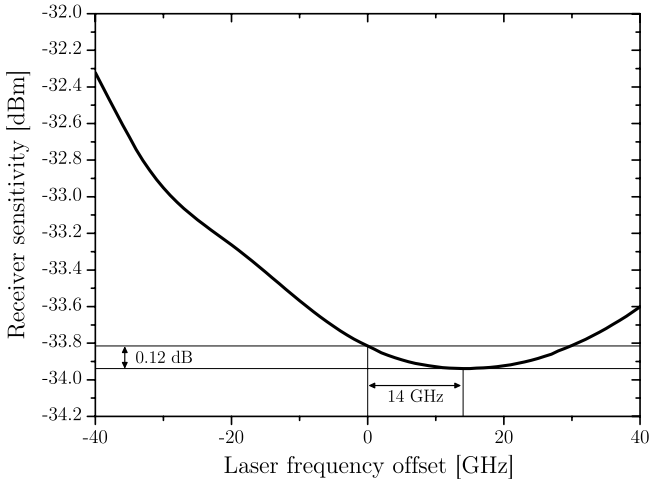

Figure 4.7: Receiver sensitivity as function of the offset between the laser frequency and the optical band-pass filter for a 40 Gbit/s SSB-RZ signal.

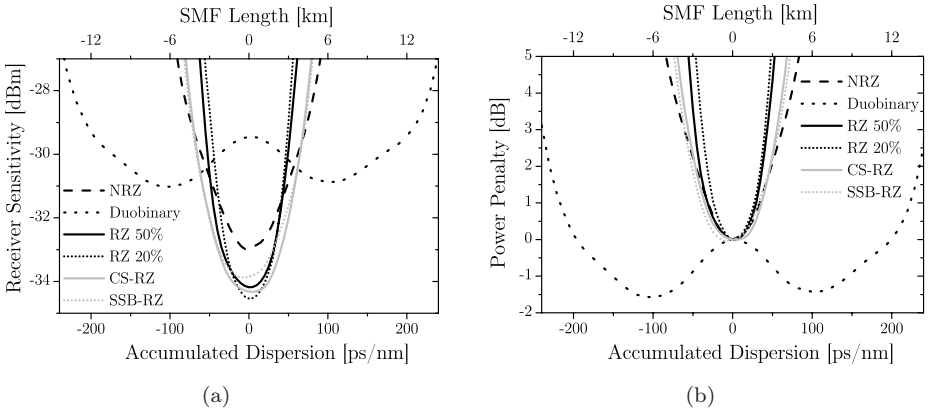

Figure 4.8: Receiver sensitivity (a) and power penalty (b) versus dispersion for the studied 40 Gbit/s modulation formats using a pre-amplified receiver.

	Rec. Sensitivity		Disp. limit		SPM limit	
	pre-amp	no pre-amp	pre-amp	no pre-amp	SMF+DCF	SMF+IDF×2
NRZ	−33.0	−19.6	65	150	11.0	9.4
Duobinary	−29.5	−18.2	440	480	10.1	10.2
RZ 50%	−34.2	−21.5	61	58	13.4	12.8
RZ 20%	−34.5	−22.1	50	44	15.4	14.6
CS-RZ	−34.3	−21.0	71	91	14.1	13.3
SSB-RZ	−33.8	−21.0	73	90	13.2	12.5

Table 4.2: Basic properties of modulation formats at 40 Gbit/s; Receiver sensitivity [dBm] and dispersion limit for a 1 dB power penalty [ps/nm] with and without pre-amplified receiver, and maximum fibre input power [dBm] for a 3 dB SPM power penalty tolerance for both fibre spans (using a pre-amplified receiver).

In order to explain why the tolerance to dispersion is so different, we compare the waveforms and eye diagrams of the 40 Gbit/s optical signals after linear transmission over 3 km SMF in Figure 4.9. We see that while the eye diagram of RZ 5% is completely closed after this distance, the eye diagram of duobinary remains wide open. With RZ 50%, dispersing neighbouring pulses interfere constructively, causing high peaks in between consecutive "ones" resulting in an eye diagram that resembles that of a NRZ signal. With CS-RZ, the π phase change between every bit causes neighbouring pulses to interfere destructively, ensuring that the power level still drops to zero between every bit. SSB-RZ results in improved eye opening compared to RZ 50% due to the reduced spectral width.

The tolerance to SPM was investigated by transmission through one dispersion compensated span comparing the resulting power penalty for various average span input powers. The fibre span consisted of 80 km SMF and 13.6 km DCF or 56 km SMF and 24 km inverse dispersion fibre (IDF)×2 without an erbium doped fibre amplifier (EDFA) after the SMF.[8] Figure 4.10 presents the plot of power penalty versus span input power.[9] The maximum input powers for a 3 dB power penalty are shown in Table 4.2. It can be seen that all the RZ-waveform

[8]Fibre parameters are listed in Table 4.3.

[9]Using a pre-amplified receiver.

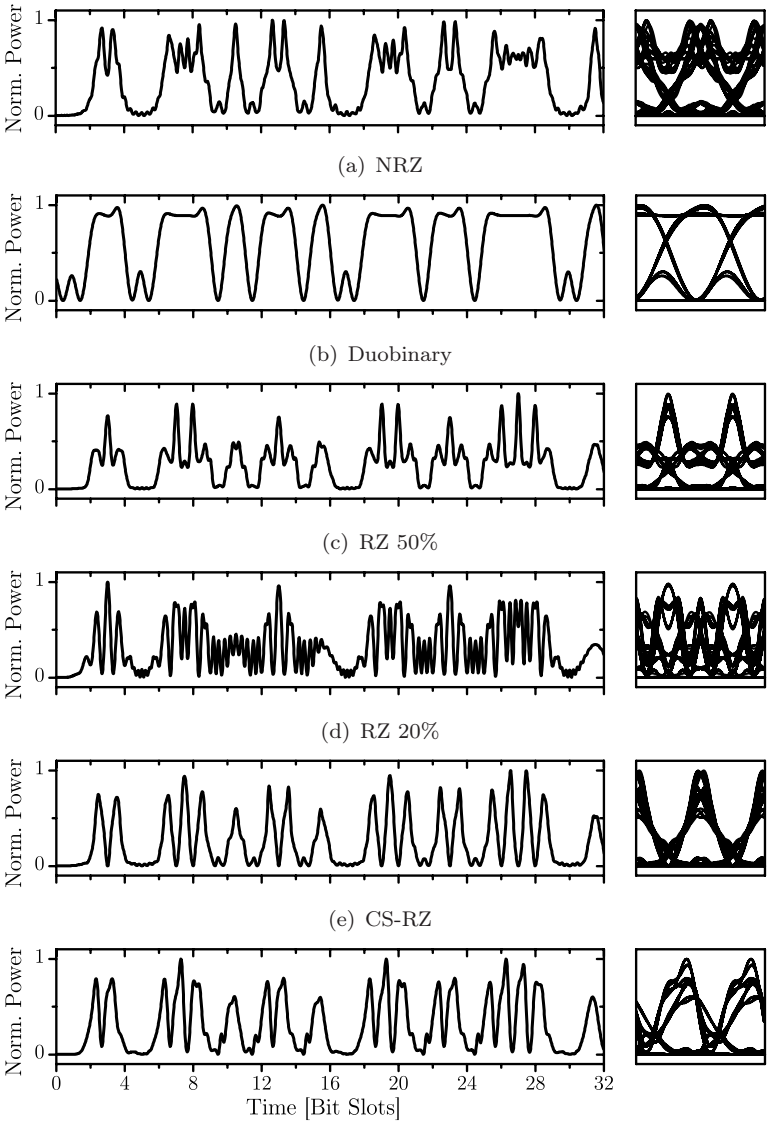

Figure 4.9: Optical waveforms and eye diagrams of the six studied modulation formats at 40 Gbit/s after linear loss-less transmission through 3 km of SMF. The bit pattern [00110011101011010011101101111001] was used for this example.

signals have a higher SPM tolerance than NRZ and duobinary, and that the narrow pulses with RZ 20% results in the highest SPM tolerance.

Using the SMF + DCF span, the 3 dB power penalty limit was 10.1 dBm for duobinary, 11.0 dBm for NRZ, 13.2 dBm for SSB-RZ, 13.4 dBm for RZ 50%, 14.1 dBm for CS-RZ and 15.4 dBm for RZ 20%. However, for a 1 dB power penalty limit, RZ 50% tolerates a higher power than CS-RZ (12.6 and 12.3 dBm, respectively). A similar behaviour was reported in [54]. The RZ waveforms have better tolerance to SPM since the pulses rapidly disperse, leading to reduced peak power. The RZ 20% has the highest SPM tolerance since the narrow pulses, having broader spectra, disperse more rapidly.

Comparing the SPM tolerances when using either DCF or IDF×2, we see that about 1 dB higher tolerance are obtained with the SMF + DCF span. As the length of SMF is 24 km shorter when using SMF + IDF×2, the peak power into the IDF×2 is much higher than into the DCF—due to both less attenuation and pulse broadening in the SMF. So even if the IDF×2 has a lower nonlinear coefficient it results in lower SPM tolerances in this case.

It is interesting to note that there exists a trade-off between dispersion tolerance on one hand and SPM tolerance on the other. The wider spectra signals disperse rapidly, but have very good SPM tolerance. Duobinary offers very good dispersion tolerance, but poor SPM tolerance. CS-RZ seems to offer a compromise with good tolerance to both dispersion and SPM.

4.5 Dispersion maps

In this chapter we compare two SMF based dispersion maps; SMF + conventional dispersion compensating fibre (DCF) and SMF + inverse dispersion fibre (IDF). The conventional DCF has a dispersion of −100 ps/nm/km, and will for the remainder of this chapter simply be referred to as DCF. The IDF we study here has a dispersion of −40 ps/nm/km, and is referred to as IDF×2 since one length of IDF×2 compensates for roughly two lengths of SMF. The fibre spans consist of either 80 km SMF followed by 13.6 km DCF or of 56 km SMF followed by 24 km IDF×2, with fibre parameters as presented in Table 4.3. The IDF×2 can be used for cabled transmission [55], thus the sum of the SMF

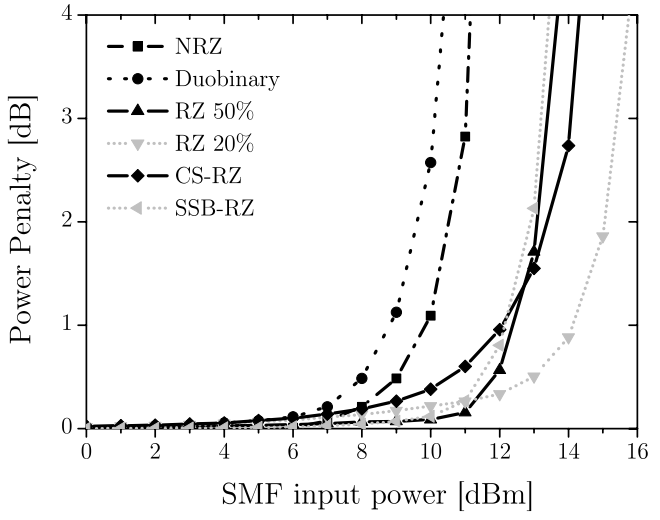

(a) SMF+DCF

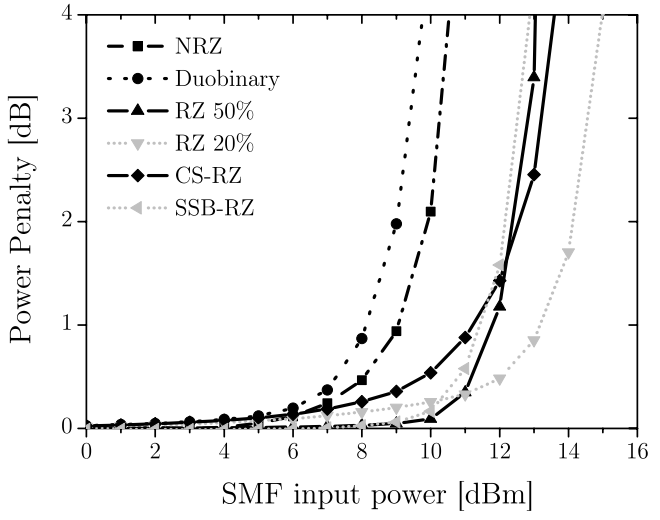

(b) SMF+IDF×2

Figure 4.10: Power penalty versus span input power for the studied 40 Gbit/s modulation formats after propagation through one 80 km SMF+DCF (a) or SMF+IDF×2 (b) fibre span.

	D [ps/nm/km]	S [ps/nm^2/km)]	Att. [dB/km]	A_{eff} [μm^2]	n_2 [m^2/W]	γ [1/W/km]
SMF	17.0	0.0578	0.18	85.0	2.17×10^{-20}	1.03
IDF×2	−40.0	−0.1360	0.26	30.4	3.19×10^{-20}	4.25
DCF	−100.0	−0.3400	0.50	19.0	3.69×10^{-20}	7.87

Table 4.3: Fibre parameters for SMF+DCF and SMF+IDF×2 dispersion maps. The nonlinear coefficient is given as $\gamma = \frac{2\pi}{\lambda}\frac{n_2}{A_{\text{eff}}}$.

and IDF×2 length is equal to the span length. Here, the DCF is assumed to be placed at the amplifier station, so with SMF + DCF the SMF length is equal to the span length.

We limit our investigation to post-compensated spans, where both the dispersion and the dispersion slope are fully compensated. The signal input power to the SMF and DCF/IDF×2 is independently controlled by two EDFAs having a noise figure of 5 dB. The gain of the amplifiers is set so that the signal input power is constant at the input of each span.

The two dispersion maps are compared in Figure 4.11, where the accumulated dispersion versus distance is shown for three periods of the map. We notice that the maximum accumulated dispersion with the SMF + IDF×2 is 30% smaller than compared with the SMF + DCF map. Since the IDF×2 is used as transmission fibre, the transmission distance equals the fibre length in this case. For DCF, the fibre length is 17% longer than the transmission distance. The extra fibre with the SMF + DCF map also results in a higher span loss of 21.2 dB, compared to 16.3 dB with the SMF + IDF×2 map.

4.6 Transmission Performance in 40 Gbit/s Single-Channel Systems

Sections 4.2–4.4 have presented the generation method and basic properties of the six studied modulation formats. In this section, the relative performance of those modulation formats are compared in a 40 Gbit/s single-channel system. WDM systems will be discussed in Section 4.7.

The system under investigation is illustrated in Figure 4.12. Transmit-

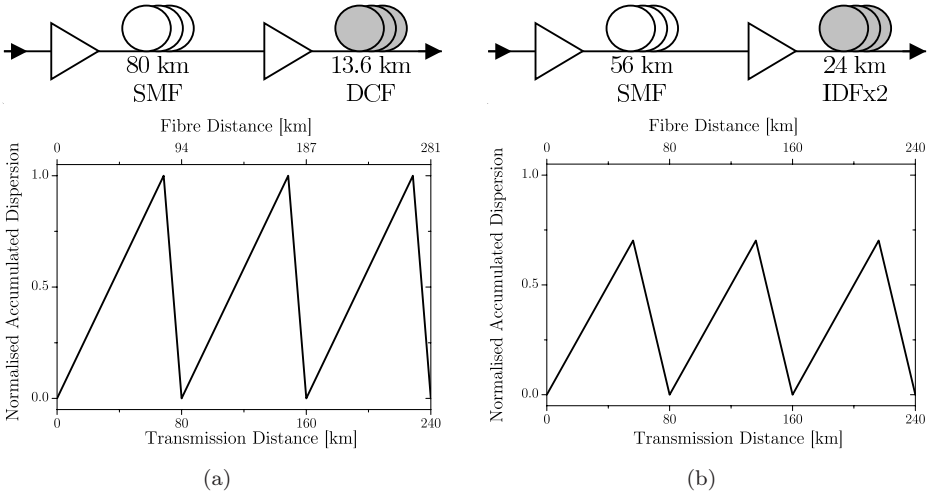

Figure 4.11: Comparisons of three periods of the dispersion maps for SMF+DCF and SMF+IDF×2. The accumulated dispersion is normalised to the maximum accumulated dispersion for the SMF+DCF map.

ters details are illustrated in Figure 4.1 and were discussed in Section 4.2. After the transmitter, the signal was transmitted through a number of concatenated 80 km SMF+DCF or SMF+IDF×2 fibre spans as discussed in Section 4.5.

In the receiver, the signal was amplified by a pre-amplifier positioned between two 100 GHz first-order Gaussian OBPFs and—after detection—filtered by a 30 GHz 4^{th} order Bessel ELPF. The split-step method was used to calculate the propagation in the fibre, taking the non-linear Kerr effect, dispersion, ASE and their interaction into account. To quantify the signal quality, the receiver sensitivity for a BER of 1.0×10^{-9} was calculated after each span by estimating the BER assuming Gaussian noise distribution and taking inter-symbol interference into account [52]. Then the 3 dB limit was found as the maximum transmission distance where the power penalty was less than or equal to 3 dB. A PRBS with a length of $2^{10}-1$ bits was used as data pattern. Further simulation parameter details are included in Appendix B.

In order to make a fair comparison between the different modulation formats, many power levels were investigated, enabling us to find and compare the optimum power level and the maximum transmission dis-

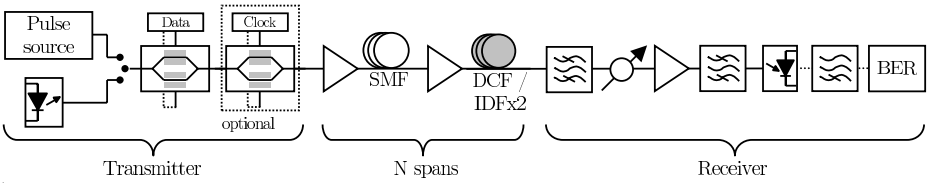

Figure 4.12: Schematic of the optical communication system under investigation. Details of the transmitters for the different modulation formats are presented in Figure 4.1.

	SMF + DCF			SMF + IDF×2		
	P_{SMF}	P_{DCF}	3 dB limit	P_{SMF}	P_{DCF}	3 dB limit
NRZ	−2	−9	720	−4	−9	1040
Duobinary	−2	−9	480	−4	−9	640
RZ 50%	−1	−8	1200	−2	−7	1600
RZ 20%	+2	−7	1360	−1	−7	1600
CS-RZ	−1	−7	1120	−2	−7	1440
SSB-RZ	−1	−8	1120	−2	−7	1440

Table 4.4: Optimum signal input power [dBm] after 800 km, and maximum 3 dB power penalty limit [km].

tance. Average signal input powers between −15 and +12 dBm to the SMF and −15 and +3 dBm to the DCF/IDF×2 were evaluated (in steps of 1 dB). In Figures 4.13 and 4.14, the results are presented as contour plots showing the 3 dB power penalty limit for the different modulation format versus SMF and DCF input power, for SMF + DCF and SMF + IDF×2, respectively. The performance at optimum power level is summarised in Table 4.4, presenting optimum signal input power and maximum transmission distance resulting in a power penalty less than 3 dB.

The straight lines in Figures 4.13 and 4.14 show the input power to the dispersion compensating fibre if no EDFA was used after the SMF. It is seen that this line is far from the optimum point for all combinations of modulation format and fibre type. Without the second EDFA, the 3 dB limit would be about 15 and 30% shorter, for the SMF + IDF×2 and SMF + DCF, respectively.

The optimum signal input power is 1–2 dB higher for the RZ signals

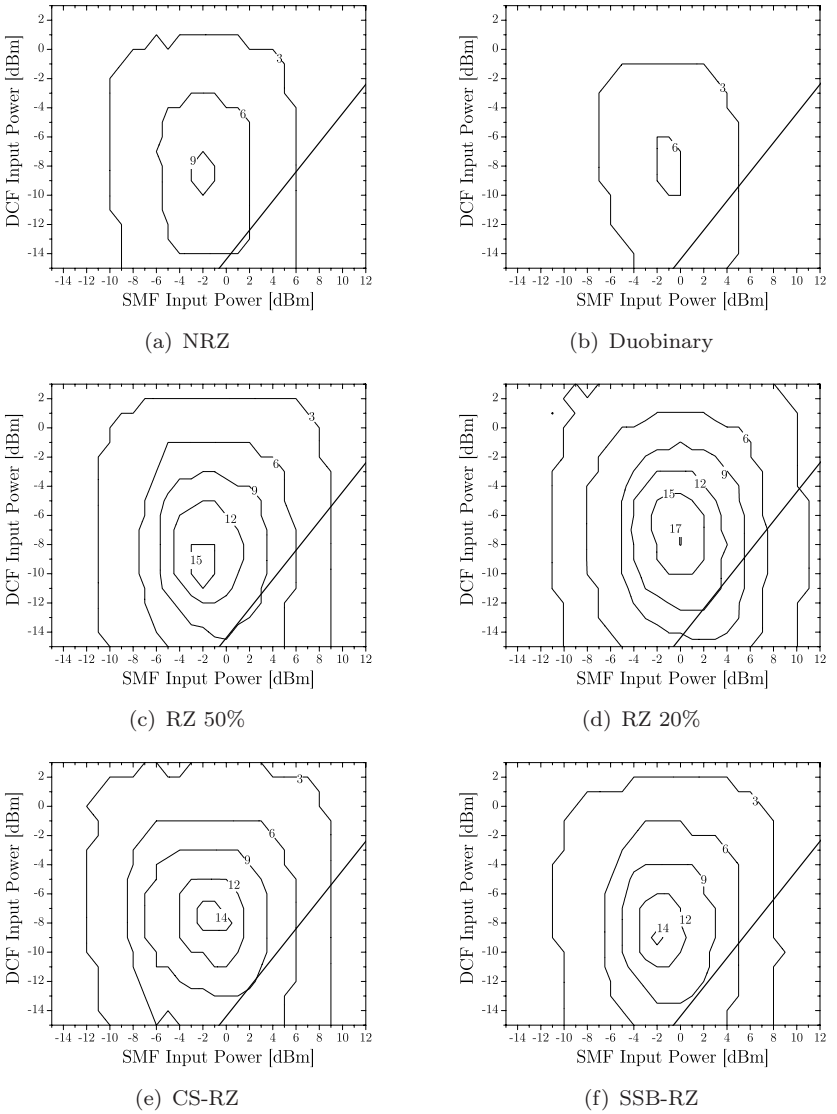

Figure 4.13: Contour plots showing the 3 dB power penalty for transmission through 80 km SMF+DCF fibre spans using various modulation formats at 40 Gbit/s. The number on the contour lines indicate the 3 dB limit in number of spans. The straight line shows the DCF input power if no EDFA was used after the SMF.

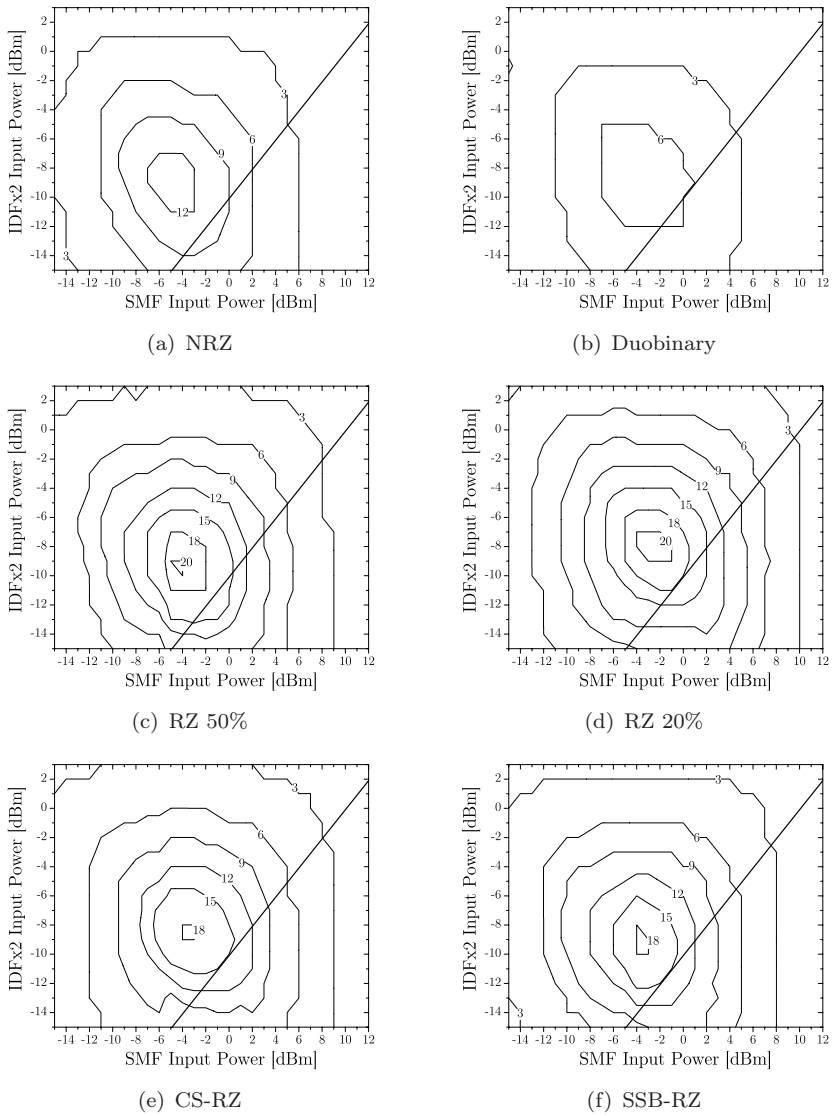

Figure 4.14: Contour plots showing the 3 dB power penalty for transmission through 80 km SMF+IDF×2 fibre spans using various modulation formats at 40 Gbit/s. The number on the contour lines indicate the 3 dB limit in number of spans. The straight line shows the IDF×2 input power if no EDFA was used after the SMF.

than for the NRZ signals, as the RZ signals have a larger tolerance to SPM. For RZ 20%, the optimal signal input power is 3–4 dB higher than for NRZ. This increase in signal power results in significantly improved optical signal to noise ratio (OSNR), allowing longer transmission distance. The maximum 3 dB limit (i.e. the 3 dB limit obtained using the optimum signal input power) is more than 50% longer with RZ 50% compared to NRZ. There are only minor differences between the RZ formats, and CS-RZ and SSB-RZ result in slightly shorter 3 dB limit than plain RZ. Duobinary suffers from low noise tolerance caused by the reduced eye opening due to the ripples in the zero level [56]

Looking at the comparison of the two fibre spans, it is seen from Table 4.4 that the SMF + IDF×2 fibre spans result in 18–44% longer 3 dB limit, depending on the modulation format, compared to SMF + DCF. The improvement is largest for NRZ and duobinary.

Careful comparison of the contour plots in the high-power region shows that the contours of SMF + DCF and SMF + IDF×2 overlap. This is illustrated in Figure 4.15, where the combination of fibre input powers resulting in a power penalty less than 3 dB after transmission over 400 km is shown. It is seen that there is identical performance for the two fibre spans in the high-power region. The investigation of tolerance to SPM after transmission over a single 80 km fibre span presented in Section 4.4, showed that there was more severe signal degradation due to SPM in the SMF + IDF×2 span. However, this was done without amplification between the SMF and DCF/IDF×2. Figure 4.15 clearly shows that for transmission over several spans with optimisation of both the SMF and DCF/IDF×2 input power levels, there is virtually no difference in the nonlinear tolerance. The difference between the two fibre spans is found in the low-power region, where the improved transmission distance of the SMF + IDF×2 span is caused by the 4.9 dB lower span loss. The lower span loss results in larger usable input power range and improved performance at the optimum power level.

In order to compare the accumulation of nonlinear signal degradation for the studied modulation formats in more detail, the power penalty versus distance was calculated when the amplifier noise was disregarded. This is shown in Figure 4.16, for the case of 80 km SMF + DCF spans using average signal input powers of -1 and -7 dBm into the SMF and DCF,

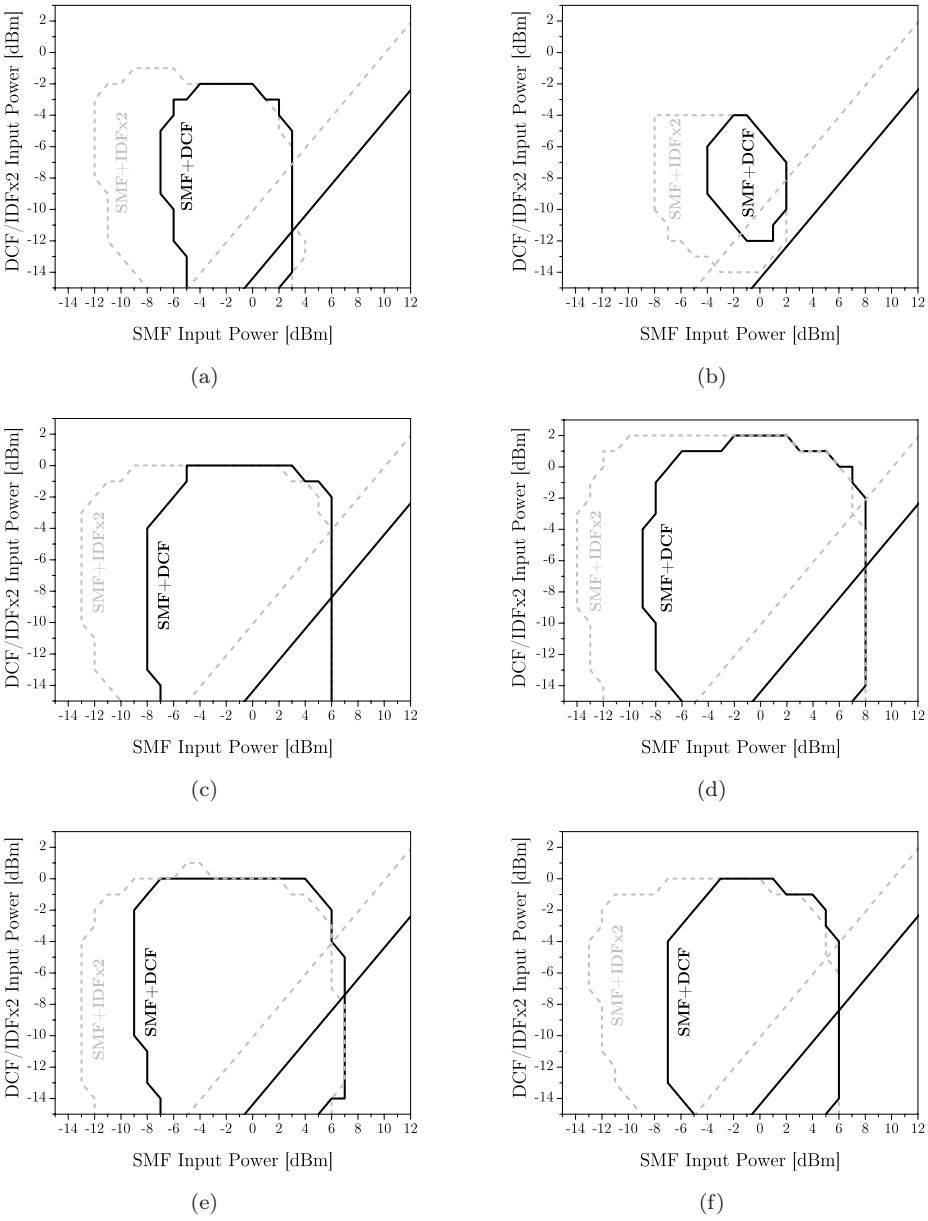

Figure 4.15: Comparison of performance of SMF+DCF (black lines) and SMF+IDF×2 (grey lines), showing input power combinations resulting in a 3 dB limit more than 400 km.

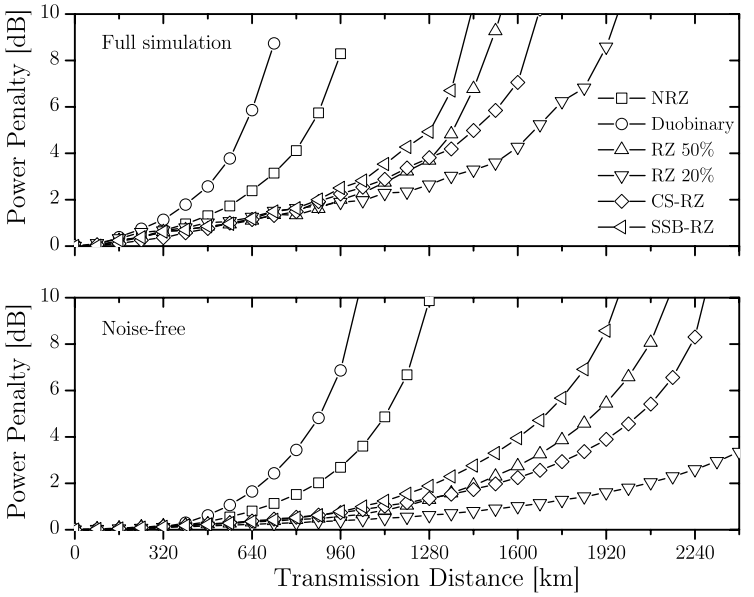

Figure 4.16: Power penalty versus distance for single-channel simulation with both noise and nonlinearities (top), without noise (centre) and without nonlinearities (bottom), using the SMF+DCF fibre span. Span input powers were −1 dBm to the SMF and −7 dBm to the DCF.

respectively.[10] The difference in the 3 dB limit between RZ and NRZ modulation formats would increase in the absence of noise, demonstrating better tolerance towards SPM in multi-span systems with RZ pulse shape. Among the RZ formats, we see that CS-RZ performs slightly better than RZ 50%, and that RZ 20% performs the best, with a significantly longer 3 dB limit. As discussed in Chapter 3, the rapidly dispersing narrow RZ pulses result in low peak power and rapidly changing waveform, which limits the detrimental effects of SPM. The results shown in Figure 4.16 corresponds well to the SPM tolerance results presented in Table 4.2.

[10]Results for the SMF + IDF×2 span show almost identical behaviour, and are included in Figure B.1 in Appendix B.

4.7 Transmission Performance in 40 Gbit/s WDM Systems

The previous section investigated the transmission performance of the six studied modulation formats for single channel 40 Gbit/s optical communication system. This section investigates an 8 channel 40 Gbit/s wavelength division multiplexing system. Using dense channel spacing of 100 GHz, we studied the performance of this WDM system after transmission through the 80 km SMF + DCF and SMF + IDF×2 dispersion compensated spans presented in Section 4.5.

Figure 4.17 presents the setup for the WDM case. The transmitters for the WDM study were identical to the single-channel transmitters discussed previously in this chapter. Eight 40 Gbit/s channels were generated, with a frequency spacing of 100 GHz, corresponding to a spectral efficiency of 0.4 bit/s/Hz. The multiplexer and demultiplexer filter transfer functions were modelled as 100 GHz FWHM second-order Gaussian. A unique bit pattern was used for each channel in order to simulate realistic cross-talk between channels. At the receiver—which was identical to the single-channel case—the receiver sensitivity of all eight channels were calculated. The signal quality of the WDM system was then quantified by the receiver sensitivity of the *worst* channel. Due to statistics of linear and non-linear crosstalk, longer bit patterns of $2^{14} - 1$ bits were used in the WDM system to get accurate BER estimation.[11]

In WDM systems, there are several additional sources of signal degradation compared to single-channel systems. These impairments come from both the multiplexing/demultiplexing and nonlinear impairments in the fibre, such as cross phase modulation (XPM) and four-wave mixing (FWM). We start by investigating the first part of this impairment—the penalty from multiplexing and then demultiplexing (MUX-DMUX penalty)—by comparing the receiver sensitivity after multiplexing and demultiplexing to that of the back-to-back case for the single-channel system. The results are presented in Table 4.5. RZ 20%, which was the

[11]The required bit pattern length was found by running the simulation with many different noise realisations, and comparing the results. The bit pattern length was increased until the different noise realisations resulted in a receiver sensitivity difference less than 0.5 dB. Details on the investigation of required number of bits is included in Appendix B.

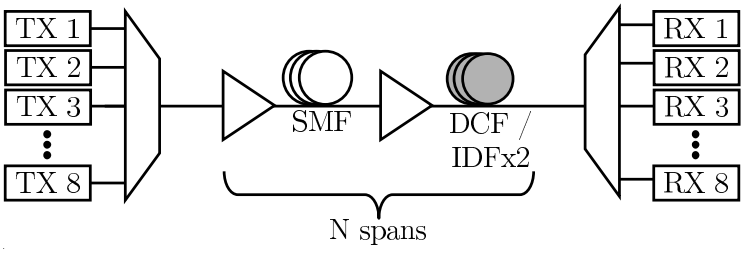

Figure 4.17: Schematic of the WDM system under investigation. Details of the transmitters for the different modulation formats are presented in Figure 4.1.

optimum for the single-channels case, suffers from a 1.8 dB power penalty due to its broad spectrum. For duobinary, a negative power penalty of −0.2 dB is observed, due to improved receiver sensitivity due to optical filtering. Tight optical band-pass filtering of duobinary signals is known to improve the receiver sensitivity—but at the cost of reduced dispersion tolerance [56, 57]. NRZ, CS-RZ and SSB-RZ all have MUX-DMUX penalty less than 0.2 dB.

We also investigated the transmission impairments due to WDM-specific non-linear effects. The signal was transmitted through the same concatenated spans as in the single-channel system. However, due to the very time-consuming simulations, only one power level was investigated for the WDM system, −1 dBm to the SMF and −7 dBm to the DCF/IDF×2.[12] These input powers are close to the optimum input power for the single-channel system. As seen in Table 4.4 the optimum input powers were not identical for the different modulation formats, but for comparison the same power level were used here for all formats. The resulting power penalty versus distance is shown in Figure 4.18 for the case of SMF + DCF spans. Here, the power penalty is defined as the receiver sensitivity of the worst channel in the WDM system compared to the back-to-back receiver sensitivity in the single-channel system. The results for SMF + IDF×2 show identical trends, and are included in Appendix B. In order to simplify the comparison, the 3 dB limits for the different combinations of fibre type and modulation format are shown in Table 4.5. It is seen that CS-RZ and SSB-RZ offer about 20% longer 3 dB limit than

[12]This is the per-channel power level. The total power is 9 dB higher, since there is a total of eight channels.

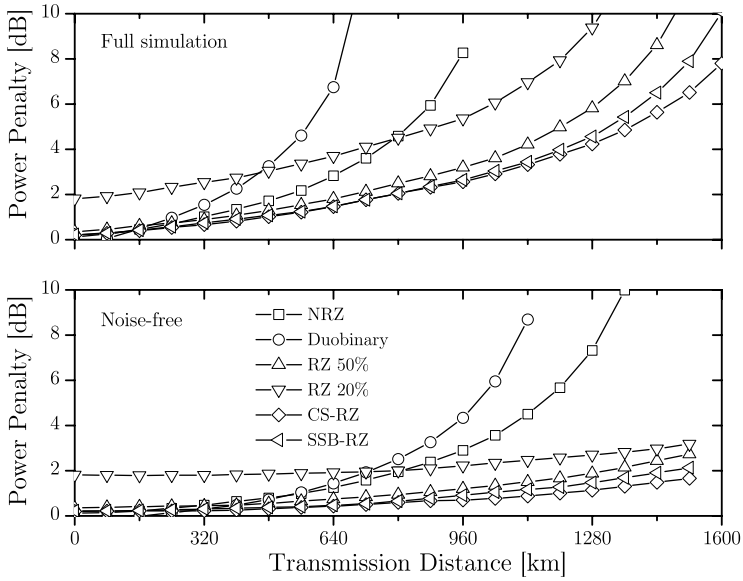

Figure 4.18: Power penalty (for the worst channel) versus distance for simulation of the WDM system when disregarding the optical noise, after transmission over SMF+DCF spans. The per channel span input powers were −1 dBm to the SMF and −7 dBm to the DCF.

RZ 50%, and that CS-RZ is slightly better than SSB-RZ. Duobinary and RZ 20% have a 3 dB limit less than half of CS-RZ. Compared to the single-channel case, it is seen that NRZ, duobinary, CS-RZ and SSB-RZ give very little additional penalty, as the 3 dB limit is no more than 10 % lower than for the single-channel case. The (plain-)RZ formats suffer from significant WDM-specific penalties compared to the single-channel case, due to the band-pass filtering in the MUX and DMUX. Using SMF + IDF×2 results in a 13–60% longer transmission distance than using SMF + DCF, depending on the modulation format—due to the lower span loss. This improvement is about the same as in the single-channel case. Figure 4.18 also shows the power penalty when the noise was excluded from the simulations. As in the single-channel case, this illustrates the good transmission properties of the RZ signals.

	MUX-DMUX	3 dB limit [km]	
	penalty [dB]	SMF+DCF	SMF+IDF×2
NRZ	0.1	640	720
Duo-NRZ	−0.2	400	560
RZ 50%	0.4	880	1040
RZ 20%	1.8	400	640
CS-RZ	0.2	1040	1280
SSB-RZ	0.2	960	1200

Table 4.5: MUX-DMUX power penalty and 3 dB limit (worst channel) for 8-channel 40 Gbit/s WDM system using SMF+DCF or SMF+IDF×2.

4.8 Summary

This chapter has presented an investigation on OOK modulation formats for 40 Gbit/s systems. Promising novel modulation formats—duobinary, RZ 20%, CS-RZ and SSB-RZ—were compared to the commonly used NRZ and RZ 50%.

NRZ and duobinary offer the highest dispersion tolerance, but suffer from reduced tolerance to SPM. On the other hand, RZ waveform signals offer higher SPM tolerance but reduced dispersion tolerance. Thus there exists a tradeoff in the choice of modulation format between high dispersion tolerance and high SPM tolerance.

The six modulation formats have been evaluated in a repeatered 40 Gbit/s dispersion managed system based on 80 km fibre spans. In the single-channel case the plain RZ formats perform the best, and there is only a small additional advantage from using narrower pulses.

CS-RZ and SSB-RZ offer better performance in the 40 Gbit/s WDM system studied here due to low MUX-DMUX penalty compared to plain RZ and low transmission penalty compared to NRZ waveforms. CS-RZ and SSB-RZ offered the best performance in the WDM system, with a small advantage for CS-RZ. RZ formats with narrow pulse width are not suitable for WDM systems due to their large spectral width.

Using SMF + IDF×2 resulted in a 13–60% longer 3 dB power penalty limit compared to SMF + DCF, depending on the modulation format. The nonlinear performance of the two fibre spans were found to be indis-

tinguishable for these systems. SMF + IDF×2 results in better performance due to 4.9 dB lower span loss.

Optimum performance was obtained by using SMF + IDF×2 fibre spans in combination with RZ 20% modulation in the single-channel case, and CS-RZ modulation in the WDM system.

References to Chapter 4

[1] Y. Miyamoto, A. Hirano, K. Yonenaga, A. Sano, H. Toba, K. Murata, and O. Mitomi. "320 Gbit/s (8×40 Gbit/s) WDM transmission over 367 km with 120 km repeater spacing using carrier-suppressed return-to-zero format", *Electronics Letters*, vol. 35, no. 23, pp. 2041–2042, November 1999. doi:10.1049/el:19991373.

[2] M. Sieben, J. Conradi, D. Dodds, B. Davies, and S. Walklin. "10 Gbit/s optical single sideband system", *Electronics Letters*, vol. 33, no. 11, pp. 971–973, May 1997. doi:10.1049/el:19970642.

[3] G. May, A. Solheim, and J. Conradi. "Extended 10 Gb/s fiber transmission distance at 1538 nm using a duobinary receiver", *IEEE Photonics Technology Letters*, vol. 6, no. 5, pp. 648–650, May 1994.

[4] G. P. Agrawal. *Fiber-Optic Communciation Systems.* Wiley, Second edition, 1997. ISBN 0-471-17540-4.

[5] O. Kjebon, M. N. Alum, and R. Schatz. "40 Gb/s transmission experiment using directly modulated 1.55 μm DBR lasers", in *Proceedings International Conference on Indium Phosphide and Related Materials,* Santa Barbara, California, U.S.A., pp. 495–498, Paper FA1.2, May 2003.

[6] A. Lender. "The duobinary technique for high-speed data transmission", *IEEE Transaction on Communication and Electronics*, vol. 82, pp. 214–218, May 1963.

[7] A. Lender. "Correlative digital communication techniques", *IEEE Transactions on Communications*, vol. 12, no. 4, pp. 128–135, December 1964.

[8] A. J. Price and N. Le Mercier. "Reduced bandwidth optical digital intensity modulation with improved chromatic dispersion tolerance", *Electronics Letters*, vol. 31, no. 1, pp. 56–57, January 1995. doi:10.1049/el:19950028.

[9] K. Yonenaga and S. Kuwano. "Dispersion-tolerant optical transmission system using duobinary transmitter and binary receiver", *Journal of Lightwave Technology*, vol. 15, no. 8, pp. 1530–1537, August 1997.

[10] S. Walklin and J. Conradi. "On the relationship between chromatic dispersion and transmitter filter response in duobinary optical communication systems", *IEEE Photonics Technology Letters*, vol. 9, no. 7, pp. 1005–1007, July 1997.

[11] W. Kaiser and W. Rosenkranz. "Simple precoder for high-speed optical duobinary transmission", *Journal of Optical Communication*, vol. 23, no. 1, pp. 26–28, February 2002.

[12] C. Rasmussen, T. Fjelde, J. Bennike, F. Liu, S. Dey, B. Mikkelsen, P. Mamyshev, P. Serbe, P. van der Wagt, Y. Akasaka, D. Harris, D. Gapontsev, V. Ivshin, and P. Reeves-Hall. "DWDM 40G transmission over trans-pacific distance (10000 km) using CSRZ-DPSK, enhanced FEC, and all-Raman-amplified 100 km UltraWave fiber spans", *Journal of Lightwave Technology*, vol. 22, no. 1, pp. 203–207, January 2004. doi:10.1109/JLT.2004.824187.

[13] H. Kim, C. X. Yu, and D. T. Neilson. "Demonstration of optical duobinary transmission system using phase modulator and optical filter", *IEEE Photonics Technology Letters*, vol. 14, no. 7, pp. 1010–1012, July 2002.

[14] J. Yu. "Generation of modified duobinary RZ signals by using one single dual-arm $LiNbO_3$ modulator", *IEEE Photonics Technology Letters*, vol. 15, no. 10, pp. 1455–1457, October 2003. doi:10.1109/LPT.2003.818242.

[15] J.-X. Cai, D. G. Foursa, L. Liu, C. R. Davidson, Y. Cai, W. W. Patterson, A. J. Lucero, B. Bakhshi, G. Mohs, P. C. Corbett, V. Gupta,

W. Anderson, M. Vaa, G. Domagala, M. Mazurczyk, H. Li, M. Nissov, A. N. Pilipetskii, and N. S. Bergano. "RZ-DPSK field trial over 13,100 km of installed non slope-matched submarine fibers", in *Technical Digest Optical Fiber Communication Conference, OFC'04,* Los Angeles, California, U.S.A., Paper PDP34, February 2004.

[16] S. D. Personick. "Receiver design for optical fiber systems", *Proceedings of the IEEE*, vol. 65, no. 12, pp. 1670–1678, December 1977.

[17] P. J. Winzer and A. Kalmar. "Sensitivity enhancement of optical receivers by impulsive coding", *Journal of Lightwave Technology*, vol. 17, no. 2, pp. 171–177, February 1999.

[18] C. Caspar, H.-M. Foisel, A. Gladisch, N. Hanik, F. Küppers, R. Ludwig, A. Mattheus, W. Pieper, B. Strebel, and H. G. Weber. "RZ versus NRZ modulation format for dispersion compensated SMF-based 10 Gb/s transmission with more than 100 km amplifier spacing", *IEEE Photonics Technology Letters*, vol. 11, no. 4, pp. 481–483, April 1999.

[19] M. Hayee and A. Willner. "NRZ versus RZ in 10–40 Gb/s dispersion-managed WDM transmission systems", *IEEE Photonics Technology Letters*, vol. 11, no. 8, pp. 991–993, August 1999.

[20] T. Tokle, C. Peucheret, and P. Jeppesen. "Transmission of 1.8 and 4.8 ps RZ signals at 10 Gbit/s over more than 2700 km of a dispersion managed link made of standard and inverse dispersion fibre", in *Proceedings OptoElectronics and Communications Conference, OECC'01,* Sydney, Australia, pp. 266–267, Paper WA4, July 2001.

[21] Y. Miyamoto, K. Yonenaga, and S. Kuwahara. "Dispersion-tolerant RZ signal transmission using baseband differential code and carrier suppressed modulation", in *Proceedings European Conference on Optical Communication, ECOC'98,* Madrid, Spain, vol. 1, pp. 351–352, September 1998.

[22] A. Hirano, Y. Miyamoto, K. Yonenaga, A. Sano, and H. Toba. "40 Gbit/s L-band transmission experiment using SPM-tolerant

carrier-suppressed RZ format", *Electronics Letters*, vol. 35, no. 25, pp. 2213–2215, December 1999. doi:10.1049/el:19991499.

[23] D.-S. Lee, M. S. Lee, Y. J. Wen, and A. Nirmalathas. "Electrically band-limited CSRZ signal with simple generation and large dispersion tolerance for 40 Gb/s WDM transmission systems", *IEEE Photonics Technology Letters*, vol. 15, no. 7, pp. 987–989, July 2003. doi:10.1109/LPT.2003.813389.

[24] G. H. Smith, D. Novak, and Z. Ahmed. "Technique for optical SSB generation to overcome dispersion penalties in fibre-radio systems", *Electronics Letters*, vol. 33, no. 1, pp. 74–75, January 1997. doi:10.1049/el:19970066.

[25] J. Conradi, B. Davies, M. Sieben, D. Dodds, and S. Walklin. "Optical single sideband (OSSB) transmission for dispersion avoidance and electrical dispersion compensation in microwave subcarrier and baseband digital systems", in *Technical Digest Optical Fiber Communication Conference, OFC'97,* Dallas, Texas, U.S.A., pp. 483–486, February 1997.

[26] L. T. Nichols and R. D. Esman. "Single sideband modulation techniques and applications", in *Technical Digest Optical Fiber Communication Conference, OFC'99,* San Diego, California, U.S.A., Paper ThW1, February 1999.

[27] M. Izutsu, S. Shikama, and T. Sueta. "Integrated optical SSB modulator/frequency shifter", *IEEE Journal of Quantum Electronics*, vol. 17, no. 11, pp. 2225–2227, November 1981.

[28] S. Shimotsu, S. Oikawa, T. Saitou, N. Mitsugi, K. Kubodera, T. Kawanishi, and M. Izutsu. "Single side-band modulation performance of a $LiNbO_3$ integrated modulator consisting of four-phase modulator waveguides", *IEEE Photonics Technology Letters*, vol. 13, no. 4, pp. 364–366, April 2001.

[29] P. M. A. Charrua and A. V. T. Cartaxo. "Single sideband demonstration using a four phase-modulator structure", in *IEEE/LEOS 2004 Workshop on Advanced Modulation Formats,* San Francisco, California, U.S.A, pp. 41–42, Paper FC2, July 2004.

[30] W. Idler, G. Charlet, R. Dischler, Y. Frignac, and S. Bigo. "0.8 bit/s/Hz of information spectral density by vestigal sideband filtering of 24.66 Gb/s NRZ", in *Proceedings European Conference on Optical Communication, ECOC'02,* Copenhagen, Denmark, vol. 3, Paper 8.1.5, September 2002.

[31] G. Charlet and S. Bigo. "Spectral reshaping by narrow optical filtering toward high information spectral density 40 Gbit/s transmission", in *IEEE/LEOS 2004 Workshop on Advanced Modulation Formats,* San Francisco, California, U.S.A, pp. 35–36, Paper FB2, July 2004.

[32] K. Tanaka, K. Takano, K. Kondo, and K. Nakagawa. "Characteristics of fiber-optic SSB modulation using optical Hilbert transformer", in *Proceedings OptoElectronics and Communications Conference, OECC'01,* Sydney, Australia, pp. 600–601, July 2001.

[33] T. Wuth, W. Kaiser, W. Rosenkranz, G. Mohs, R. Neuhauser, and C. Glingener. "200 km repeaterless 10 Gb/s transmission on standard single-mode fiber with single-sideband (SSB) modulation and Raman amplification", in *Proceedings OptoElectronics and Communications Conference, OECC'01,* Sydney, Australia, pp. 8–9, July 2001.

[34] M. Sieben, J. Conradi, and D. Dodds. "Optical single sideband transmission at 10 Gb/s using only electrical dispersion compensation", *Journal of Lightwave Technology*, vol. 17, no. 10, pp. 1742–1749, 1999.

[35] A. Hodžić, B. Konrad, and K. Petermann. "Alternative modulation formats in N×40 Gb/s WDM standard fiber RZ-transmission systems", *Journal of Lightwave Technology*, vol. 20, no. 4, pp. 598–607, April 2002.

[36] B. Zsigri. *Investigation of single side band transmission in high spectral efficiency optical communication systems.* Master's thesis, Research Center COM, Technical University of Denmark, Kgs. Lyngby, Denmark, October 2002.

[37] B. Zsigri, C. Peucheret, A. Buxens, and P. Jeppesen. "Performance comparison of optical single side band generation techniques", in *Proceedings European Conference on Optical Communication, ECOC'03,* Rimini, Italy, vol. 3, pp. 524–525, Paper We3.5.3, September 2003.

[38] N. S. Bergano, C. R. Davidson, C. J. Chen, B. Pedersen, M. A. Mills, N. Ramanujam, H. D. Kidorf, A. B. Puc, M. D. Levonas, and H. Abdelkader. "640 Gb/s transmission of sixty-four 10 Gb/s WDM channels over 7200 km with 0.33 (bits/s)/Hz spectral efficiency", in *Technical Digest Optical Fiber Communication Conference, OFC'99,* San Diego, California, U.S.A., Paper PD2, February 1999.

[39] E. A. Golovchenko, A. N. Pilipetskii, and N. S. Bergano. "Transmission properties of chirped return-to-zero pulses and nonlinear intersymbol interference in 10 Gb/s WDM transmission", in *Technical Digest Optical Fiber Communication Conference, OFC'00,* Baltimore, Maryland, U.S.A., vol. 3, pp. 38–40, Paper FC3, March 2000.

[40] N. S. Bergano, M. Nissov, A. Pilipetskii, J.-X. Cai, C. Davidson, and B. Bakhshi. "Chirped return-to-zero formats for ultra long-haul fiber communications", in *IEEE/LEOS 2004 Workshop on Advanced Modulation Formats,* San Francisco, California, U.S.A, pp. 1–2, Paper ThA1, July 2004.

[41] M. Wichers, W. Kaiser, T. Wuth, and W. Rosenkranz. "Experimental demonstration of chirped duobinary transmission", *Electronics Letters*, vol. 38, no. 4, pp. 191–193, February 2002. doi:10.1049/el:20020118.

[42] M. Wichers, W. Kaiser, T. Wuth, and W. Rosenkranz. "10 Gb/s chirped duobinary transmission (CDBT) over 277 km of uncompensated standard single mode fibre", in *Proceedings International Conference on Transparent Optical Networks,* Cracow, Poland, Paper We.A.6, April 2002.

[43] K. S. Cheng and J. Conradi. "Reduction of pulse-to-pulse interaction using alternative RZ formats in 40 Gb/s systems", *IEEE Photonics Technology Letters*, vol. 14, no. 1, pp. 98–100, January 2002.

[44] A. Hirano, Y. Miyamoto, K. Yonenaga, S. Kuwahara, H. Miyazawa, K. Murata, K. Sato, and Y. Tada. "SSB direct detection scheme in duobinary-carrier-suppressed RZ transmission", *Electronics Letters*, vol. 38, no. 12, pp. 585–587, June 2002. doi:10.1049/el:20020408.

[45] Y. Miyamoto, K. Yonenaga, A. Hirano, H. Toba, K. Murata, and H. Miyazawa. "Duobinary carrier-suppressed return-to-zero format and its application to 100 GHz-spaced 8×43 Gbit/s DWDM unrepeatered transmission over 163 km", in *Technical Digest Optical Fiber Communication Conference, OFC'01,* Anaheim, California, U.S.A., Paper TuU4, March 2001.

[46] P. M. A. Charrua and A. V. T. Cartaxo. "Performance of AMI-RZ and DCS-RZ single-sideband signals in an 80% spectral-efficient UDWDM ultra long-haul transmission system", in *IEEE/LEOS 2004 Workshop on Advanced Modulation Formats,* San Francisco, California, U.S.A, pp. 43–44, Paper FC3, July 2004.

[47] P. Kabal and S. Pasupathy. "Partial-response signaling", *IEEE Transactions on Communications*, vol. 23, no. 9, pp. 921–934, September 1975.

[48] A. Matsuura, K. Yonenaga, Y. Miyamoto, and H. Toba. "High-speed transmission based on optical modified duobinary signals", *Electronics Letters*, vol. 35, no. 9, pp. 736–737, April 1999. doi:10.1049/el:19990480.

[49] X. Liu, X. Wei, A. H. Gnauck, C. Xu, and L. K. Wickham. "Suppression of intrachannel four-wave-mixing-induced ghost pulses in high-speed transmissions by phase inversion between adjacent marker blocks", *Optics Letters*, vol. 27, no. 13, pp. 1177–1179, July 2002.

[50] X. Wei, A. H. Gnauck, X. Liu, and J. Leuthold. "Nonlinearity tolerance of RZ-AMI format in 42.7 Gbit/s long-haul transmission over standard SMF spans", *Electronics Letters*, vol. 39, no. 20, pp. 1459–1460, October 2003. doi:10.1049/el:20030898.

[51] P. J. Winzer, A. H. Gnauck, G. Raybon, S. Chandrasekhar, Y. Su, and J. Leuthold. "40 Gb/s return-to-zero alternate-mark-inversion (RZ-AMI) transmission over 2000 km", *IEEE Photonics Technology Letters*, vol. 15, no. 5, pp. 766–768, May 2003. doi:10.1109/LPT.2003.809982.

[52] C. J. Anderson and J. A. Lyle. "Technique for evaluating system performance using Q in numerical simulations exhibiting intersymbol

interference", *Electronics Letters*, vol. 30, no. 1, pp. 71–72, January 1994. doi:10.1049/el:19940045.

[53] S. Bigo, W. Idler, J.-C. Antona, G. Charlet, C. Simonneau, M. Gorleir, M. Molina, S. Borne, C. de Barros, P. Sillard, P. Tran, R. Dischler, W. Poehlmann, P. Nouchi, and Y. Frignac. "Transmission of 125 WDM channels at 42.7 Gbit/s (5 Tbit/s capacity) over 12×100 km of TeraLight Ultra fibre", in *Proceedings European Conference on Optical Communication, ECOC'01,* Amsterdam, The Netherlands, vol. 6, pp. 2–3, Paper PD.M.1.1, September 2001.

[54] Y. Akiyama, H. Ooi, T. Takahara, J. C. Rasmussen, and G. Ishikawa. "A comparison of performance in 40 Gbit/s NRZ, RZ, CS-RZ and optical duobinary modulation schemes", in *Proceedings OptoElectronics and Communications Conference, OECC'01,* Sydney, Australia, pp. 176–177, Paper TUI2, July 2001.

[55] S. N. Knudsen, M. Ø. Pedersen, and L. Grüner-Nielsen. "Optimisation of dispersion compensating fibres for cabled long-haul applications", *Electronics Letters*, vol. 36, no. 25, pp. 2067–2068, December 2000. doi:10.1049/el:20001445.

[56] D. Penninckx. "Enhanced-phase-shaped binary transmission", *Electronics Letters*, vol. 36, no. 5, pp. 478–480, March 2000. doi:10.1049/el:20000349.

[57] H. Kim and C. X. Yu. "Optical duobinary transmission system featuring improved receiver sensitivity and reduced optical bandwidth", *IEEE Photonics Technology Letters*, vol. 14, no. 8, pp. 1205–1207, August 2002.

Chapter 5

Dispersion Map Comparison with 160 km Fibre Spans

5.1 Introduction

Chapters 3 and 4 discussed dispersion maps for 10 and 40 Gbit/s systems with fibre span lengths of 80 km. Normally, fibre spans have lengths around 40 km for transoceanic systems and around 80 km for terrestrial systems [1]. Therefore, most work on optimising the dispersion maps has focussed on span lengths less than 80 km.

This chapter presents an experimental investigation of optimum dispersion maps for a 40 Gbit/s system using ultra-long fibre spans of 160 km. Increasing the span length can be an effective way to reduce system cost, as fewer amplifier stations are needed. Unfortunately, in order to maintain a high optical signal to noise ratio (OSNR) the distance between the amplifiers should be as low as possible [2]. Thus, there exists a trade-off between cost on one hand and OSNR of the received signal on the other hand.

In order to partly overcome OSNR degradations associated with long fibre spans, we use a combination of distributed Raman amplification and conventional lumped erbium doped fibre amplifiers (EDFAs) to compensate for the span loss. This approach enables the use of far longer span lengths than when using EDFAs only.

We study a 40 Gbit/s system using return-to-zero (RZ) coding and fibre spans based on non-zero dispersion shifted fibre (NZDSF) and dis-

persion compensating fibre (DCF). Three different dispersion schemes for this span length are compared: pre-compensation (DCF at the start of the span), post-compensation (DCF at the end of the span) and a symmetrical compensation scheme where the DCF is placed at the centre of the span.

Good performance for this 40 Gbit/s system with ultra-long span lengths of 160 km is experimentally demonstrated. Comparing the performance of the three dispersion compensation schemes, we show significant better performance using the symmetrical compensation [3].

5.2 Ultra-long Fibre Spans

Using ultra-long fibre spans can reduce the system cost and management complexity by reducing the number of amplifier stations. Having a large loss (coming from a long fibre span) between two optical amplifiers decreases the OSNR of the signal at the receiver. This is discussed in details in e.g. [1, Ch. 10], where it is found that the optimum amplifier spacing is 10–20 km for transoceanic systems.[1] For a given system, the span length should be as large as possible (to save cost) while satisfying the OSNR requirement at the receiver.

The use of ultra-long fibre spans changes the link design in several ways. First, as the span length is increased, the maximum value of the accumulated dispersion also increases. This leads to transmission of very dispersed pulses. Second, the higher span loss requires higher input power or distributed amplification to achieve the same OSNR as shorter spans. Figure 5.1 compares a system with 40 and 160 km span lengths, showing link schematics and accumulated dispersion versus distance. Here the span length is increased by a factor of four, leading to the same reduction of number of amplifiers. The maximum accumulated dispersion is accordingly four times larger.[2]

Due to these differences between systems with long and short span lengths, the optimum dispersion compensation schemes—optimum dispersion value and relative position of the different fibre segments—can not be assumed to be the same. Therefore a separate study for long span lengths is necessary.

[1] When only considering amplified spontaneous emission and excess amplifier loss.
[2] Assuming that the same fibre types are used for both span lengths.

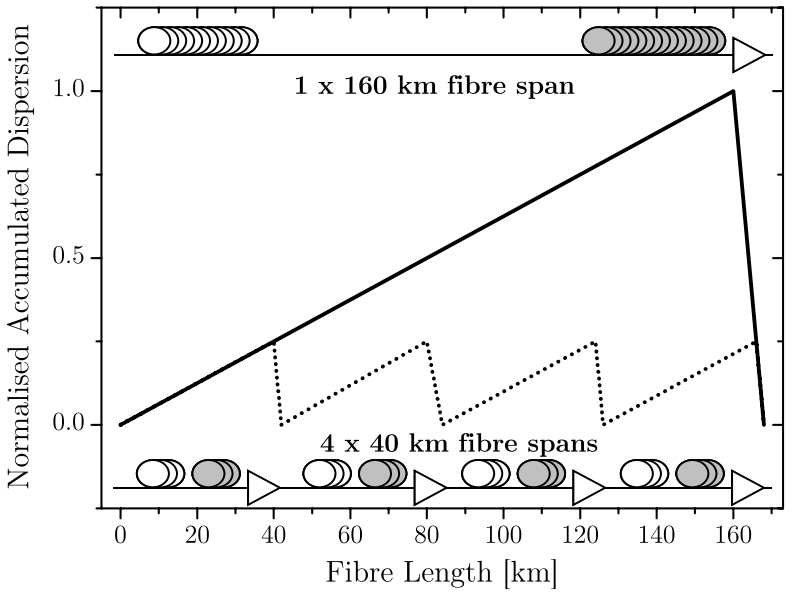

Figure 5.1: Comparison of dispersion maps for 40 and 160 km fibre spans, showing the link schematic and the accumulated dispersion versus distance for a post-compensated link.

Many recent publications present experimental or numerical studies of optimum dispersion compensation scheme for various bit rates and span lengths (see e.g. [4–15]), but not for 40 Gbit/s systems with ultra-long span lengths.

5.3 System under Investigation

To compare different dispersion compensation schemes for ultra-long fibre spans, an experimental 40 Gbit/s single-channel system was set up. The 40 Gbit/s signal was generated using optical time division multiplexing (OTDM), where a 10 Gbit/s RZ signal was multiplexed to 40 Gbit/s using passive delay lines. The full width at half maximum (FWHM) pulse width was 3 ps, corresponding to 12% of the 25 ps bit slot.

The experimental setup is illustrated in Figure 5.2. A mode locked fibre ring laser (MLFRL) produced a 10 GHz pulse train with 3 ps FWHM

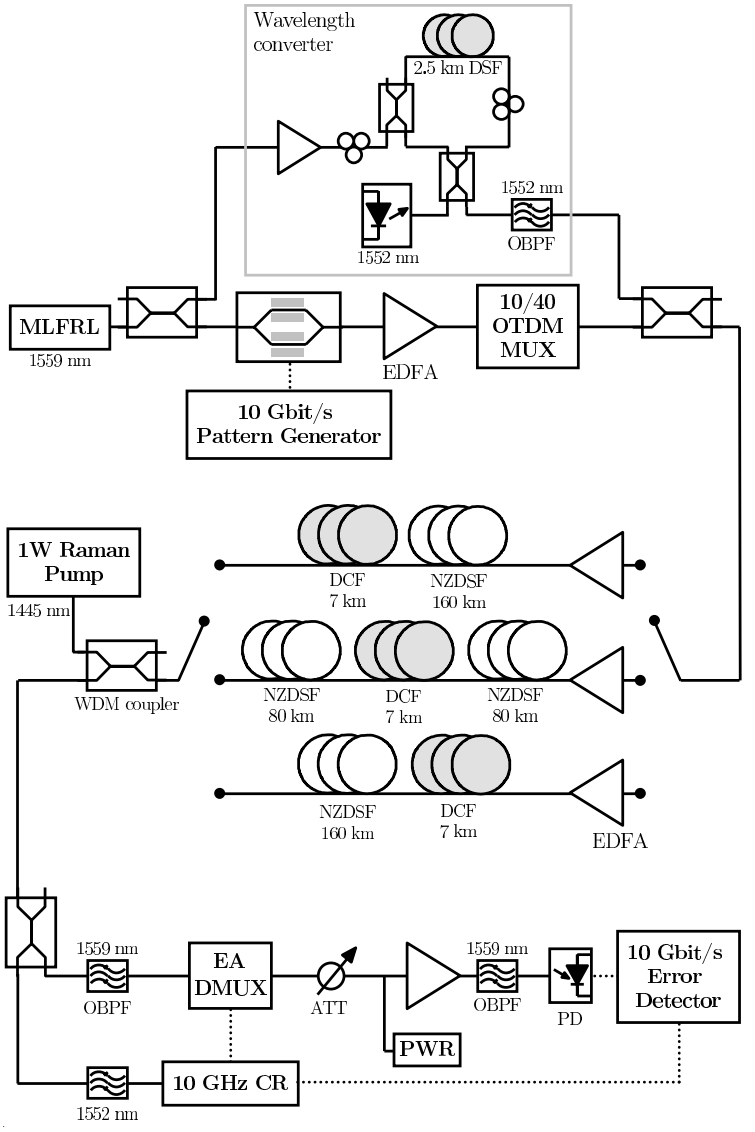

Figure 5.2: Experimental setup showing the transmitter (top), the three span configurations (centre) and the receiver (bottom).
MLFRL: Mode-locked fibre ring laser, OBF: Optical band-pass filter, EA: Electro-absorbtion modulator, CR: Clock recovery, PWR: Optical power metre, PD: Photodiode.

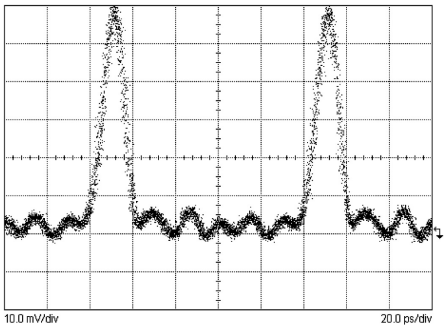

Figure 5.3: Eye diagram of the 10 GHz pulse train from the MLFRL. The FWHM pulse width was 3 ps.

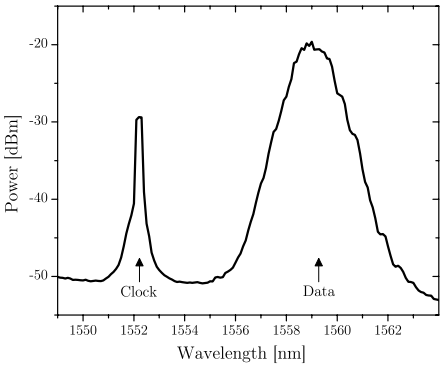

Figure 5.4: Optical spectrum of the generated signal, showing both clock and data signals.

pulse width. This pulse train was modulated at 10 Gbit/s using a Mach-Zehnder (MZ) modulator driven with a $10^{31} - 1$ bit pseudo random bit sequence (PRBS). The "eye diagram" of the optical 10 GHz pule train is shown in Figure 5.3. A 40 Gbit/s signal was generated by optically multiplexing the 10 Gbit/s RZ signal using passive delay lines. Figure 5.9(a) shows the eye diagram of the generated 40 Gbit/s RZ signal.

Due to the lack of a 40 GHz clock recovery at the time of this experiment, a rather complicated clock recovery setup had to be implemented. An optical 10 GHz clock signal was transmitted at a wavelength of 1552 nm to provide clock recovery in the receiver. The clock signal was generated by wavelength converting the 10 GHz pulse train from the MLFRL to a wavelength of 1552 nm. The wavelength conversion was performed by a nonlinear optical loop mirror (NOLM) with 2.5 km of dispersion shifted fibre (DSF). A continuous wave (CW) signal at 1552 nm with a power of 10 dBm was inserted into the NOLM, along with the pulse train having an average power of 18 dBm.[3] The data and clock signals were multiplexed using a 3 dB coupler, and the optical spectrum of the generated signal is shown in Figure 5.4. In order to prevent the clock signal from interfering with the data signal, the power of the clock signal was kept at least 10 dB lower than the data signal.

The 40 Gbit/s RZ signal was then transmitted through a link consist-

[3]For details on wavelength conversion using NOLMs, please refer to e.g. [16].

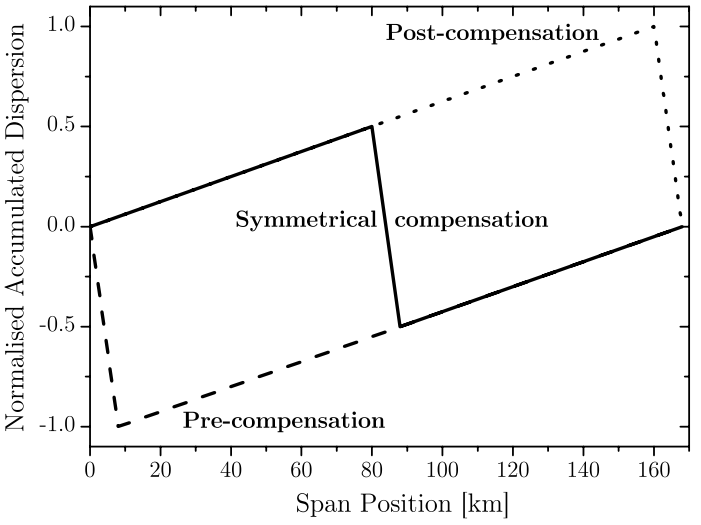

Figure 5.5: Dispersion maps for pre-, post-, and symmetrical compensation schemes.

ing of one span made of 160 km NZDSF and 7 km DCF fibre segments. We investigated three different dispersion management schemes—pre-, post- and symmetrical compensated fibre spans. Figure 5.5 illustrates the difference between these dispersion maps, showing the accumulated dispersion versus distance.

The respective lengths of the NZDSF and DCF were matched to offer very close to 100% dispersion compensation at the signal wavelength of 1559 nm. A novel DCF was used, which was specifically designed to provide simultaneous dispersion and dispersion slope compensation of the NZDSF [17, 18]. The per span accumulated dispersion and dispersion slope were -1.1 ps/nm and 0.05 ps/nm^2 at the signal wavelength, respectively. This corresponds to a dispersion compensation ratio of 99.9%. The per span accumulated dispersion and dispersion slope is illustrated in Figure 5.6. Fibre parameters were $D = 5.5$ ps/nm/km, $S = 0.055$ ps/nm^2/km, $A_{\text{eff}} = 55$ μm^2 for the NZDSF and $D = -110$ ps/nm/km, $S = -1.1$ ps/nm^2/km, $A_{\text{eff}} = 15$ μm^2 for the DCF, all at a wavelength of 1550 nm.

The total loss of the 160 km fibre span was 44 dB, which proved

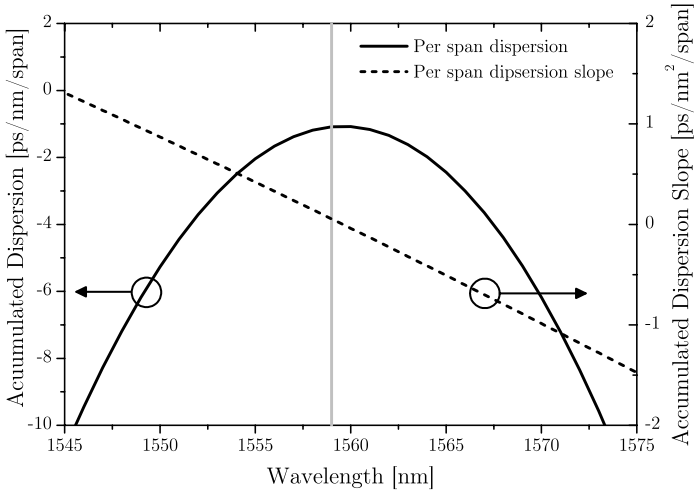

Figure 5.6: Measured dispersion profile of the studied 160 km fibre span, showing total accumulated dispersion of the span versus wavelength. At the signal wavelength of 1559 nm, the dispersion and dispersion slope was -1.1 ps/nm/span and 0.05 ps/nm^2/span, respectively. The vertical line indicates the signal wavelength.

too high to be covered by EDFA amplification only. It should be noted that this span loss is about 7 dB higher than what would be expected from the fibre loss itself since the fibre was placed on six different fibre spools. This caused significant excess loss from splices and connections. In order to overcome this high span loss, a combination of EDFA and Raman amplification scheme was used. The span was backward-pumped using a Raman pump offering 1 W of average power at a wavelength of 1455 nm. Figure 5.7 shows the optical power spectrum of the signal after transmission through one 160 km span with and without Raman pumping, for each of the three dispersion compensation schemes. The Raman pumping resulted in an on-off gain of 17 dB for the pre- and symmetrical compensation schemes. The loss of the last 80 km NZDSF was so large ($\sim$20 dB) that there was no significant gain in the DCF in neither of the two configurations. Thus, all the Raman gain comes from the last 80 km NZDSF. For the post-compensated scheme, a higher gain of 26 dB was obtained, due to the higher Raman gain (smaller A_{eff}) of the

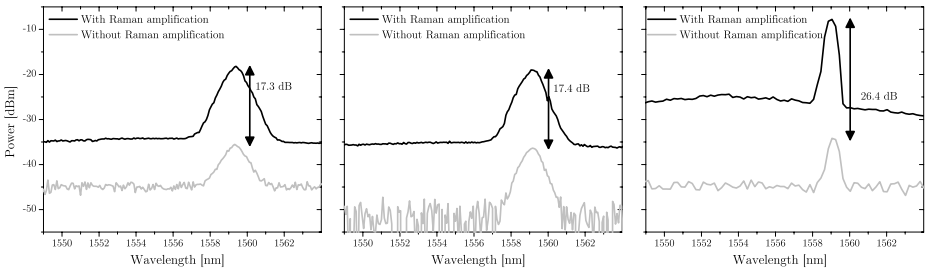

Figure 5.7: Optical spectrum at the end of the link with and without Raman gain for pre-compensation (a), symmetrical compensation (b) and post-compensation (c). The spectra were recorded with a 1 nm resolution bandwidth, after disabling the clock signal at 1552 nm.

DCF compared to the NZDSF. In this case, there is significant Raman gain both in the DCF and the NZDSF.

At the receiver, the clock and data signal were demultiplexed into two separate branches by a 3 dB coupler and two optical bandpass filters (OBPFs), as illustrated in Figure 5.2. An electrical 10 GHz clock signal was recovered from the optical clock signal and was used for demultiplexing. An electro-absorption modulator (EAM) was used to demultiplex the data signal from 40 Gbit/s down to 10 Gbit/s.[4]

The signal quality was quantified as the receiver sensitivity of one of the demultiplexed 10 Gbit/s channels at a bit error rate (BER) of 1.0×10^{-9} using a pre-amplified receiver. The back-to-back sensitivity of the demultiplexed 10 Gbit/s signal was -38.1 dBm at a BER of 1.0×10^{-9}.

5.4 System Performance

The input power to the fibre span was adjusted to get optimum performance—in term of best possible receiver sensitivity. Due to the high span loss, the optimum input power was as high as 11 dBm, which was the maximum output power of the booster EDFA. This was the optimum power level for all three span configurations.

We compare the relative performance of the three dispersion maps by

[4]For details on EAMs, please refer to e.g. [19].

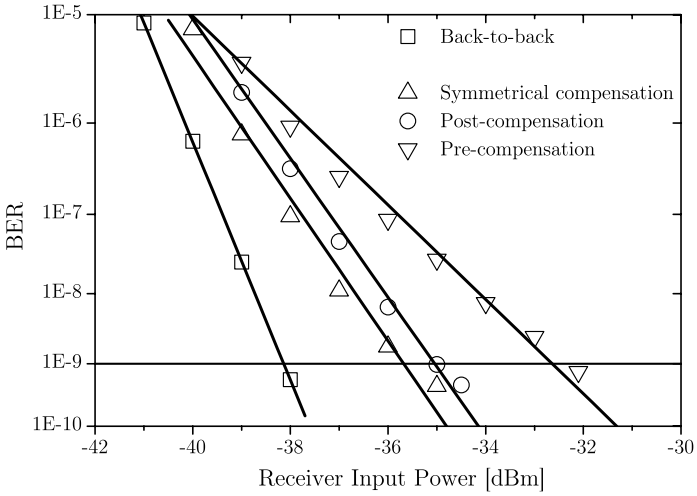

Figure 5.8: BER curves of one of the demultiplexed 10 Gbit/s tributaries in the 40 Gbit/s signal for the back-to-back case and after transmission over 160 km.

comparing the power penalty after transmission through one 160 km fibre span. The power penalty is defined as the receiver sensitivity degradation after transmission compared to the back to back case. The measured BER curves after transmission are shown in Figure 5.8. The resulting power penalty was found to be 5.4, 3.1 and 2.4 dB for pre-, post- and symmetrical compensation schemes, respectively. Eye diagrams of the signal at the output of the transmitter and after transmission through one symmetrical 160 km fibre span are shown in Figure 5.9. We see that even though the signal has considerably more noise, the pulse shape is maintained due to accurate dispersion compensation.

Even though the post-compensated scheme offered 9 dB higher Raman gain, the symmetrical scheme resulted in the best performance. The extra Raman gain increased the optical power at the end of the link, but did not improve the signal quality. Actually, the high gain in the DCF leads to non-linear signal degradation and enhanced multi-path interference (MPI) [20–22], limiting the performance compared to symmetrical compensation. The pre-compensated span suffers from severe nonlinear degradation due to the high input power to the DCF. The symmetrical map offers high amplification where the signal power is lowest, and reduces at the same

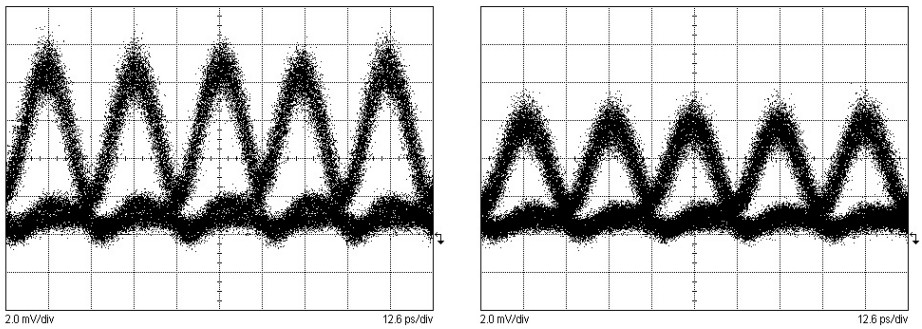

(a) (b)

Figure 5.9: Eye diagram of the 40 Gbit/s signal at the output of the transmitter (left) and after transmission through the symmetrical span (right).

time nonlinear signal degradation and MPI by having the DCF in the centre of the span where both the pump and signal have been attenuated. Therefore, the symmetrical map has best performance.

5.5 Summary

Ultra-long fibre spans can be an efficient way of reducing both the installation and operational costs of optical communication system by reducing the number of amplifier stations.

We have presented an experimental comparison of transmission performance of 40 Gbit/s RZ signals over pre-, post- and symmetrical dispersion compensated 160 km NZDSF + DCF fibre spans. A combination of lumped EDFA and distributed Raman amplification was used to overcome the high span loss associated with long fibre spans. By combining high gain at the point where the signal power is low, with reduced nonlinear signal degradation and MPI, the symmetrical map results in the best performance.

References to Chapter 5

[1] I. P. Kaminov and T. L. Koch, editors. *Optical Fiber Telecommunications IIIA*. Academic Press, 1997. ISBN 0-12-39-5171-2.

[2] G. P. Agrawal. *Fiber-Optic Communciation Systems.* Wiley, Second edition, 1997. ISBN 0-471-17540-4.

[3] T. Tokle, Q. N. T. Le, C. Peucheret, and P. Jeppesen. "Optimum dispersion map for Raman amplified 160 km NZDSF + DCF fibre spans with 40 Gbit/s RZ signals", *Electronics Letters*, vol. 40, no. 22, pp. 1443–1444, October 2004. doi:10.1049/el:20040605.

[4] D. Breuer, F. Küppers, A. Mattheus, E. G. Shapiro, I. Gabitov, and S. K. Turitsyn. "Symmetrical dispersion compensation for standard monomode-fiber-based communication systems with large amplifier spacing", *Optics Letters*, vol. 22, no. 13, pp. 982–984, July 1997.

[5] D. Breuer, K. Jürgensen, F. Küppers, A. Mattheus, I. Gabitov, and S. K. Turitsyn. "Optimal schemes for dispersion compensation of standard monomode fiber based links", *Optics Communication*, vol. 140, no. 1-3, pp. 15–18, July 1997. doi:10.1016/S0030-4018(97)00167-3.

[6] D. Breuer, K. Petermann, A. Mattheus, and S. K. Turitsyn. "Combatting fibre nonlinearity in symmetrical compensation schemes using RZ-modulation format at 120 km amplifier spacing over standard fibre", in *Proceedings European Conference on Optical Communication, ECOC'97,* Edinburgh, Scotland, U.K., vol. 2, pp. 261–264, September 1997.

[7] L. E. Nelson, L. D. Garrett, A. B. Chraplyvy, and R. W. Tkach. "NZ-DSF dispersion maps in 2000 km 8×10 Gb/s WDM transmission", in *Proceedings European Conference on Optical Communication, ECOC'98,* Madrid, Spain, vol. 1, pp. 315–316, September 1998.

[8] A. K. Røyset, S. Bjørnstad, and D. R. Hjelme. "Optimal dispersion management for 40 Gbit/s non-repeatered transmission systems using positive and negative dispersion fibre", in *Technical Digest IEEE Lasers and Electro-Optics Society Annual Meeting, LEOS'99,* Orlando, Florida, U.S.A., vol. 1, pp. 364–365, Paper TuCC3, November 1999.

[9] C. Peucheret, N. Hanik, R. Freund, L. Molle, and P. Jeppesen. "Optimization of pre- and post-dispersion compensation schemes for

10 Gbits/s NRZ links using standard and dispersion compensating fibers", *IEEE Photonics Technology Letters*, vol. 12, no. 8, pp. 992–994, August 2000.

[10] T. Okuno, T. Ooishi, T. Kato, Y. Yokoyama, M. Yoshida, Y. Takahashi, Y. Makio, and M. Nishimura. "Optimum dispersion of nonzero dispersion shifted fiber for high bit rate DWDM systems", in *Technical Digest Optical Fiber Communication Conference, OFC'01,* Anaheim, California, U.S.A., vol. 2, Paper TuH4, March 2001.

[11] C. Peucheret, T. Tokle, S. N. Knudsen, C. J. Rasmussen, and P. Jeppesen. "System performance of new types of dispersion compensating fibres", in *Technical Digest Conference on Lasers and Electro-Optics, CLEO'01,* Baltimore, Maryland, U.S.A., p. 544, Paper CFA2, May 2001.

[12] B. Konrad, A. Hodžić, and K. Petermann. "Dispersion compensation schemes for 160 Gb/s TDM-transmission over SSMF and NZDSF", in *Proceedings European Conference on Optical Communication, ECOC'01,* Amsterdam, The Netherlands, vol. 2, pp. 188–189, September 2001.

[13] Y. Frignac, J.-C. Antona, S. Bigo, and J.-P. Hamaide. "Numerical optimization of pre- and in-line dispersion compensation in dispersion-managed systems at 40 Gbit/s", in *Technical Digest Optical Fiber Communication Conference, OFC'02,* Anaheim, California, U.S.A., pp. 612–613, Paper ThFF5, March 2002.

[14] A. Pizzinat, A. Schiffini, F. Alberti, F. Matera, A. N. Pinto, and P. Almeida. "40 Gb/s systems on G.652 fibers: comparison between periodic and all-at-the-end dispersion compensation", *Journal of Lightwave Technology*, vol. 20, no. 9, pp. 1673–1679, September 2002. doi:10.1109/JLT.2002.802222.

[15] T. Tokle, C. Peucheret, and P. Jeppesen. "System optimisation of dispersion maps using new cabled dispersion compensating fibers", *Journal of Optical Communication*, vol. 25, no. 2, pp. 75–78, March 2004.

[16] N. Chi, L. Xu, K. S. Berg, T. Tokle, and P. Jeppesen. "All optical wavelength conversion and multichannel 2R regeneration based on highly nonlinear dispersion-imbalanced loop mirror", *IEEE Photonics Technology Letters*, vol. 14, no. 11, pp. 1581–1583, November 2002. doi:10.1109/LPT.2002.803343.

[17] Q. N. T. Le. *Fibers for 160 Gbit/s transmission and above.* Ph.D. thesis, Research Center COM, Technical University of Denmark, Kgs. Lyngby, Denmark, June 2003. ISBN 87-90974-44-1.

[18] Q. N. T. Le, T. Veng, and L. Grüner-Nielsen. "New dispersion compensating module for compensation of dispersion and dispersion slope of non-zero dispersion fibres in the C-band", in *Technical Digest Optical Fiber Communication Conference, OFC'01,* Anaheim, California, U.S.A., Paper TuH5, March 2001.

[19] L. K. Oxenløwe. *Optical signal processing with semiconductor components.* Ph.D. thesis, Research Center COM, Technical University of Denmark, Kgs. Lyngby, Denmark, May 2002. ISBN 87-90974-23-9.

[20] C. R. S. Fludger, V. Handerek, and R. J. Mears. "Pump to signal RIN transfer in Raman fiber amplifiers", *Journal of Lightwave Technology*, vol. 19, no. 8, pp. 1140–1148, August 2001.

[21] S. Tenenbaum and P. Poggiolini. "A comparison between IMDD and DPSK on the impact of MPI in all-Raman dispersion-compensated links", in *Proceedings European Conference on Optical Communication, ECOC'04,* Stockholm, Sweden, vol. 3, pp. 522–523, Paper We4.P026, September 2004.

[22] C. R. S. Fludger, Y. Zhu, V. Handerek, and R. J. Mears. "Impact of MPI and modulation format on transmission systems employing distributed Raman amplification", *Electronics Letters*, vol. 37, no. 15, pp. 970–972, July 2001. doi:10.1049/el:20010659.

Chapter 6

Differential Quadrature Phase Shift Keying

6.1 Introduction

Differential phase shift keying (DPSK) modulation is well-known from digital radio communication, and was investigated as a modulation format for optical coherent communication system about two decades ago (see e.g. [1–4]). In 2000, DPSK was "rediscovered" in the field of optical communication systems by Rohde et. al. [5]. Since then, differential binary phase shift keying (DBPSK) has been intensely studied, and recent experiments have demonstrated good performance for long-haul transmission with high spectral efficiency (see e.g. [6–8]).

Four-level DPSK, differential quadrature phase shift keying (DQPSK), is also known from radio communication (see e.g. [1, 2, 9]), and there has also been some interest in four-level phase modulation for coherent systems [10–12]. Griffin et. al. suggested the use of direct detection DQPSK for optical communication systems in 2002 [13], and recent experiments have demonstrated long haul transmission, high spectral efficiency and 80 Gbit/s per channel bit rates using DQPSK (see e.g. [14–18]).

This chapter presents a study of direct detection DQPSK, discussing generation, transmission and reception for long-haul system applications for per channel bit rates above 10 Gbit/s. First, an introductory description of DQPSK is given for direct detection optical communication systems, presenting different designs for transmitters and receivers. The

effect of imperfect components is discussed, and conclusions are made on basic design requirements. The dispersion tolerance of DQPSK is compared to that of on-off keying (OOK), showing an improvement of almost a factor of four when using DQPSK (at the same bit rate). DQPSK transmission experiments were performed in a wavelength division multiplexing (WDM) system with a per channel bit rate of 12.5 Gbit/s, obtaining transmission distances of up to 6500 km [14], thus demonstrating DQPSK as a suitable modulation format for transoceanic transmission systems. We show that DQPSK is suitable for very close channel spacing by demonstrating transmission over 6500 km with up to 0.66 bit/s/Hz spectral density [15]. Finally, results from the first wavelength conversion experiment of ultra-high speed phase modulated signals is presented. Using four-wave mixing (FWM) in a highly nonlinear fibre, we successfully wavelength converted an 80 Gbit/s non return-to-zero differential quadrature phase shift keying (NRZ-DQPSK) with only 2.8 dB power penalty [19].

6.2 DQPSK Overview

DQPSK is a four-level phase modulation format, where each symbol is coded with one out of four possible phase transitions, i.e. the phase change between two consecutive symbols. As each symbol has four possible states, two bits are transmitted for each symbol, and the symbol rate is therefore half of the bit rate B.

Instead of detecting the phase *change* as with DPSK, the *absolute* phase can also be detected. This modulation format is referred to as phase shift keying (PSK).[1] PSK benefits from a better receiver sensitivity than DPSK, but puts very strict requirements on the phase stability of the system. For example, phase noise from the source laser can be a significant problem. The laser linewidth must be four orders of magnitude smaller than the bit rate for it to be negligible [20]. This is one of few limitations that is actually relaxed for an increased bit rate, and can normally be disregarded for high bit rates such as 10 or 40 Gbit/s. When transmitting over optical fibres, even the smallest change in temperature will cause significant phase change at the receiver, making PSK not suitable for optical communication systems. However, when the information is coded

[1] Referred to as quadrature phase shift keying (QPSK) for four-level systems.

in the phase change, the system only needs to have phase stability over the duration of two symbol periods, as only the phase *change* between two symbols is detected. At high bit rates, this is a very short time period (400 ps for a 10 Gbit/s DQPSK system), and thus the phase drift in that period is normally negligible. The laser linewidth of the source laser in a direct detection DQPSK system should be three orders of magnitude less than the symbol rate [21].

Detection of phase modulated signals is not possible using normal receivers. Photodiodes only detect the optical power, thus losing all information about the phase of the signal. By mixing the incoming phase modulated signal with the light from a laser at the receiver, the photocurrent can be made dependent on the phase of the incoming signal (or rather, the phase difference between the laser at the receiver and the incoming signal) [20]. Thus the phase modulation in the optical signal can be demodulated to an amplitude modulated photocurrent. Systems using this type of receiver are referred to as *coherent systems*.[2]

Phase modulated signals can also be demodulated by so-called *delay demodulators*, where the incoming signal is split into two branches, and the signal in one of the branches is delayed for a time corresponding to one symbol period. The phase change between two consecutive symbols determines the amount of contructive/destructive interference when recombining the signals. Thus, the phase information has been transferred into an optical amplitude modulation, and can be converted into an electrical signal with a normal photodiode. This receiver method is referred to as *direct detection*, and if one of the signals from the demodulator is received, it is referred to as *single-ended detection*. Preferably, *balanced detection* would be used, where both outputs of the demodulator are detected, and one photocurrent subtracted from the other. Balanced detection offers a 3 dB receiver sensitivity improvement compared to single-ended detection [23].

Optical coherent DQPSK systems have been investigated in the past—see e.g. [12, 24, 25]—and offer up to 20 dB better receiver sensitivity than direct detection systems [20], but require very complex and expensive receivers that prohibit commercial use. Furthermore, the advent of the optical amplifier has limited the interest in coherent systems.

Direct detection receivers for phase modulated signals allow for much

[2]For details on coherent systems, the interested reader is directed to e.g. [20, 22].

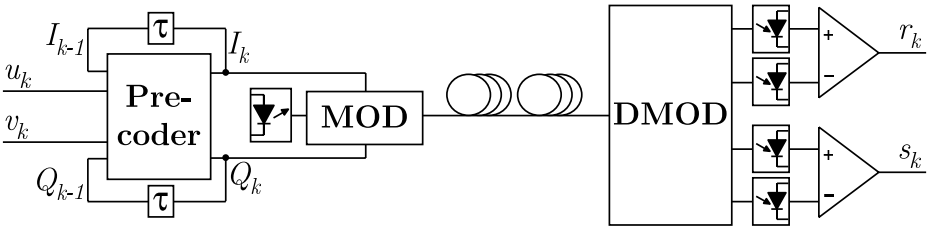

Figure 6.1: Overview of a direct detection DQPSK system. The delay τ is equal to the symbol length.

simpler receiver designs and more stable operation. Therefore, this work focuses solely on direct detection DQPSK.

6.3 Direct Detection DQPSK

A basic DQPSK[3] system is illustrated in Figure 6.1. Two data signals, u and v at a bit rate $B/2$, are input to a precoder, which generates two pre-coded signals I and Q. The pre-coded signals are then used to drive the modulator(s). Every symbol is coded into one of four possible phase levels, representing one of the four combinations of the two bits I and Q. The input signals u and v could be demultiplexed from a signal b at the bit rate, or be two independent data inputs at half the bit rate.

In a direct detection receiver, a demodulator converts the phase modulated DQPSK signal into four amplitude modulated signals. After detection by two pairs of balanced photodiodes the received signals r and s are obtained. The most frequently used demodulators for DPSK direct detection systems are one symbol delay interferometers. The light is split into two paths, one of the paths is delayed one symbol, and then the light is combined again. The amplitude of the combined light then depends on the phase difference between two consecutive symbols. However, due to this differential decoding, the system is no longer bit transparent. A pre-coder is therefore needed in order to ensure that the received data is identical to the transmitted data.

In a DQPSK system operating at a bit rate B, all electronic and

[3]From this point on, only direct detection DQPSK is discussed, and is thus simply referred to as DQPSK.

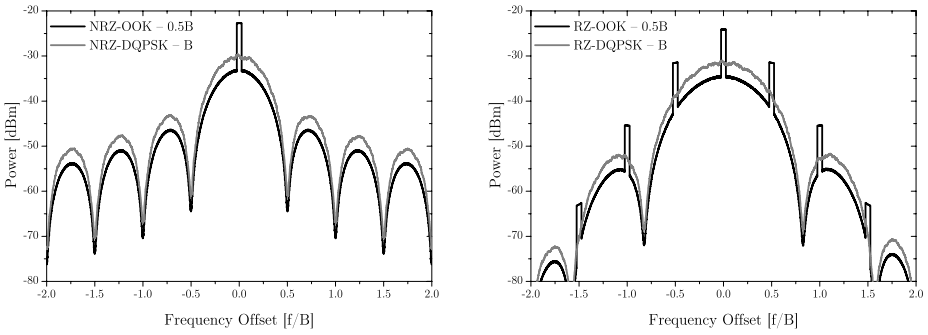

(a) NRZ (b) RZ

Figure 6.2: Comparison of calculated optical power spectra of DQPSK signals at bit rate B and OOK signals at bit rate $B/2$. Both NRZ (a) and RZ (b) waveforms are shown (with the same peak power). The resolution bandwidth is $0.08B$.

electro-optic components operate at the symbol rate equal to $B/2$. This reduced bandwidth leads to significant cost reduction compared to a binary system where all components need a bandwidth sufficient for a bit rate B. For example, in order to generate and receive a 40 Gbit/s signal, bandwidth sufficient for only 20 Gbit/s communication is needed. However, the more complex receiver required for DQPSK will lead to a cost increase compared to a binary system, and a detailed investigation would be required to determine the overall cost perspective.

As the symbol rate is reduced, the spectral width is significantly reduced. A DQPSK signal at bit rate B has the same spectral width as an OOK signal at bit rate $B/2$, as shown in Figure 6.2 for both return-to-zero (RZ) and non return-to-zero (NRZ) waveforms. The reduced symbol rate leads to significant dispersion tolerance improvements: DQPSK has about four times larger dispersion tolerance compared to an OOK signal at the same bit rate.

DQPSK can be a good method for upgrading the capacity of existing OOK WDM systems. A DQPSK channel at bit rate $2B$ can be added to an OOK WDM system with per channel bit rate of B. Since the DQPSK channel has the same spectral width and pulse shape as the OOK channel, existing filters and dispersion compensation will still be suitable

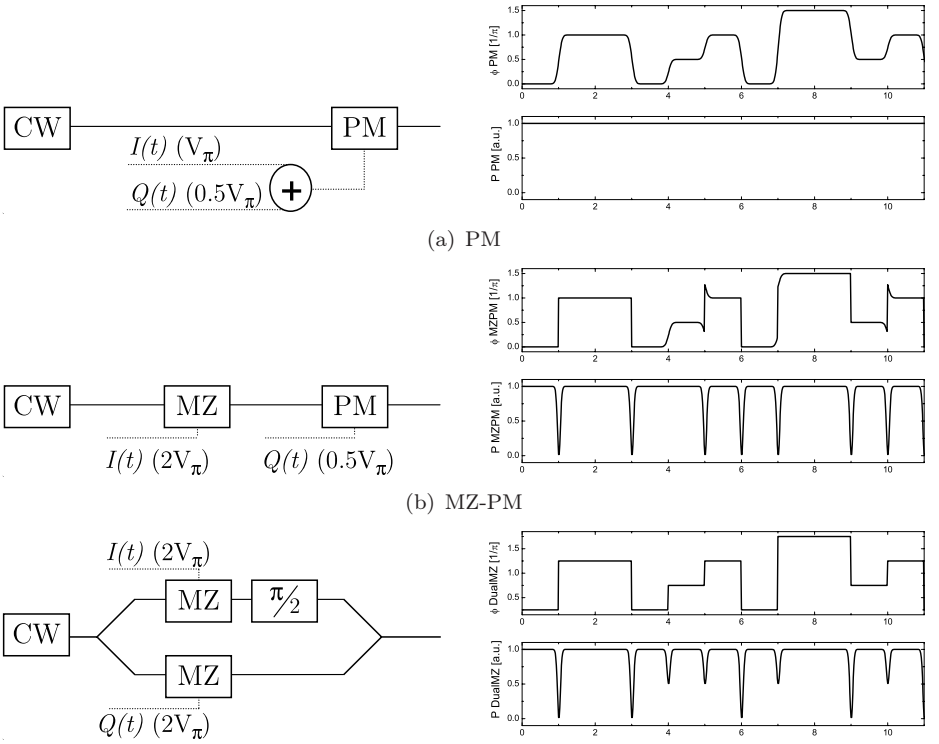

(a) PM

(b) MZ-PM

(c) Dual MZ

Figure 6.3: Three different methods to generate DQPSK (left) and the phase and power versus time of the modulated signal (right), using a rise-time of $0.2/B$ of the drive signals.

for DQPSK, as shown in [26]. If the system is fully loaded, OOK channels can be replaced by DQPSK channels to further increase the capacity.

6.3.1 Transmitter

Three different methods to generate a DQPSK signal will be described; using a phase modulator only, using phase modulator and a Mach-Zehnder (MZ) modulator in series and using two MZ modulators in parallel. The generation methods, along with the resulting phase modulation and waveforms are illustrated in Figure 6.3.

The following sections describe the three generation methods.

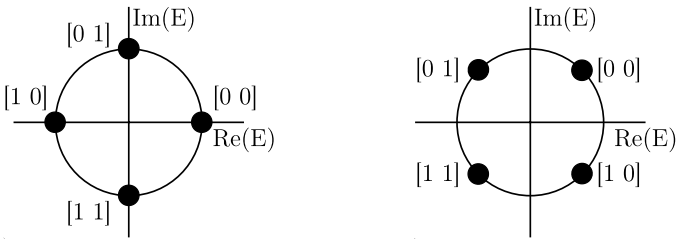

(a) PM or MZ-PM (b) Dual-MZ

Figure 6.4: Symbol allocation for DQPSK using PM or MZ-PM (a) or dual-MZ (b) generation. The states are referred to as $[I_k\ Q_k]$. Note that the states [1 0] and [1 1] are coded differently in the two cases.

Phase Modulator

The phase modulator method uses electrical processing to generate a four-level electrical signal that is used to directly drive a phase modulator, as illustrated in Figure 6.3(a). The drive signal is generated by adding I and Q, with I having twice as large voltage as Q, such that the drive signal has values within $\{0, \frac{V_\pi}{2}, V_\pi, \frac{3V_\pi}{2}\}$. The resulting signal has phase levels within $\{0, \frac{\pi}{2}, \pi, \frac{3\pi}{2}\}$, with the symbol allocation as shown in Figure 6.4(a). This method is simple to implement, since only one optical modulator is needed. However—due to the linear transfer function of the phase modulator—any imperfection in the drive signal will be directly transferred to a deviation from the intended phase level. The distribution of the electrical drive levels caused by inter-symbol interference (ISI) and noise will reduce the eye opening of the demodulated signal.

The output field from the transmitter using the PM generation method can be written as

$$E(t_k) = E_0 e^{i\pi\left(I_k + \frac{Q_k}{2}\right)}, \tag{6.1}$$

where the time $t = t_k$ indicates the centre of the symbol.

Mach-Zehnder + Phase Modulator

With the Mach-Zehnder + Phase Modulator (MZ-PM) method, two optical modulators in series are used. As seen in Figure 6.3(b), a MZ modulator driven with the precoded signal I having an amplitude equal to $2V_\pi$

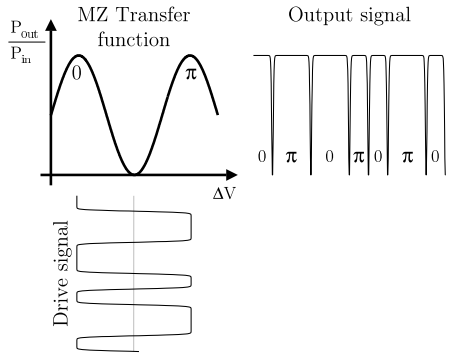

Figure 6.5: Illustration of NRZ-DBPSK generation using a MZ modulator. A two-level data signal drives the modulator from one peak of the transfer function to another, generating equal-amplitude pulses with 0 or π phase. Every time the drive signal changes value, the zero point of the modulator is crossed, resulting in a power dip of the generated signal.

generates a non return-to-zero differential binary phase shift keying (NRZ-DBPSK) signal.[4] NRZ-DBPSK generation using a MZ modulator is illustrated in Figure 6.5. After the MZ modulator, a phase modulator driven with the precoded signal Q, having an amplitude of $V_\pi/2$, adds a $\frac{\pi}{2}$ phase modulation. The resulting data signal is then four-level phase modulated with phase levels within $\{0, \frac{\pi}{2}, \pi, \frac{3\pi}{2}\}$, with symbol allocation shown in Figure 6.4(a). The symbol allocation is identical to that of the phase modulator generation method.

An advantage of using a MZ modulator to modulate the phase is that there will be a perfect π phase modulation in the first stage, since the null transmission point of the MZ transfer function is crossed. On the other hand, driving the MZ modulator this way causes the optical power to drop to zero for each phase change. This amplitude modulation can degrade NRZ coded signals, but RZ coded signal are unaffected, as these transitions are suppressed by the RZ pulse carving [27].[5]

A distribution of the amplitude of the drive signal to the MZ modulator does not change the phase modulation, but it will cause a small

[4] In the case of a single-drive MZ. For a dual-drive MZ in push-pull configuration, two drive signals each having a voltage swing of V_π would be used.

[5] The waveforms of NRZ-DQPSK and RZ-DQPSK will be compared in Section 6.4.1.

residual amplitude modulation. The amplitude fluctuations will be small due to the nonlinear transfer function of the MZ modulator. However, the distribution of the data signal that drives the phase modulator will still cause a distribution on the modulated phase.

The output field from the dual-MZ transmitter will be equivalent to that of the phase modulator generation method (at time $t = t_k$) as shown in Eq. 6.1.

Dual Mach-Zehnder

With the dual-MZ transmitter option, two MZ modulators are inserted in a MZ interferometer, as illustrated in Figure 6.3(c). Two NRZ-DBPSK signals are generated from the precoded signals I and Q, and the signal in the upper arm is phase shifted with $\frac{\pi}{2}$ before both signals are combined, resulting in a four-level phase modulated signal with phase values within $\{\frac{\pi}{4}, \frac{3\pi}{4}, \frac{5\pi}{4}, \frac{7\pi}{4}\}$. The power drops to zero when both I and Q change value at the same time. When *either* I or Q change value, the power drops to half. From Figure 6.4(b), it is seen that the symbol allocation is different from the two previous generation methods. Disregarding the constant $\frac{\pi}{4}$ phase offset, it is seen that the position of the states [1 0] and [1 1] have been switched. Therefore, as we will see in the next section, the pre-coding is not the same for all generation methods.

The MZ modulators give exact phase changes and only the $\frac{\pi}{2}$ phase shift in the upper arm needs to be tuned. Since this is a constant phase shift, it can easily be tuned to the optimum value. Thus, this transmitter structure gives very close to optimum four-level phase modulation. However, this implementation requires that there is a constant phase shift between the two arms of the interferometer structure. These stability issues can be overcome by integrating the entire transmitter structure as demonstrated in [28, 29].

At the centre of the bit slot the output signal from the dual-MZ transmitter will be

$$E(t_k) = E_0 \cos\left[\frac{\pi(I_k - Q_k) + \frac{\pi}{2}}{2}\right] e^{j\left(\frac{\pi(I_k+Q_k)+\frac{\pi}{2}}{2}\right)}. \tag{6.2}$$

In Table 6.1 the pre-coding, encoding and decoding of a DQPSK system using a dual-MZ transmitter is illustrated. It is seen that the transmitted data equals the received data, thus verifying that the precoding is

u_k	0	0	1	1	0	1	1	1	1	0	0
v_k	0	1	0	0	0	1	0	1	0	1	1
I_k	0	1	0	0	0	1	0	1	1	1	0
Q_k	0	0	0	1	1	0	0	1	0	1	1
P_k	$\frac{E_0^2}{2}$	$\frac{E_0^2}{2}$	$\frac{E_0^2}{2}$	$\frac{E_0^2}{2}$	$\frac{E_0^2}{2}$	$\frac{E_0^2}{2}$	$\frac{E_0^2}{2}$	$\frac{E_0^2}{2}$	$\frac{E_0^2}{2}$	$\frac{E_0^2}{2}$	$\frac{E_0^2}{2}$
ϕ_k	$\frac{\pi}{4}$	$\frac{7\pi}{4}$	$\frac{\pi}{4}$	$\frac{3\pi}{4}$	$\frac{3\pi}{4}$	$\frac{7\pi}{4}$	$\frac{\pi}{4}$	$\frac{5\pi}{4}$	$\frac{7\pi}{4}$	$\frac{5\pi}{4}$	$\frac{3\pi}{4}$
$\Delta\phi_k$	–	$\frac{3\pi}{2}$	$\frac{\pi}{2}$	$\frac{\pi}{2}$	0	π	$\frac{\pi}{2}$	π	$\frac{\pi}{2}$	$-\frac{\pi}{2}$	$-\frac{\pi}{2}$
r_k	–	0	1	1	0	1	1	1	1	0	0
s_k	–	1	0	0	0	1	0	1	0	1	1

Table 6.1: Input, pre-coded, encoded and received data at time $t = t_k$ for a DQPSK system with Dual-MZ generation.

correct. We also notice that the power of each symbol $P(t_k) = E_k \cdot E_k^*$ from the transmitter is constant, showing that there is no residual amplitude modulation. The corresponding analysis for the PM or MZ-PM generation method is given in Table C.1 in Appendix C.

6.3.2 Precoding

As already mentioned, the transmitted data needs to be precoded to ensure that it is correctly detected following the differential demodulation. For DBPSK, researchers have enjoyed the special property of pseudo random bit sequences (PRBSs) that causes a PRBS precoded with the DBPSK precoder to maintain its information. Thus, no precoding is necessary for testing DBPSK systems using PRBSs. Unfortunately, this is not the case for DQPSK, and precoding must be implemented also for system testing using PRBSs.

In the previous section, we saw that the symbol allocation was not the same for all generation methods. Therefore, the precoding is also different. For the dual-MZ transmitter, the precoding formula is known from radio communication theory [2], and can be written as

$$I_k = \overline{(u_k \oplus v_k)}(u_k \oplus I_{k-1}) + (u_k \oplus v_k)(v_k \oplus Q_{k-1}) \tag{6.3}$$

$$Q_k = \overline{(u_k \oplus v_k)}(v_k \oplus Q_{k-1}) + (u_k \oplus v_k)(u_k \oplus I_{k-1}). \tag{6.4}$$

With the PM or MZ-PM transmitter methods, the precoding formula can be found to be

$$I_k = \overline{v_k \oplus I_{k-1}} \cdot \overline{Q_{k-1}} + \overline{u_k \oplus I_{k-1}} \cdot Q_{k-1} \tag{6.5}$$

$$Q_k = u_k \oplus v_k \oplus Q_{k-1}. \tag{6.6}$$

For laboratory testing, the precoding is normally not implemented in hardware. Two methods based on software-based precoding have been used in recent DQPSK experiments. One method implements the precoding in software on a computer, using a PRBS and an inverted PRBS as the input signals u and v, respectively. The precoded signals I and Q are then calculated using Eqs. 6.3 and 6.4 or Eqs. 6.5 and 6.6, depending on the generation method. I and Q can then be programmed to a pattern generator, and used to drive the DQPSK modulator. The signal at the receiver will either be a PRBS or an inverted PRBS depending on the sign of the $\pm\frac{\pi}{4}$ phase shift in the demodulator. Alternatively, the precoding in the transmitter can be replaced by a "postcoding" in the receiver. By using a PRBS and an inverted and/or time-shifted PRBS to directly drive the modulators, the expected signal at the receiver can be calculated in software on a computer and transferred to a programmable error detector. Both methods were used for the experimental work presented later in this chapter.

It is worth noting that a precoding method that does not include feedback circuits has recently been demonstrated for DQPSK [30], similar to feedback-free precoding for DBPSK and duobinary as presented in [31]. This method is based on simple logical gates and uses T flip-flop gates instead of feedback circuits, and thus allows for easier implementation at high bit rates.

6.3.3 Receiver

A receiver for DQPSK basically consists of two DBPSK one symbol delay demodulators offset $\pm\frac{\pi}{4}$ from the maximum transmission point, as illustrated in Figure 6.6. First, the incoming signal is split into two branches, one for each tributary. Then the signal is demodulated by a MZ interferometer with a delay of one symbol period, corresponding to a free spectral range (FSR) equal to the symbol rate (half the bit rate). Balanced detection offers a 3 dB improvement in receiver sensitivity compared to

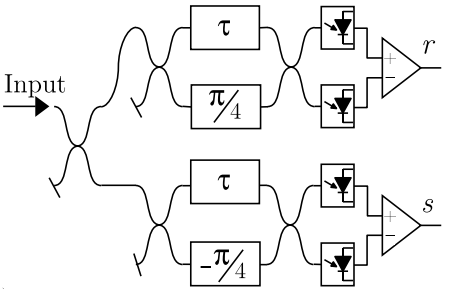

Figure 6.6: DQPSK demodulator and receiver schematic. The time delay τ is equal to one symbol period.

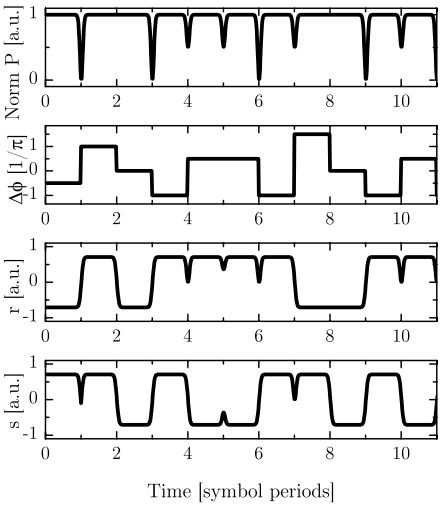

Figure 6.7: Illustration of the signals in a DQPSK receiver for a signal generated with the dual-MZ generation method.

single-ended reception [23]. The same 3 dB improvement is also seen for DBPSK [32].

If the input signal to the demodulator is $E_0 e^{i\phi(t)}$, and we assume identical photo diode responsitivities R, the balanced receiver currents will be

$$r(t_k) = -R\frac{E_0^2}{2}\left[\cos(\Delta\phi_k) - \sin(\Delta\phi_k)\right] \tag{6.7}$$

$$s(t_k) = -R\frac{E_0^2}{2}\left[\cos(\Delta\phi_k) + \sin(\Delta\phi_k)\right] \tag{6.8}$$

where $\Delta\phi_k = \phi(t_k) - \phi(t_{k-1})$ is the phase difference between two consecutive symbols.

Figure 6.7 illustrates some of the signals in a DQPSK receiver for a signal generated with the dual-MZ generation method, showing the waveforms of the received signals r and s. The corresponding illustrations for MZ-PM and PM generation methods are presented in Figure C.1 in Appendix C.

Demodulators for DQPSK can easily be made from two standard 3 dB couplers, but this method suffers from severe stability problems. Due to small temperature drift in the demodulator, the phase change between

the two arms will vary. Therefore, the demodulator needs to be temperature stabilised, and the interferometer length should be made as short as possible. By minimising the interferometer delay and using temperature controlled packaging, fibre-based demodulators can be sufficiently stable.

The DQPSK demodulator can also be made with planar integration. In [33] a demodulator for 20 Gbit/s DQPSK signals was integrated on an area less than 1.5 cm^2 using high index contrast SiON technology. The small size of planar integration is an important advantage, but a significant drawback is an increased polarisation dependence.

For both methods, the $\pm\frac{\pi}{4}$ phase shift applied to one of the arms of each delay interferometer can be generated by temperature tuning. This method is also used for DBPSK, in order to tune the demodulator to the laser frequency. Today, only fibre based demodulators are commercially available, for example from [34].

In this work, two different demodulators were used. For experiments with 12.5 Gbit/s bit rate, a "home-made" fibre-based demodulator was used. It consisted of one delay interferometer, with length of about 28 cm.[6] One arm of the interferometer was about 33 mm longer than the other, corresponding to free spectral range of 6.25 GHz. The interferometer was packaged with a heater element to obtain phase tuning in a foam-insulated box and inserted in a temperature controlled chamber to obtain sufficient temperature stability. For experiments with 80 Gbit/s bit rate, a commercial fibre-based demodulator was used. This demodulator has a shorter interferometer length and good packaging, resulting in very good stability.

6.4 Receiver Sensitivity

In this section we present experimental investigations of the receiver sensitivity of DQPSK, and compare it to that of DBPSK. All comparisons were performed at the same symbol rate, such that the same setup could be used—allowing for a fair comparison. Thus, the bit rate of the DQPSK signal was twice that of the DBPSK signal.

[6] Early implementations of this demodulator were made with longer interferometer lengths, but suffered from excessive instability due to very high temperature and polarisation sensitivity. 28 cm was the shortest interferometer length we could make by splicing 3 dB couplers.

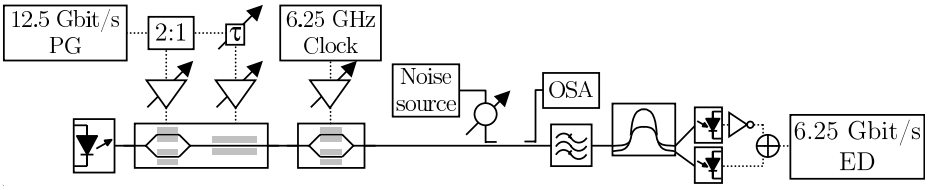

(a) 6.25 Gbaud

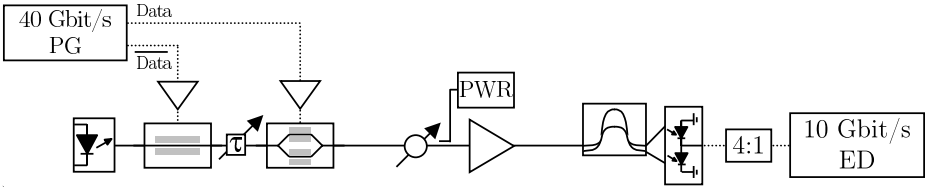

(b) 40 Gbaud

Figure 6.8: Schematics of experimental setups for investigation of DQPSK receiver sensitivity using 6.25 Gbaud (a) and 40 Gbaud (b) symbol rate.
PG: Pattern generator, ED: Error detector, PWR: Optical power metre.

First, the receiver sensitivity of 12.5 Gbit/s return-to-zero differential quadrature phase shift keying (RZ-DQPSK) and 6.25 Gbit/s return-to-zero differential binary phase shift keying (RZ-DBPSK) was compared. The setup consisted of an external cavity laser (ECL) followed by a MZ modulator and a phase modulator in series, as illustrated in Figure 6.8(a). The precoded sequences I and Q were calculated in software for input data streams $2^{15} - 1$ PRBS and inverted $2^{15} - 1$ PRBS.[7] A 12.5 Gbit/s pattern generator followed by a 2:1 demultiplexer was used to apply the 6.25 Gbit/s precoded data signals to the modulators. A second MZ modulator driven with a 12.5 GHz clock signal was used to carve 50% RZ pulses. We measured the optical signal to noise ratio (OSNR) receiver sensitivity by adding a variable amount of noise from an broadband noise source. The OSNR was measured by an optical spectrum analyser (OSA) in a 0.1 nm bandwidth. At the receiver, the signal was filtered using an optical bandpass filter with a 3 dB bandwidth of 0.25 nm and demodulated using our "home-made" demodulator designed for a symbol rate of

[7] A PRBS sequence of $2^{15} - 1$ bits was selected because it was the longest pre-coded sequence that would fit in the pattern generator memory.

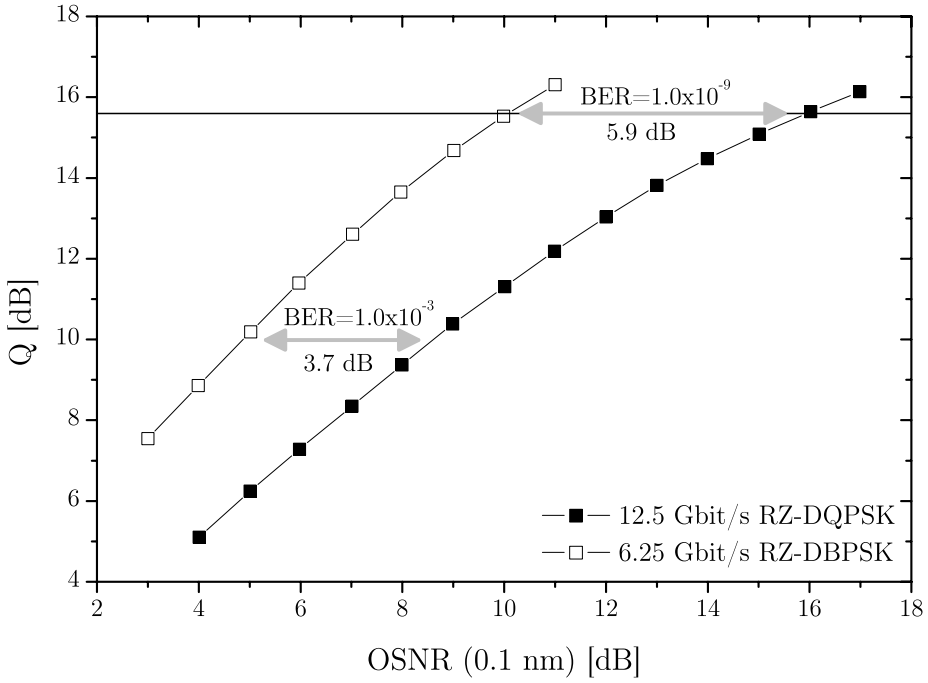

Figure 6.9: OSNR receiver sensitivity measurements for 12.5 Gbit/s RZ-DQPSK and 12.5 Gbit/s RZ-DBPSK.

6.25 Gbaud. The received pattern was $2^{15} - 1$ PRBS or inverted $2^{15} - 1$, depending on the sign of the $\pm\frac{\pi}{4}$ phase shift in the demodulator. Two 15 GHz photodiodes in a balanced configuration were used to detect the signal. As a differential amplifier was not available for this experiment, an inverting amplifier was used to invert the signal in one of the arms before adding the two signals using a 6 dB power splitter. The signal quantity was quantified by the Q-factor, found by converting the bit error rate (BER) measured by a 6.25 Gbit/s error detector.

Figure 6.9 presents the Q-factor versus OSNR measurement of the input signal for 12.5 Gbit/s RZ-DQPSK and 6.25 Gbit/s RZ-DBPSK. At a Q-factor of 15.6 dB—corresponding to a BER of 1.0×10^{-9}—the RZ-DQPSK signal requires 5.9 dB higher OSNR than the RZ-DBPSK signal. At a Q factor of 10 dB or a BER of 1.0×10^{-3}, the difference is 3.7 dB.

Second, we compared the receiver sensitivity of NRZ-DQPSK and NRZ-DBPSK using 40 Gbaud symbol rate. Light from a distributed

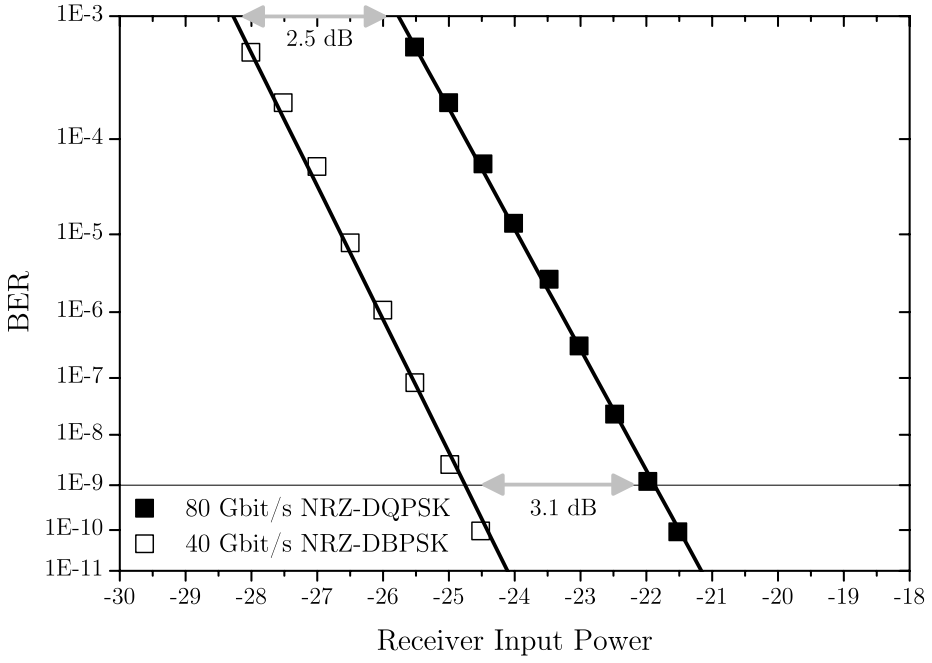

Figure 6.10: BER versus receiver input power measurements for 80 Gbit/s NRZ-DQPSK and 40 Gbit/s NRZ-DBPSK.

feedback (DFB) laser was modulated by a phase modulator and MZ modulator in series, as illustrated in Figure 6.8(b). The phase modulator was driven with an inverted $2^7 - 1$ PRBS, and the MZ modulator was driven with a $2^7 - 1$ PRBS delayed 48 bits to decorrelate the two signals. For this setup, we investigated the receiver sensitivity, and varied the optical power into the pre-amplified receiver. The signal was demodulated using a commercial demodulator designed for a symbol rate of 43 Gbaud, and received with a 45 GHz balanced detector. As precoding was not implemented in this experiment, instead the error detector was programmed with the expected pattern. Due to the lack of a 40 Gbit/s error detector with programmable data pattern, the signal was electrically demultiplexed to 10 Gbit/s and a programmable 10 Gbit/s error detector was used.

The resulting BER versus receiver input power is presented in Figure 6.10, and it is seen that 80 Gbit/s NRZ-DQPSK requires 3.1 dB more receiver input power compared to 40 Gbit/s NRZ-DBPSK in order to

achieve a BER of 1.0×10^{-9}. For a BER of 1.0×10^{-3}, the difference was 2.5 dB.

In conclusion, we see that the receiver sensitivity of our DQPSK signals is only slightly more than 3 dB higher than DBPSK at half the bit rate. We can compare the performance at the same bit rate by taking into account that DBPSK would perform 3 dB worse by doubling the bit rate. Then, at a BER of 1.0×10^{-9} we see an excess penalty of 0.7 dB for our 12.5 Gbit/s RZ-DQPSK signal and 0.1 dB for the 80 Gbit/s NRZ-DQPSK signal.

Other reports suggest that there should be a 1.5 to 2 dB worse sensitivity for DQPSK compared to DBPSK at the same bit rate, as shown experimentally for 20 Gbit/s optical DQPSK in [23] and theoretically for radio communication in [1]. We attribute the difference between those works and the work presented in this chapter to experimental uncertainty, and conclude that—at the same bit rate—DQPSK has slightly worse receiver sensitivity compared to DBPSK, and better sensitivity compared to OOK.

6.4.1 RZ vs. NRZ

In on-off keying it is well-known that the use of RZ coding results in an improved receiver sensitivity, due to better peak power to noise ratio in the receiver. Already in 1977, Personick noted that if the received pulse energy is constant, the best performance is obtained with a pulse width less than the bit slot [35]. About 2 dB improved receiver sensitivity is obtainable with RZ compared to NRZ, as discussed in Chapter 3 and in [36].

The phase modulated DQPSK signal is converted into an amplitude modulated signal after demodulation. A demodulated RZ-DQPSK signal has a RZ shape while a demodulated NRZ-DQPSK signal has a NRZ shape. Thus, it is to be expected that there should be the same 2 dB advantage for RZ coding with DQPSK as with OOK systems. The waveforms of NRZ-DQPSK and RZ-DQPSK are compared in Figure 6.11.[8] It is seen that the power-dips in symbol transitions caused by the MZ modulator are no longer visible after the RZ pulse carving.

[8]The waveforms in Figure 6.11 are created using the Dual-MZ transmitter option.

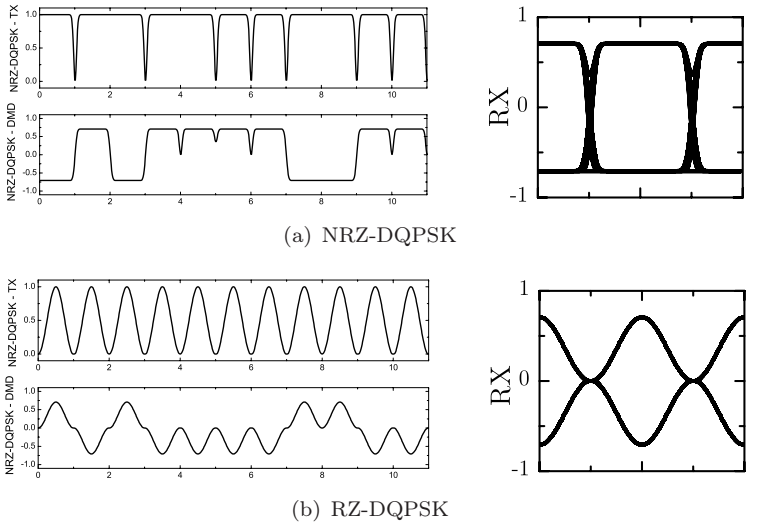

Figure 6.11: Waveforms and eye diagrams of transmitted and received NRZ (a) and RZ (b) DQPSK signals.

To demonstrate the advantage of RZ in DQPSK systems an experiment was carried out to compare NRZ-DQPSK and RZ-DQPSK at a bit rate of 12.5 Gbit/s. The results are presented in Figure 6.12, showing the Q-factor versus OSNR of the received signal. It is seen that the RZ-DQPSK requires 2 dB less OSNR for the same Q-factor as NRZ-DQPSK. Thus, we verify the advantage of RZ waveform for DQPSK. The same 2 dB improvement was also demonstrated for RZ-DBPSK compared to NRZ-DBPSK.

6.5 Component Tolerance

In a real system, there will be several factors degrading the performance compared to the ideal case. The most likely problem areas are the $\frac{\pi}{2}$ phase modulation, demodulator extinction ratio, demodulator delay and demodulator phase shift. Using numerical simulations, we quantify the impact of deviations from the optimum values of these parameters and find design requirements.

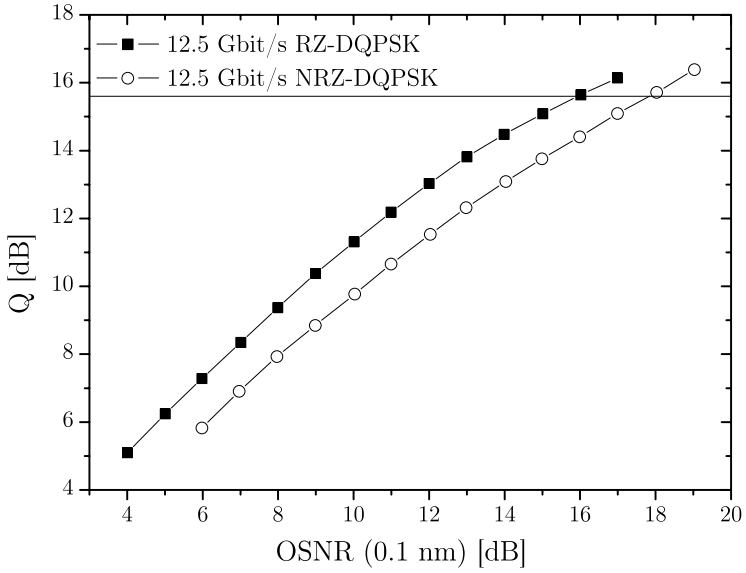

Figure 6.12: Receiver sensitivity comparison of NRZ-DQPSK vs. RZ-DQPSK at a bit rate of 12.5 Gbit/s, verifying the 2 dB advantage of the RZ waveform. The line at Q=15.6 dB corresponds to a BER of 1.0×10^{-9}.

All of these imperfections will degrade the quality of the demodulated signal. Figure 6.13 illustrates the effect of various imperfections, showing the eye diagrams of the demodulated electrical signal for a RZ-DQPSK input signal.[9] From Figure 6.13(b) it is seen that the effect of the imperfect delay is to shift the centre of the eye in time and to reduce the amplitude of the demodulated signal. An imperfect phase offset in the demodulator results in two distinct traces for both the "1" and "0" levels, as seen in Figure 6.13(c). A low demodulator extinction ratio simply reduces the amplitude of the received signal, as seen in Figure 6.13(d). Imperfect phase modulation levels of the DQPSK signal creates three distinct traces on both "1" and "0" levels, as seen in Figure 6.13(e). This effect is enhanced since the worst case deviation on $\Delta\phi_k = \phi_k - \phi_{k-1}$ is twice the worst case deviation on ϕ_k.

It is interesting to note that in some cases using a demodulator delay other than the symbol period might be beneficial. Using a shorter delay

[9]The RZ-DQPSK signal was generated using the PM method, assuming 1/5 symbol period rise time of the electrical signal.

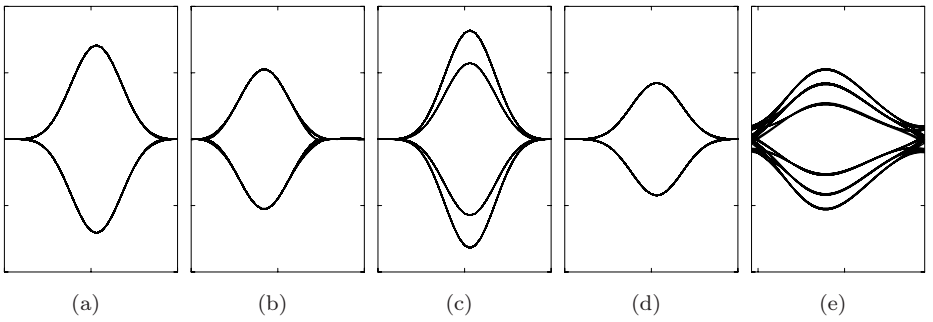

Figure 6.13: Calculated eye diagrams of the balanced electrical received signal in an imperfect RZ-DQPSK receiver for a noise-free case back-to-back. For reference, the ideal case is shown in (a). The imperfections studied were a 40% longer interferometer delay (b), a 35° demodulator phase offset (c), a demodulator extinction ratio of 6 dB (d) and phase modulation of $\pi/5$ in the phase modulator (e). The same scale is used for all plots.

length can cause a conversion from NRZ to RZ waveform, as described in [37].

We studied the effect of key parameters using numerical simulations in order to conclude on design requirements for a RZ-DQPSK receiver. A 12.5 Gbit/s RZ-DQPSK was generated using the PM method, assuming square drive signals. By changing different variables, and calculating the Q-factor at the receiver, the impact of various imperfections could be quantified. Using the Q-factor penalty[10] as the quality measure, we found the tolerable variations from the optimum values for a 0.1 dB and 1.0 dB penalty. The results are summarised in Table 6.2.

From a practical point of view, the requirement most difficult to meet in practice is the transmitter phase modulation, with allowable deviation of ±1.5° for a 0.1 dB Q factor penalty. It is most likely only the Dual-MZ transmitter option that can generate signals with such low deviation. For a signal generated with a phase modulator to reach such values, the drive signal must deviate only 3.3% from $V_\pi/2$. The laser stability tolerance of ±20 MHz is also very strict, but could be solved by tracking the frequency of the laser with the tuning of the demodulator. The requirements on the

[10]Defined as the difference between Q-factor for the ideal and imperfect case, Penalty(dB)) = Q_{ideal}(dB) − Q(dB).

	0.1 dB	**1 dB**
CW laser stability	±20 MHz	±105 MHz
Transmitter $\pi/2$ phase modulation	±1.5°	±6.3°
Demodulator extinction ratio	>21 dB	>13 dB
Demodulator delay	±9.1 ps	±25 ps
Demodulator $\pi/4$ phase offset	±2.0°	±7.0°

Table 6.2: Component tolerance of a 12.5 Gbit/s RZ-DQPSK signal found by numerical calculations, for a 0.1 and 1 dB Q-factor penalty.

extinction ratio and delay of the demodulator—±9.1 ps and > 21 dB, respectively—should be relatively easy to obtain.

6.5.1 Polarisation Dependent Frequency Shift

A special case of interest for DPSK signals demodulated using delay interferometers is the polarisation dependent frequency shift (PDFS) of the demodulator.

The wave propagation constant in optical fibres, and thus the speed of propagation, depends on the state of polarisation (SOP) of the light [38]. When the propagation speed of the light changes, the relative delay of the two arms of the DQPSK demodulator also changes. Thus, the phase shift seen by the light going through the demodulator becomes polarisation dependent. Varying the polarisation shifts the transfer function of the demodulator in frequency, referred to as a polarisation dependent frequency shift. We investigated the effect of PDFS at a bit rate of 12.5 Gbit/s using our "home-made" delay interferometer.[11]

A 12.5 Gbit/s RZ-DQPSK signal was generated using the MZ-PM transmitter method. The OSNR of the signal into the receiver was adjusted by varying the amount of noise added from a noise source based on erbium doped fibre amplifiers (EDFAs). To investigate the effect of PDFS, the Q-factor versus OSNR was measured for optimised SOP, averaged SOP and worst-case SOP. In the case of the average SOP, a polarisation controller was used to continuously adjust the state of polarisation. The

[11] This was the same demodulator used for all 12.5 Gbit/s DQPSK experiments presented in this chapter.

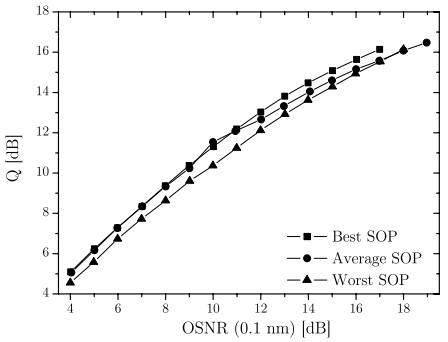

Figure 6.14: Experimental investigation of PDFS for 12.5 Gbit/s RZ-DQPSK, showing Q-factor versus OSNR for the optimum, average and worst SOP into the demodulator.

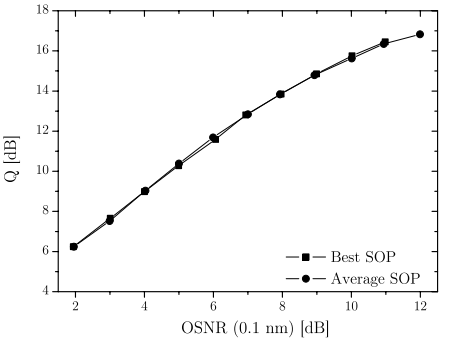

Figure 6.15: Experimental investigation of PDFS for 6.25 Gbit/s RZ-DBPSK, showing Q-factor versus OSNR for the optimum and average SOP into the demodulator.

results of this investigation are shown in Figure 6.14. For comparison, an investigation of DBPSK was also performed (at a bit rate of 6.25 Gbit/s so that the same demodulator could be used), and these results are presented in Figure 6.15.

We observed no measurable effect of the PDFS with the DBPSK signal, but for DQPSK there was 1 dB OSNR penalty at a Q-factor of 16 dB when switching from optimum to average or worst SOP. The performance of the average SOP was similar to that of the best-case SOP for low OSNR and similar to worst-case for high OSNR. For low OSNR, the system is limited by noise which dominates over the effects of PDFS. However, in the case of high OSNR, PDFS from the worst-case SOP is the dominating source of errors, and then the difference between average and worst SOP decreases.

6.6 Dispersion Tolerance

One of the main benefits of DQPSK is the improved tolerance to chromatic dispersion. In this section, the dispersion tolerance of 12.5 Gbit/s RZ-DQPSK and 12.5 Gbit/s return-to-zero on-off keying (RZ-OOK) is compared.

Using numerical simulations, the OSNR sensitivity was calculated

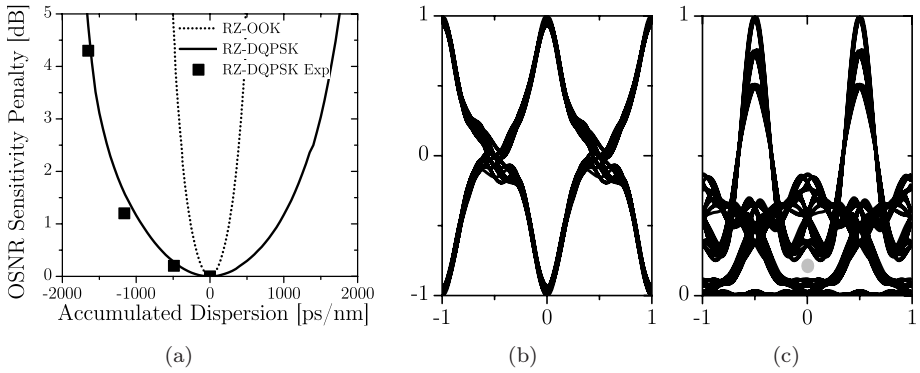

Figure 6.16: Dispersion tolerance of 12.5 Gbit/s RZ-DQPSK compared to 12.5 Gbit/s RZ-OOK; Calculated (lines) and measured (squares) OSNR sensitivity penalty versus dispersion (a) and calculated eye diagrams of RZ-DQPSK (b) and RZ-OOK (c) after applying 500 ps/nm dispersion. The grey dot in (c) indicates the centre of the eye.

after propagation through a linear, lossless dispersive element. Figure 6.16(a) presents the resulting OSNR sensitivity penalty versus accumulated dispersion, and it is seen that the dispersion tolerance for a 1 dB penalty is 1860 ps/nm for RZ-DQPSK, corresponding to about 110 km single mode fibre (SMF), which is 3.5 times larger than the 525 ps/nm limit for RZ-OOK. Figures 6.16(b) and 6.16(c) show the eye diagrams of a 12.5 Gbit/s RZ-DQPSK and RZ-OOK signal, respectively, after applying 500 ps/nm of dispersion (corresponding to about 30 km of SMF). While the RZ-OOK eye is (almost) completely closed, the RZ-DQPSK stays wide open.

These simulation results are compared with experimental results for 12.5 Gbit/s RZ-DQPSK (represented as squares in Figure 6.16). The receiver OSNR sensitivity was measured after transmission through different lengths of fibre, keeping the input power sufficiently low to ensure linear propagation.[12] We see a very good correlation between the experimental and numerical results, demonstrating the good dispersion tolerance of DQPSK.

[12]Due to lack of a clock recovery for this investigation, only short lengths of negative dispersion fibre were used.

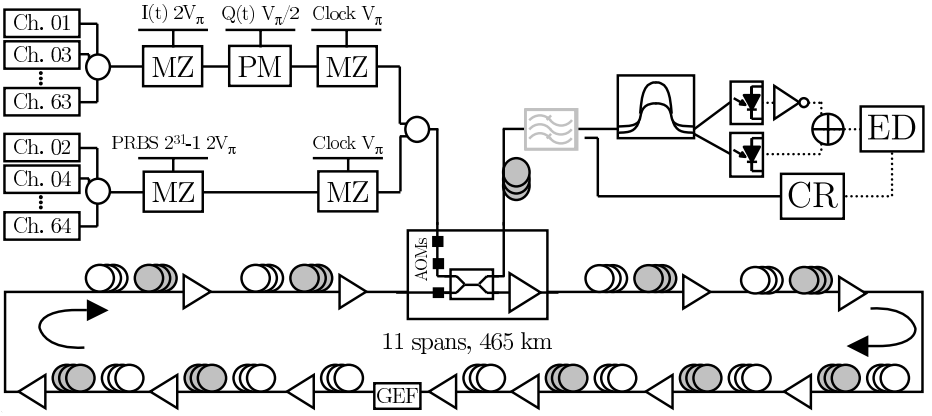

Figure 6.17: Simplified schematic of setup used for transoceanic 12.5 Gbit/s DQPSK WDM system demonstration.
AOM: acousto-optic modulator, ED: error detector, CR: clock recovery, GEF: gain-equalising filter.

6.7 Transoceanic 12.5 Gbit/s DQPSK WDM System Demonstration

This section describes an experiment set out to demonstrate that DQPSK can be a suitable modulation format for WDM systems even over transoceanic distances. Using 12.5 Gbit/s RZ-DQPSK channels in a 64 channel WDM system, we demonstrated good performance over distances up to 6500 km [14].

The experimental setup showing transmitter, re-circulating loop testbed and receiver is illustrated in Figure 6.17. Transmitter details are identical to the setup presented in Figure 6.8(a). Even channels were modulated with 12.5 Gbit/s RZ-DQPSK using the MZ-PM transmitter option. A 12.5 Gbit/s pattern generator was programmed with a data signal that was demultiplexed to the two 6.25 Gbit/s signals, I_k and Q_k. These signals had been precoded using Eqs. 6.5 and 6.6 so that the signal at the receiver was a $2^{15}-1$ bit PRBS or a inverted $2^{15}-1$ bit PRBS, depending on the sign of the $\pm\frac{\pi}{4}$ phase shift in the demodulator. Figure 6.18(a) shows the eye diagram of the generated optical 12.5 Gbit/s RZ-DQPSK signal.

Odd channels were modulated with 6.25 Gbit/s RZ-DBPSK in order to reduce system complexity. Since 6.25 Gbit/s RZ-DBPSK has the same

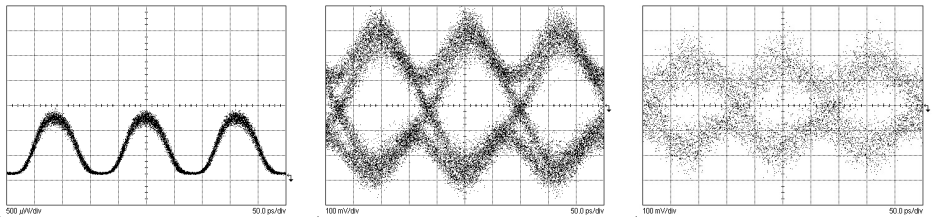

(a) (b) (c)

Figure 6.18: Eye diagrams of the generated 12.5 Gbit/s DQPSK signal. The generated optical signal (a), the electrical received signal in the back-to-back configuration (b) and after transmission over 6500 km (c). All eye diagrams were recorded for the channel at 1553.1 nm.

waveform and spectral shape as 12.5 Gbit/s RZ-DQPSK, this simplification does not affect the inter-channel crosstalk.[13]

The amplifier chain was 465 km long and consisted of 11 fibre spans made of large effective area fibre with a dispersion of 20 ps/nm/km SMF, and IDF×2 with dispersion of −40 ps/nm/km, with two of the fibre span consisting of SMF only. The average span length of the SMF + IDF×2 spans was 45 km, and the respective lengths of the SMF and IDF×2 fibres had been adjusted to get a dispersion and dispersion slope compensated map. The amplifier chain was inserted in a re-circulating loop to reach longer distances.

At the receiver, the WDM demultiplexing was achieved using a series of optical bandpass filters, where the narrowest filter had a full width at half maximum (FWHM) of 0.25 nm.[14] After filtering, the signal was demodulated in our demodulator with a free spectral range of 6.25 GHz. The signal was detected using a balanced detector, and the resulting eye diagram of one of the received channels in the back-to-back configuration is shown in Figure 6.18(b). The signal quality was quantified by measuring the BER of one of the demodulated DQPSK tributaries, and then finding the Q-factor as $Q_{dB} = 20 \times \log_{10}[\sqrt{2}\mathrm{erfc}^{-1}(2 \times \mathrm{BER})]$.

The signals were transmitted through 14 roundtrips in the recirculating loop, corresponding to a distance of 6500 km. We measured the

[13]The spectral shape of 6.25 Gbit/s RZ-DBPSK and 12.5 Gbit/s RZ-DQPSK signals are compared in Figure C.2 in Appendix C.

[14]Using the same configuration as the 66 GHz case shown in Figure 6.23.

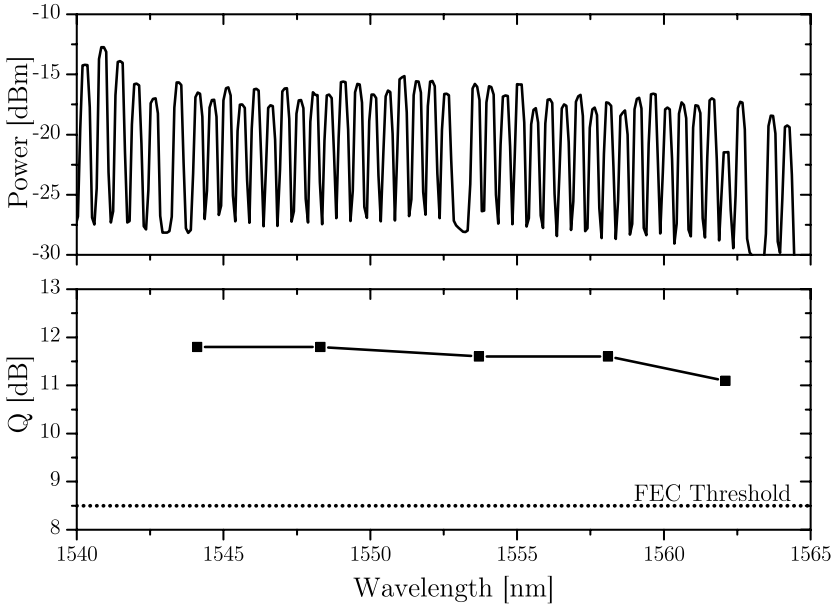

Figure 6.19: Optical spectrum (top), and Q-factor measurement (bottom) of 12.5 Gbit/s RZ-DQPSK after transmission over 6500 km. A resolution bandwidth of 0.5 nm was used when recording the spectrum.

Q-factor of the received signal for a number of channels after that distance, as presented in Figure 6.19. The optical power spectrum of the received signal is also shown. We see that the Q-factor is above 11 dB for all measured channels. When using 25% overhead for forward error correction (FEC), a Q-factor of 8.5 dB is required to achieve error free performance [39]. Thus, after 6500 km we have more than 2.5 dB margin to the FEC threshold.

System performance was limited by the dispersion map in the link available for this experiment. This particular dispersion map was designed for symbol rates at or above 10 Gbaud. The under-compensation of the SMF + IDF×2 spans was too small to significantly disperse the wide pulses of our 12.5 Gbit/s RZ-DQPSK signal. Thus, the pulse shape was preserved throughout the link, leading to enhanced nonlinear signal degradation. If a dispersion map optimised for 6.25 Gbaud symbol rate had been used, significant performance improvement would be expected.

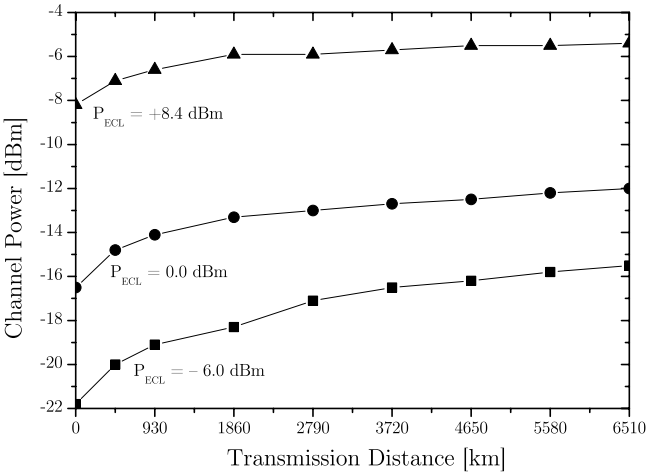

Figure 6.20: Illustration of the power evolution of the channel at 1553.1 nm, showing signal power versus distance for different launched powers from the ECL.

6.8 Comparison of 6.25 Gbit/s RZ-DBPSK and 12.5 Gbit/s RZ-DQPSK over 6500 km

In the previous section we demonstrated WDM transmission over transoceanic distances using RZ-DQPSK. However, it did not tell us how the performance of RZ-DQPSK is compared to other modulation formats. This section presents a comparison 12.5 Gbit/s RZ-DQPSK and 6.25 Gbit/s RZ-DBPSK.

Using the same setup as in the previous section, 12.5 Gbit/s RZ-DQPSK and 6.25 Gbit/s RZ-DBPSK signals were transmitted in a 64 channel WDM system. We study the channel at 1553.1 nm, and by applying a power pre-emphasis on the channel of interest, we were able to study different span input powers. When a large negative power pre-emphasis was used, the power of that channel would grow with increasing transmission distance. The power evolution for different input power levels is shown in Figure 6.20. The channel power was measured using an optical spectrum analyser on a tap port from the input of the first span in the last loop.

Adjusting the power of the continuous wave (CW) laser at 1553.1 nm

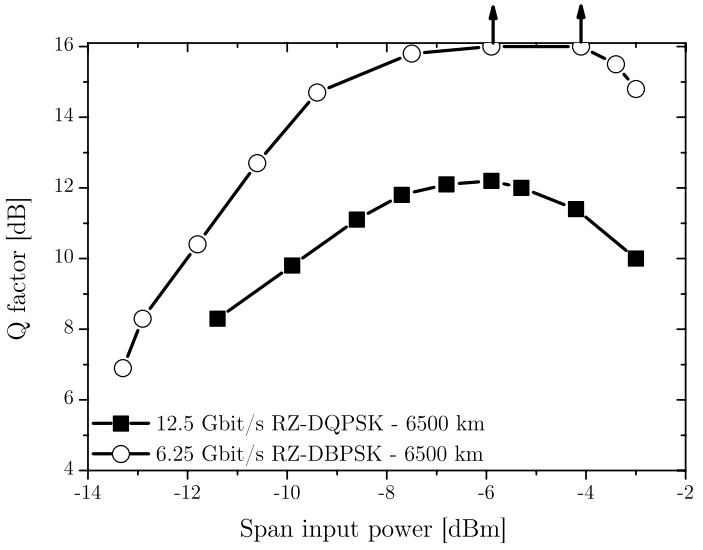

Figure 6.21: Comparison of Q-factor versus channel power level for 6.25 Gbit/s RZ-DBPSK and 12.5 Gbit/s RZ-DQPSK after transmission over 6500 km. Arrows indicate Q-factors above 16 dB (BER $< 1.5\times10^{-10}$).

and measuring the resulting Q-factor of the signal after transmission, we could study both the case of noise-limited low-power case and the nonlinearity-limited high-power case.

By turning the phase modulator off, and changing the drive signal to the MZ modulator to a $2^{15}-1$ bit PRBS, we could change between RZ-DQPSK and RZ-DBPSK.[15]

Figure 6.21 presents the resulting Q-factor versus span input power after transmission over 6500 km for 12.5 Gbit/s RZ-DQPSK and 6.25 Gbit/s RZ-DBPSK. We see that the DBPSK performs about 4 dB better than the RZ-DQPSK signal. Taking into account that the 6.25 Gbit/s RZ-DBPSK would perform 3 dB worse at 12.5 Gbit/s, the results indicate that our RZ-DQPSK signal performs about 1 dB worse than RZ-DBPSK for this system. Eye diagrams of the two signals after

[15]For RZ-DBPSK we could simply have measured on one of the even channels, but we chose to modify the odd channels in order to use exactly the same components for the comparison.

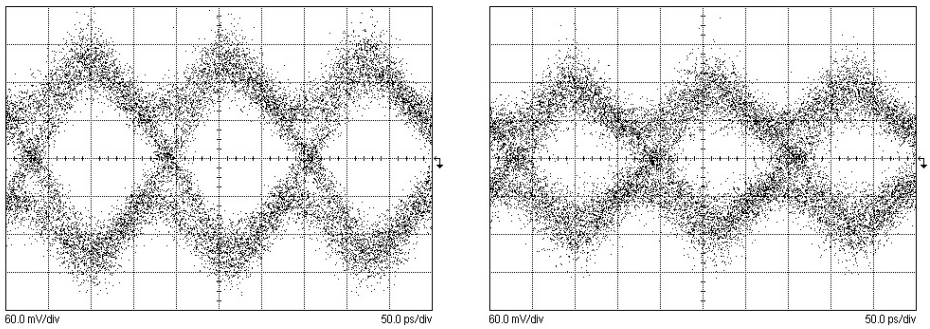

(a) 6.25 Gbit/s RZ-DBPSK (b) 12.5 Gbit/s RZ-DQPSK

Figure 6.22: Comparison of eye diagram of the electrical received signal of the channel at 1553.1 nm from the 6.25 Gbit/s RZ-DBPSK and 12.5 Gbit/s RZ-DQPSK signals after transmission over 6500 km.

transmission at optimum power are shown in Figure 6.22. Significantly better eye opening is obtained with the RZ-DBPSK signal.

It is clear from Figure 6.21 that the optimum span input power is 1–2 dB higher for the RZ-DBPSK signal, compared to RZ-DQPSK. This indicates that the non-linear tolerance of RZ-DBPSK is higher than that of RZ-DQPSK, and partly explains the difference in performance.

6.9 High Spectral Efficiency Demonstration

As previously mentioned, DQPSK has half the spectral width compared to binary modulation formats at the same bit rate. This reduced spectral width will naturally lead to better tolerance to narrow channel spacing in WDM systems. In order to demonstrate these benefits in a system environment, a WDM transmission experiment over 6500 km was carried out using five different channel spacings [15].

The experimental setup was based on that presented in Figure 6.17. By moving a group of seven channels around 1553 nm closer together, we were able to vary the channel spacing from 66 GHz down to 15 GHz. Also, by turning off the even channels, we could measure with a channel spacing of 133 GHz. With the reduced channel spacing, more receiver filtering was required to get sufficient suppression of neighbouring channels. The filtering setup is illustrated in Figure 6.23, along with the optical power

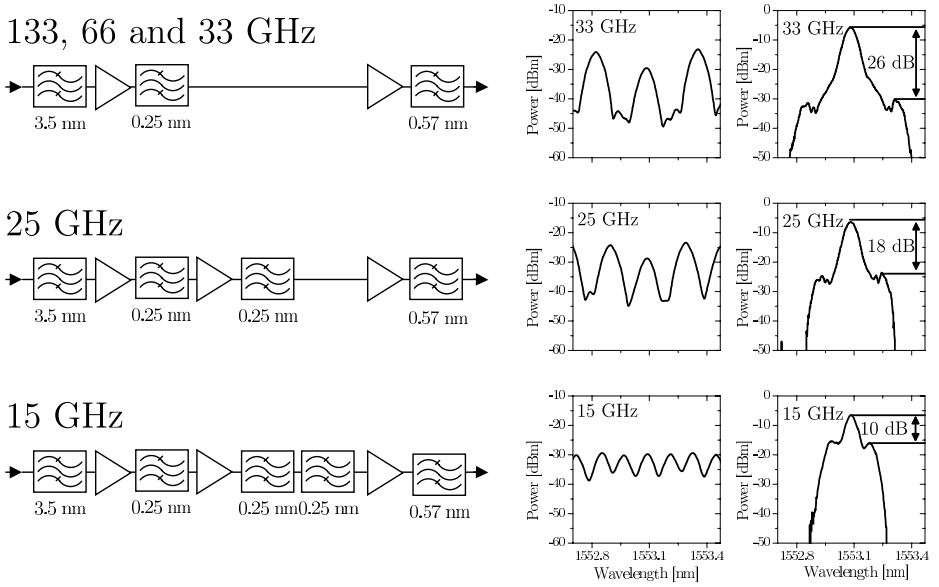

Figure 6.23: Illustration of channel selection filtering at the receiver for different channel spacings (left), optical power spectra at the transmitter (centre) and after transmission over 6500 km and filtering (right). The optical spectra were recorded with a resolution bandwidth of 0.01 nm.

spectra out of the transmitter and after filtering. Neighbouring channels were launched in the same polarisation state (parallel launch) for channel spacings from 133 to 25 GHz. When using 15 GHz channel spacing, it was necessary to launch neighbouring channels with orthogonal state of polarisation (orthogonal launch) in order to get Q-factors above the FEC threshold.

The Q-factor for the different channel spacings was measured after transmission over 6500 km. Figure 6.24 presents the measurements of the tributaries of the 12.5 Gbit/s RZ-DQPSK channel at 1553.1 nm. We see that there is a very small difference between the case of 133, 66 and 33 GHz channel spacing, with resulting Q-factors of 11.5, 11.4 and 11.2 dB, respectively. When the channel spacing is decreased to 25 GHz, the obtainable Q-factor becomes 10.2 dB. Further decreasing the channel spacing to 15 GHz did not allow for a Q-factor above the FEC threshold with parallel

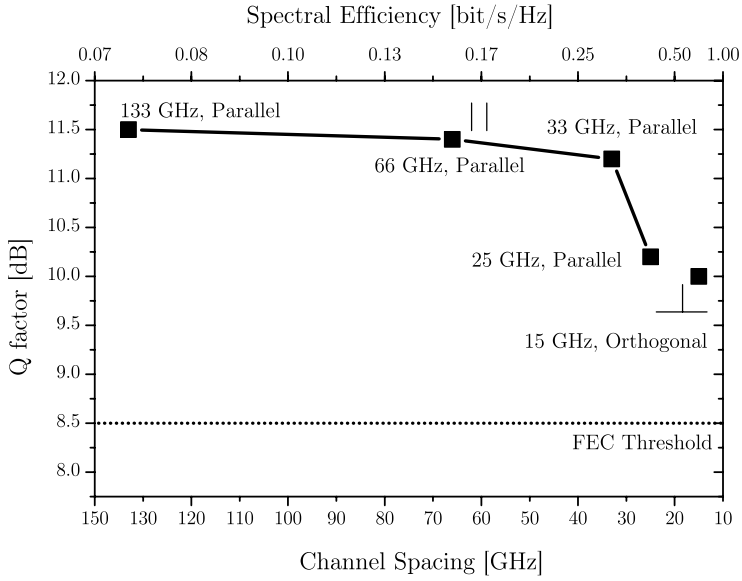

Figure 6.24: Q-factor of the 12.5 Gbit/s RZ-DQPSK channel at 1553.1 nm as a function of channel spacing after transmission over 6500 km.

launch. However, by introducing orthogonal launch, where odd and even channels were transmitted on orthogonal SOPs, a Q-factor of 10.0 dB was obtained after 6500 km. Thus even with the very dense channel spacing of 15 GHz, there is a 1.5 dB margin to the FEC threshold.

The spectral efficiency of a system is defined as the per channel bit rate without FEC overhead divided by the channel spacing. For the case with 15 GHz channel spacing with and a pre-FEC data rate of 10 Gbit/s we thus get a spectral efficiency of 0.66 bit/s/Hz.

In Figure 6.25 the optical spectrum and the eye diagrams of the signal after transmission are shown for the case with 15 GHz channel spacing. It is seen that the neighbouring channels are suppressed by only 10 dB. The optical filters used for demultiplexing the WDM channels had a filter bandwidth of 0.25 nm, corresponding to 31 GHz. Therefore, it is believed that if filters with narrower bandwidth had been used even denser channel spacing would be achievable.

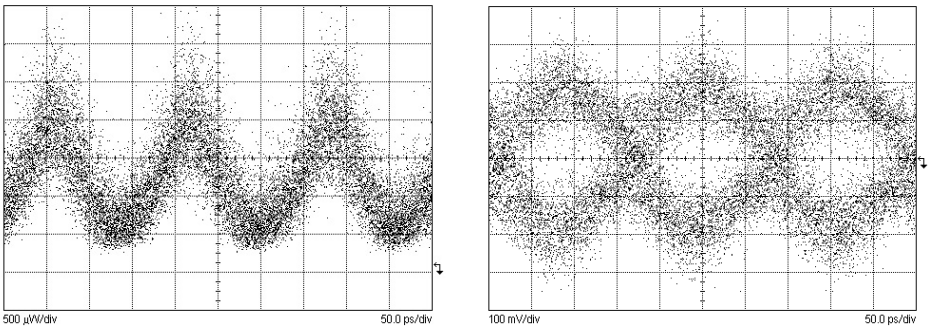

(a) (b)

Figure 6.25: Eye diagram of the received optical (a) and electrical (b) signal after transmission over 6500 km with 15 GHz channel spacing.

6.10 Wavelength Conversion of Phase Modulated Signals

The high spectral efficiency makes DQPSK an attractive modulation format for designing new or upgrading existing optical links in order to maximise the capacity in a given bandwidth. Large dispersion tolerance is required in reconfigurable optical networks where the fibre path—and thus the accumulated dispersion—is dynamically changed. DQPSK can increase the reach of such systems.

Wavelength conversion is expected to be an essential feature of future all optical networks. However, conventional wavelength conversion methods—such as those based on cross gain modulation (XGM) in a semiconductor optical amplifier (SOA) or cross phase modulation (XPM) in SOA interferometric structures [40]—disregard the phase information and thus prevent the conversion of phase modulated signals. FWM can be utilised to obtain phase-preserving wavelength conversion, as demonstrated in [41] for a 2.5 Gbit/s DBPSK signal using FWM in non-linear fibre, and in [42] for a 10 Gbit/s DBPSK signal using FWM in a SOA.

This section presents an experiment demonstrating wavelength conversion of 40 Gbit/s NRZ-DBPSK and 80 Gbit/s NRZ-DQPSK signals [19]. Wavelength conversion is performed by using FWM in a 1 km highly nonlinear fibre (HNLF).

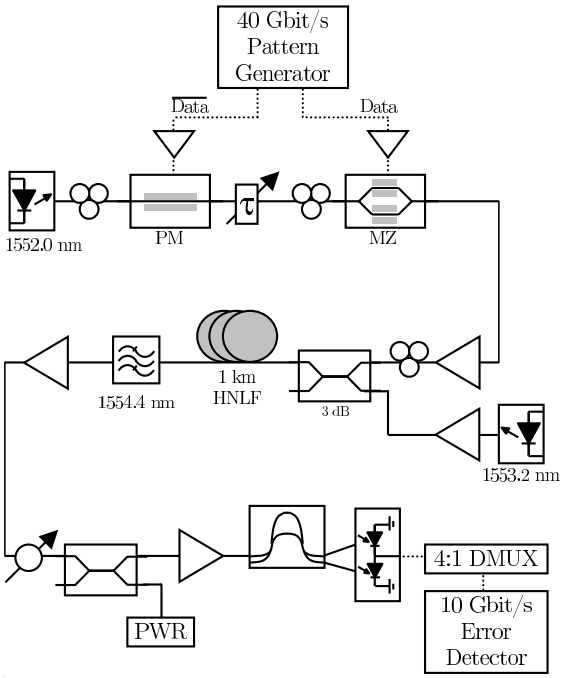

Figure 6.26: Experimental setup, showing transmitter, wavelength converter and receiver.

As shown in Figure 6.26, the 80 Gbit/s NRZ-DQPSK signal was generated using a phase modulator and a MZ modulator in series. CW light from a laser at a wavelength of 1552.0 nm was first modulated by a phase modulator driven by a 40 Gbit/s data signal having an amplitude resulting in a $\frac{\pi}{2}$ phase change. After the phase modulator, a single-drive MZ modulator driven with a $2V_\pi$ drive signal added a π phase shift. By turning off the drive signal to the phase modulator, a 40 Gbit/s NRZ-DBPSK signal could be generated instead.

Due to the low bandwidth—28 GHz—of the drive amplifier for the MZ modulator, the drive signal has significant amount of ISI. This is illustrated in Figure 6.27, where the eye diagrams of the electrical drive signals are shown. The drive signal to the phase modulator was amplified by an amplifier with 38 GHz bandwidth, and shows no sign of significant ISI.

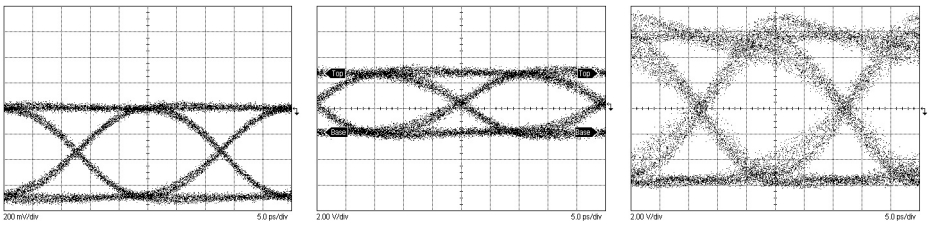

(a) (b) (c)

Figure 6.27: Eye diagrams of the electrical drive signals used to generate the 80 Gbit/s DQPSK signal. The output of the pattern generator is shown in (a), and the amplified drive signal to the PM and MZ modulators are shown in (b) and (c), respectively. Significant ISI is present in the MZ drive signal due to insufficient amplifier bandwidth.

The eye diagram of the generated optical signal is shown in Figure 6.28(a). No difference on the optical eye diagram was observed between the NRZ-DBPSK and NRZ-DQPSK signal, as the phase modulator did not add significant amplitude modulation. The signal has the classical characteristic of a MZ-generated NRZ-DBPSK signal.

In the receiver, the signal was pre-amplified before demodulation in a one bit delay demodulator. The demodulator had a time-delay of 23.5 ps, optimised for a symbol rate of 43 Gbaud. For 40 Gbit/s NRZ-DBPSK, the phase offset between the two demodulator arms was tuned to the peak of the transfer function, whereas for 80 Gbit/s NRZ-DQPSK it was offset by $\pm\pi/4$. After the demodulator, the signal was received using a 45 GHz balanced photo detector. Eye diagrams of electrical back-to-back signals are shown in Figures 6.28(b) and 6.28(c), for 40 Gbit/s NRZ-DBPSK and 80 Gbit/s NRZ-DQPSK, respectively. It is seen that the distorted drive signal to the MZ modulator results in significant ISI on the generated signals. Going from two to four phase levels (DBPSK to DQPSK) clearly adds more ISI primarily caused by a very limited bandwidth—22 GHz—of the phase modulator.

A $2^7 - 1$ PRBS and a $2^7 - 1$ PRBS were used for the MZ modulator and phase modulator, respectively. The two patterns were decorrelated by a relative delay of 48 bits. Pre-coding was not applied to the transmitted data, instead the error detector was programmed with the expected bit

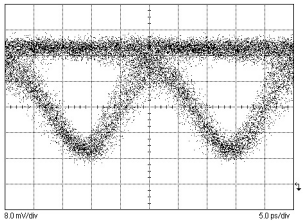

(a) Generated optical signal

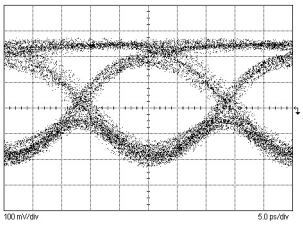

(b) 40 Gbit/s DBPSK back-to-back electrical

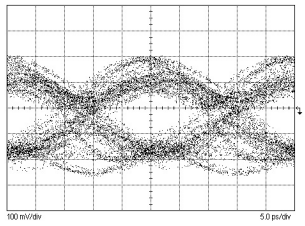

(c) 80 Gbit/s DQPSK back-to-back electrical

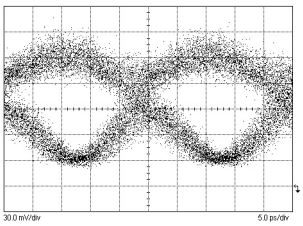

(d) 40 Gbit/s DBPSK converted optical

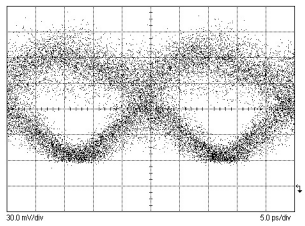

(e) 80 Gbit/s DQPSK converted optical

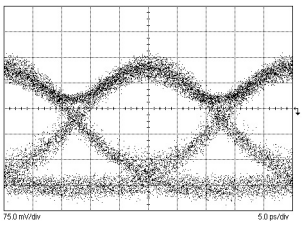

(f) 40 Gbit/s DBPSK converted electrical

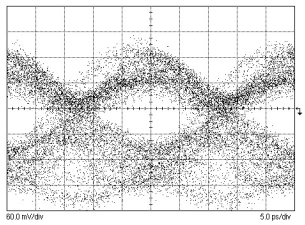

(g) 80 Gbit/s DQPSK converted electrical

Figure 6.28: Eye diagrams of signals at various points in the system. The generated signal shown in (a) is identical for both 40 Gbit/s NRZ-DBPSK and 80 Gbit/s DQPSK.

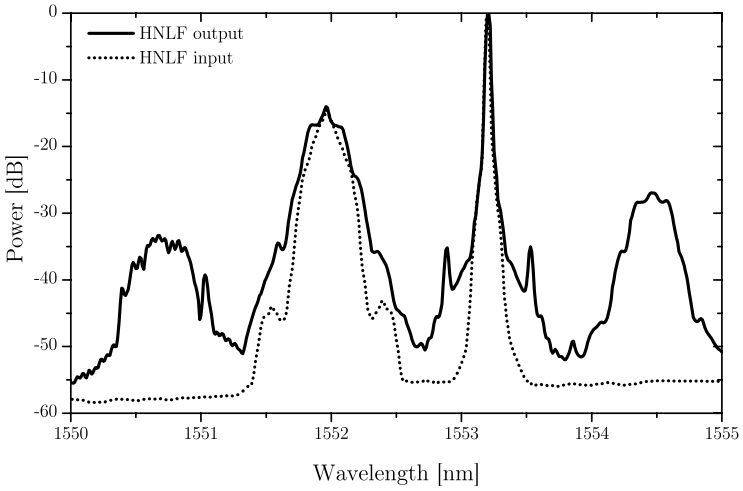

Figure 6.29: Optical power spectrum at the input and output of the HNLF, illustrating the generation of the FWM products at 1550.8 and 1554.4 nm.

pattern. As no programmable 40 Gbit/s error detector was available at the time of this experiment, the received signal was electrically demultiplexed to 10 Gbit/s, and the errors counted on a programmable 10 Gbit/s error detector.

Wavelength conversion was realised using FWM in a 1 km HNLF with a non-linear coefficient $\gamma = 10.9$ W^{-1}km^{-1}. The signal was fed into the HNLF along with a CW pump at a wavelength of 1553.2 nm. At the fibre input, the power of the data and pump was 14 and 17 dBm, respectively. Due to FWM between the pump and the signal, two new signals were generated at wavelengths of 1550.8 and 1554.4 nm, as seen in Figure 6.29 where the optical power spectrum of the signals at the input and output of the HNLF is shown. Detailed description of FWM is beyond the scope of this thesis, and the interested reader is directed to e.g. [38, 43–45]. After the HNLF, the converted signal at 1554.4 nm is filtered by an optical bandpass filter and amplified by an EDFA. The conversion efficiency, defined as the ratio of the power of the converted signal and the power of the original signal at the output of the HNLF, was −12.4 dB.

In Figure 6.30, the receiver sensitivity measurements are presented, showing the measured BER as a function of the receiver input power.

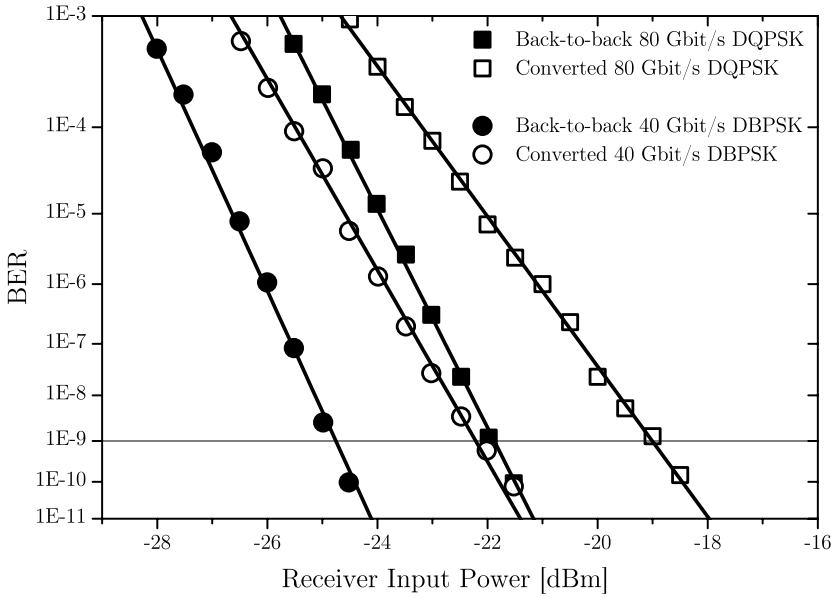

Figure 6.30: Measured BER vs. receiver input power for 80 Gbit/s DQPSK (one of the two tributaries are shown) and 40 Gbit/s DBPSK before and after wavelength conversion.

The BER was measured on one of the four 10 Gbit/s electrical tributaries demultiplexed from the 40 Gbit/s received signal. A receiver sensitivity of −21.8 dBm for 80 Gbit/s NRZ-DQPSK was measured in the back-to-back case. After conversion we measured a receiver sensitivity of −19.0 dBm, corresponding to a conversion power penalty of 2.8 dB.

For 40 Gbit/s NRZ-DBPSK, an almost identical conversion power penalty of 2.6 dB was measured. It is interesting to note that the increased number of symbol levels of DQPSK does not lead to significant extra wavelength conversion penalty compared to DBPSK.

Eye diagrams of the converted optical signals are shown in Figures 6.28(d) and 6.28(e). The corresponding electrical received signals are shown in Figures 6.28(f) and 6.28(g). It is seen that the optical signals are quite distorted compared to the back-to-back signal. It is seen that the waveforms of the electrical signal after conversion is not significantly degraded compared to the back-to-back case, and that the main degrad-

ation is due to reduced optical signal-to-noise ratio after the wavelength conversion.

6.11 Summary

Differential quadrature phase shift keying has been presented as a promising modulation format for optical communication systems. DQPSK four-level encoding results in half the spectral width of binary signals at the same bit rate, offering four times larger dispersion tolerance and double spectral efficiency. The use of DQPSK in optical communication systems allows for design of high bit rate systems using lower symbol rate to reduce impact of transmission impairments and electronic bandwidth requirements. Alternatively, DQPSK can be used to generate signals with twice the bit rate of state-of-the-art electronics. This chapter has described both approaches.

We presented an introduction to DQPSK including different transmitter/receiver designs and precoding methods. Receiver sensitivity, tolerance to dispersion, polarisation dependent frequency shift and transmitter/receiver imperfections were studied and design requirements based on RZ-DQPSK systems were found.

Transmission experiments have demonstrated the feasibility of WDM transmission over transoceanic distances. We successfully transmitted 12.5 Gbit/s DQPSK in a 64 channel WDM system over 6500 km. The performance of 12.5 Gbit/s RZ-DQPSK was compared with that of 6.25 Gbit/s RZ-DBPSK, and we found a 4 dB difference in Q-factor after transmission over 6500 km. The inherent tolerance of DQPSK to close channel spacings was demonstrated by transmitting 12.5 Gbit/s RZ-DQPSK over 6500 km using very dense channel spacing of 15 GHz, corresponding to a spectral density of 0.66 bit/s/Hz.

Using a symbol rate of 40 Gbaud, we demonstrated an 80 Gbit/s NRZ-DQPSK system. We presented the first wavelength conversion experiment of such high speed phase modulated signals. Using FWM in a 1 km HNLF we obtained a conversion penalty of 2.8 dB, which was only 0.2 dB more than the conversion penalty for a 40 Gbit/s NRZ-DBPSK.

References to Chapter 6

[1] J. G. Proakis. *Digital communication.* McGraw Hill, Third edition, 1995.

[2] F. Xiong. *Digital modulation techniques.* Artech House, 2000.

[3] J. M. P. Delavaux, L. D. Tzeng, and M. Dixon. "1.4 Gbit/s optical DPSK heterodyne transmission system experiment", *Electronics Letters*, vol. 24, no. 15, pp. 941–942, July 1988.

[4] M. J. Creaner, R. C. Steele, I. Marshall, G. R. Walker, N. G. Walker, J. Mellis, S. Al Chalabi, I. Sturgess, M. Rutherford, J. Davidson, and M. Brain. "Field demonstration of 565 Mbit/s DPSK coherent transmission system over 176 km of installed fibre", *Electronics Letters*, vol. 24, no. 22, pp. 1354–1356, October 1988.

[5] M. Rohde, C. Caspar, N. Heimes, M. Konitzer, E.-J. Bachus, and N. Hanik. "Robustness of DPSK direct detection transmission format in standard fibre WDM systems", *Electronics Letters*, vol. 36, no. 17, pp. 1483–1484, August 2000. doi:10.1049/el:20000981.

[6] J.-X. Cai, D. G. Foursa, C. R. Davidson, Y. Cai, G. Domagala, H. Li, L. Liu, W. W. Patterson, A. N. Pilipetskii, M. Nissov, and N. S. Bergano. "A DWDM Demonstration of 3.73 Tb/s over 11,000 km using 373 RZ-DPSK Channels at 10 Gb/s", in *Technical Digest Optical Fiber Communication Conference, OFC'03,* Atlanta, Georgia, U.S.A., Paper PD22, March 2003.

[7] L. Becouarn, G. Vareille, P. Pecci, and J. F. Marcerou. "3 Tbit/s transmission (301 DPSK channels at 10.709 Gb/s) over 10270 km with a record efficiency of 0.65 (bit/s)/Hz", in *Proceedings European Conference on Optical Communication, ECOC'03,* Rimini, Italy, Paper PD45, September 2003.

[8] C. Rasmussen, T. Fjelde, J. Bennike, F. Liu, S. Dey, B. Mikkelsen, P. Mamyshev, P. Serbe, P. van der Wagt, Y. Akasaka, D. Harris, D. Gapontsev, V. Ivshin, and P. Reeves-Hall. "DWDM 40G transmission over trans-pacific distance (10000 km) using CSRZ-DPSK, enhanced FEC, and all-Raman-amplified 100 km UltraWave fiber

spans", *Journal of Lightwave Technology*, vol. 22, no. 1, pp. 203–207, January 2004. doi:10.1109/JLT.2004.824187.

[9] F. G. Jenks, P. D. Morgan, and C. S. Warren. "Use of four-level phase modulation for digital mobile radio", *IEEE Transaction on Electromagnetic Compatibility*, vol. 14, no. 4, pp. 113–128, November 1972.

[10] F. Derr. "Optical QPSK homodyne transmission of 280 Mbit/s", *Electronics Letters*, vol. 26, no. 6, pp. 401–403, March 1990.

[11] S. Yamazaki and K. Emura. "Feasibility study on QPSK optical-heterodyne detection system", *Journal of Lightwave Technology*, vol. 8, no. 11, pp. 1646–1653, November 1990.

[12] H. Furuta, M. Yamamoto, M. Maeda, K. Oyamada, and N. Toyama. "Phase-diversity demodulation of an optical DQPSK signal", in *Proceedings European Conference on Optical Communication, ECOC'98,* Madrid, Spain, vol. 1, pp. 427–428, September 1998.

[13] R. Griffin and A. Carter. "Optical differential quadrature phase-shift key (oDQPSK) for high capacity optical transmission", in *Technical Digest Optical Fiber Communication Conference, OFC'02,* Anaheim, California, U.S.A., pp. 367–368, Paper WX6, March 2002.

[14] T. Tokle, C. R. Davidson, M. Nissov, J.-X. Cai, D. G. Foursa, and A. Pilipetskii. "6500 km transmission of RZ-DQPSK WDM signals", *Electronics Letters*, vol. 40, no. 7, pp. 444–445, April 2004. doi:10.1049/el:20040274.

[15] T. Tokle, C. R. Davidson, M. Nissov, J.-X. Cai, D. G. Foursa, and A. Pilipetskii. "Transmission of RZ-DQPSK over 6500 km with 0.66 bit/s/Hz spectral efficiency", in *IEEE/LEOS 2004 Workshop on Advanced Modulation Formats,* San Francisco, California, U.S.A, pp. 3–4, Paper ThA2, July 2004.

[16] N. Yoshikane and I. Morita. "1.14 b/s/Hz spectrally-efficient 50×85.4 Gb/s transmission over 300 km using copolarized CS-RZ DQPSK signals", in *Technical Digest Optical Fiber Communication Conference, OFC'04,* Los Angeles, California, U.S.A., Paper PDP38, February 2004.

[17] P. S. Cho, G. Harston, C. J. Kerr, A. S. Greenblatt, A. Kaplan, Y. Achiam, G. Levy-Yurista, M. Margalit, Y. Gross, and J. B. Khurgin. "Investigation of 2 b/s/Hz 40 Gb/s DWDM transmission over 4×100 km SMF-28 fiber using RZ-DQPSK and polarization multiplexing", *IEEE Photonics Technology Letters*, vol. 16, no. 2, pp. 656–658, February 2004. doi:10.1109/LPT.2002.807934.

[18] P. Boffi, L. Marazzi, L. Paradiso, P. Parolari, A. Righetti, D. Setti, R. Siano, R. Cigliutti, D. Mottarella, P. Franco, and M. Martinelli. "20 Gb/s differential quadrature phase-shift keying transmission over 2000 km in a 64-channel WDM system", *Optics Communication*, vol. 237, pp. 319–323, July 2004. doi:10.1016/j.optcom.2004.04.008.

[19] T. Tokle, Y. Geng, C. Peucheret, and P. Jeppesen. "Wavelength conversion of 80 Gbit/s optical DQPSK using FWM in a highly nonlinear fibre". Submitted to Conference on Lasers and Electro-Optics, CLEO'05.

[20] G. P. Agrawal. *Fiber-Optic Communciation Systems.* Wiley, Second edition, 1997. ISBN 0-471-17540-4.

[21] S. Savory and A. Hadjifotiou. "Laser linewidth requirements for optical DQPSK systems", *IEEE Photonics Technology Letters*, vol. 16, no. 3, pp. 930–932, March 2004. doi:10.1109/LPT.2004.823720.

[22] S. Betti, G. De Marchis, and E. Iannone. *Coherent Optical Communications Systems.* Wiley, January 1995. ISBN 0-471-57512-7.

[23] C. Wree, J. Leibrich, J. Eick, and W. Rosenkranz. "Experimental investigation of receiver sensitivity of RZ-DQPSK modulation format using balanced detection", in *Technical Digest Optical Fiber Communication Conference, OFC'03,* Atlanta, Georgia, U.S.A., Paper ThE5, 2003.

[24] P. Hill and R. Olshansky. "Bandwidth efficient transmission of 4 Gb/s on two microwave QPSK subcarriers over a 48 km optical link", *IEEE Photonics Technology Letters*, vol. 2, no. 7, pp. 510–512, July 1990.

[25] R. Gross and R. Olshansky. "Optical DQPSK video system with heterodyne detection", *IEEE Photonics Technology Letters*, vol. 3, no. 3, pp. 262–264, March 1991.

[26] O. Vassilieva, T. Hoshida, S. Choudhary, and H. Kuwahara. "Non-linear tolerant and spectrally efficient 86 Gbit/s RZ-DQPSK format for a system upgrade", in *Technical Digest Optical Fiber Communication Conference, OFC'03,* Atlanta, Georgia, U.S.A., Paper ThE7, March 2003.

[27] M. Serbay, C. Wree, and W. Rosenkranz. "Comparison of six different RZ-DQPSK transmitter set-ups regarding their tolerance towards fibre impairments in 8×40 Gb/s WDM-systems", in *IEEE/LEOS 2004 Workshop on Advanced Modulation Formats,* San Francisco, California, U.S.A, pp. 9–10, Paper ThB3, July 2004.

[28] R. A. Griffin, R. I. Johnstone, R. G. Walker, S. D. Wadsworth, A. C. Carter, and M. J. Wale. "Integrated DQPSK transmitter for dispersion-tolerant and dispersion-managed DWDM transmission", in *Technical Digest Optical Fiber Communication Conference, OFC'03,* Atlanta, Georgia, U.S.A., Paper FP6, March 2003.

[29] R. A. Griffin, R. G. Walker, and R. I. Johnstone. "Integrated devices for advanced modulation formats", in *IEEE/LEOS 2004 Workshop on Advanced Modulation Formats,* San Francisco, California, U.S.A, pp. 39–40, Paper FC1, July 2004.

[30] M. Serbay, C. Wree, and W. Rosenkranz. "Cost-efficient realisation of a robust transmission with the DQPSK-modulation format including precoding", in *ITG Conference Photonische Netze,* Leipzig, Germany, pp. 181–186, May 2004.

[31] W. Kaiser and W. Rosenkranz. "Simple precoder for high-speed optical duobinary transmission", *Journal of Optical Communication*, vol. 23, no. 1, pp. 26–28, February 2002.

[32] P. J. Winzer and H. Kim. "Degradations in balanced DPSK receivers", *IEEE Photonics Technology Letters*, vol. 15, no. 9, pp. 1282–1284, September 2003. doi:10.1109/LPT.2003.816112.

[33] F. Morichetti, R. Costa, G. Cusmai, A. Cabas, M. Ferè, M. C. Ubaldi, A. Melloni, and M. Martinelli. "Integrated optical receiver for RZ-DQPSK transmission systems", in *Technical Digest Optical*

Fiber Communication Conference, OFC'04, Los Angeles, California, U.S.A, Paper FC8, February 2004.

[34] ITF Optical Technologies, 400 Montpellier Boulevard, Montreal, Québec, Canada, H4N 2G7. http://www.itfoptical.com.

[35] S. D. Personick. "Receiver design for optical fiber systems", *Proceedings of the IEEE*, vol. 65, no. 12, pp. 1670–1678, December 1977.

[36] P. J. Winzer and A. Kalmar. "Sensitivity enhancement of optical receivers by impulsive coding", *Journal of Lightwave Technology*, vol. 17, no. 2, pp. 171–177, February 1999.

[37] P. J. Winzer and J. Leuthold. "Return-to-zero modulator using a single NRZ drive signal and an optical delay interferometer", *IEEE Photonics Technology Letters*, vol. 13, no. 12, pp. 1298–1300, December 2001.

[38] G. P. Agrawal. *Nonlinear Fiber Optics.* Academic Press, Second edition, 1995. ISBN 0-12-045142-5.

[39] C. R. Davidson, C. J. Chen, M. Nissov, A. Pilipetskii, N. Ramanujam, H. D. Kidorf, B. Pedersen, M. A. Mills, C. Lin, M. I. Hayee, J.-X. Cai, A. B. Puc, P. C. Corbett, R. Menges, H. Li, A. Elyamani, C. Rivers, and N. S. Bergano. "1800 Gb/s transmission of one hundred and eighty 10 Gb/s WDM channels over 7,000 km using the full EDFA C-band", in *Technical Digest Optical Fiber Communication Conference, OFC'00,* Baltimore, Maryland, U.S.A., vol. 4, pp. 242–244, Paper PD25, March 2000.

[40] K. E. Stubkjær. "Semiconductor optical amplifier-based all-optical gates for high-speed optical processing", *IEEE Journal of Selected Topics in Quantum Electronics*, vol. 6, no. 6, pp. 1428–1435, November 2000.

[41] N. Chi, J. Zhang, P. V. Holm-Nielsen, C. Peucheret, and P. Jeppesen. "Transmission and transparent wavelength conversion of an optically labeled signal using ASK/DPSK orthogonal modulation", *IEEE Photonics Technology Letters*, vol. 15, no. 5, pp. 760–762, May 2003. doi:10.1109/LPT.2003.809922.

[42] Z. Li, Y. Dong, J. Mo, Y. Wang, and C. Lu. "Cascaded all-optical wavelength conversion for RZ-DPSK signal based on four-wave mixing in semiconductor optical amplifier", *IEEE Photonics Technology Letters*, vol. 16, no. 7, pp. 1685–1687, July 2004. doi:10.1109/LPT.2004.828463.

[43] M. C. Tatham, G. Sherlock, and L. D. Westbrook. "20 nm optical wavelength conversion using nondegenerate four-wave mixing", *IEEE Photonics Technology Letters*, vol. 5, no. 11, pp. 1303 –1306, November 1993.

[44] A. E. Kelly, A. D. Ellis, D. Nesset, R. Kashyap, and D. G. Moodie. "100 Gbit/s wavelength conversion using FWM in an MQW semiconductor optical amplifier", *Electronics Letters*, vol. 34, no. 20, pp. 1955–1956, October 1998. doi:10.1049/el:19981388.

[45] A. T. Clausen, L. K. Oxenløwe, C. Peucheret, H. N. Poulsen, P. Jeppesen, S. N. Knudsen, and L. Grüner-Nielsen. "10 GHz return-to-zero pulse source tunable in wavelength with a single- or multi-wavelength output based on four-wave mixing in a newly developed highly nonlinear fiber", *IEEE Photonics Technology Letters*, vol. 13, no. 1, pp. 70–72, January 2001.

Chapter 7

Conclusion

Dispersion management and modulation formats have been studied for single-channel and wavelength division multiplexing (WDM) optical communication systems with per channel bit rates at or above 10 Gbit/s.

Dispersion Management

New dispersion compensating fibres (DCFs) referred to as inverse dispersion fibres (IDFs) allow more freedom in fibre span design, as the DCF itself can be cabled and used as transmission fibre. Three novel fibre types were investigated, with dispersion ranging from -17 to -54 ps/nm/km. These fibres are referred to as IDF$\times n$, with $n = \{1, 2, 3\}$ being the single mode fibre (SMF) to IDF length ratio. We show that IDFs can effectively reduce the accumulation of amplified spontaneous emission (ASE), compared to the conventional DCF with a dispersion of -100 ps/nm/km, due to significantly lower span loss. We found that IDF$\times$1 suffers from enhanced nonlinear signal degradation due to less attenuation and pulse dispersion in the SMF before the IDF$\times$1. IDF$\times$2 and IDF$\times$3 offer a combination of good nonlinear signal propagation and low span loss, resulting in good performance for all power levels.

We experimentally compare three different dispersion management schemes in a 40 Gbit/s system with ultra-long 160 km fibre spans. A combination of amplification using lumped erbium doped fibre amplifiers (EDFAs) and distributed Raman amplification was used to overcome the high span loss of such long fibre spans. Comparing pre-, post- and sym-

metrical dispersion compensation, we showed that the symmetrical scheme offers best performance, primarily due to reduced nonlinear signal interaction.

Modulation Formats

There has been a fierce debate regarding "optimum" modulation formats for optical communication systems for some time, starting with the debate of non return-to-zero (NRZ) vs. return-to-zero (RZ), and later with the suggestion of advanced modulation formats such as CS-RZ, SSB-RZ and duobinary.

We investigated the question of pulse width in 10 Gbit/s system with 80 km span lengths, comparing the performance of NRZ and RZ coding using pulse widths of 50%, 10%, and 5% of the bit slot. Results clearly showed that all the studied RZ formats outperformed the traditional NRZ formats—due to a 2 dB improved receiver sensitivity and greatly improved nonlinear tolerance. We found that, as the narrow RZ pulses disperse rapidly and have a rapidly changing waveform, the nonlinear signal degradation due to self phase modulation (SPM) is significantly relaxed.

Advanced on-off keying (OOK) modulation formats were studied for 40 Gbit/s single-channel and WDM systems with 80 km fibre spans. We studied the relative performance of six modulation formats—NRZ, RZ (50% and 20% pulse width), duobinary, CS-RZ and SSB-RZ. For the single-channel case we found that the narrow RZ pulses were optimum, as in the 10 Gbit/s system. However, the broad spectrum associated with narrow pulses puts a natural limitation on use in WDM systems. We found that CS-RZ and SSB-RZ resulted in optimum performance in a 100 GHz spaced 40 Gbit/s WDM system, as these formats offer a combination of good transmission properties and high receiver sensitivity with a relatively narrow spectrum.

DQPSK

Differential quadrature phase shift keying (DQPSK) is a modulation format well-known from radio communication, where multilevel signalling is frequently used to enhance the spectral efficiency. We show that multilevel phase modulation is suitable for use in optical communication sys-

tems, and can be used either to generate high speed signals using low symbol rates, or to generate ultra-high bit rates signals with bit rates higher than obtainable with OOK.

Following the proven success of differential binary phase shift keying (DBPSK) in recent experiments, we demonstrate the suitability of four-level DQPSK for transoceanic optical communication systems. We show successful transmission of DQPSK signals in a 12.5 Gbit/s 64 channel WDM system over a transatlantic distance of 6500 km. Furthermore, we use DQPSK to achieve high spectral efficiency, obtaining up to 0.66 bit/s/Hz even after transmission over 6500 km.

Using components with bandwidth suitable for 40 Gbit/s OOK, we experimentally demonstrated a 80 Gbit/s non return-to-zero differential quadrature phase shift keying (NRZ-DQPSK) system. Using four-wave mixing (FWM) in a highly nonlinear fibre (HNLF), we demonstrated for the first time wavelength conversion of ultra-high speed phase modulated signals. We obtained a conversion power penalty of 2.8 dB for 80 Gbit/s NRZ-DQPSK, which was only 0.2 dB higher than the penalty for 40 Gbit/s non return-to-zero differential binary phase shift keying (NRZ-DBPSK).

Summary

The work presented in this thesis has shown that novel dispersion management schemes and advanced modulation formats offer significant benefits compared to traditional systems, in some cases allowing three times longer transmission distance. However, there is no universal optimum combination of modulation format and dispersion management, and a detailed study is required for each system.

DQPSK has been demonstrated as a suitable modulation format for optical communication systems, even for spectrally efficient transoceanic WDM systems. We also showed that DQPSK can be implemented at bit rates as high as 80 Gbit/s with 40 Gbit/s electronics.

Hopefully, the benefits of the advanced modulation formats demonstrated in this work will be sufficient to overcome the drawbacks of extra transmitter and receiver complexity. If so, these formats will allow for future ultra-high capacity spectrally efficient optical communication systems.

List of Acronyms

AMI	alternate mark inversion
ASE	amplified spontaneous emission
BER	bit error rate
CS-RZ	carrier suppressed return-to-zero
CW	continuous wave
DBPSK	differential binary phase shift keying
DCF	dispersion compensating fibre
DFB	distributed feedback
DPSK	differential phase shift keying
DSF	dispersion shifted fibre
DQPSK	differential quadrature phase shift keying
ECL	external cavity laser
EAM	electro-absorption modulator
EDFA	erbium doped fibre amplifier
ELPF	electrical low-pass filter
FEC	forward error correction
FOM	figure of merit
FSR	free spectral range
FWHM	full width at half maximum
FWM	four-wave mixing
GVD	group-velocity dispersion

HNLF	highly nonlinear fibre
IDF	inverse dispersion fibre
ISI	inter-symbol interference
MLFRL	mode locked fibre ring laser
MPI	multi-path interference
MZ	Mach-Zehnder
NOLM	nonlinear optical loop mirror
NRZ	non return-to-zero
NRZ-DBPSK	non return-to-zero differential binary phase shift keying
NRZ-DQPSK	non return-to-zero differential quadrature phase shift keying
NZDSF	non-zero dispersion shifted fibre
OBPF	optical bandpass filter
OOK	on-off keying
OTDM	optical time division multiplexing
OSA	optical spectrum analyser
OSNR	optical signal to noise ratio
PDFS	polarisation dependent frequency shift
PRBS	pseudo random bit sequence
PSK	phase shift keying
QPSK	quadrature phase shift keying
RDF	reverse dispersion fibre
RZ	return-to-zero
RZ-OOK	return-to-zero on-off keying
RZ-DBPSK	return-to-zero differential binary phase shift keying
RZ-DQPSK	return-to-zero differential quadrature phase shift keying
SOA	semiconductor optical amplifier
SMF	single mode fibre
SOP	state of polarisation
SPM	self phase modulation

SSB	single side band
SSB-RZ	single side band return-to-zero
WDM	wavelength division multiplexing
XPM	cross phase modulation
XGM	cross gain modulation

Appendices

Appendix A

Details from Chapter 3

This Appendix presents detailed list of parameters and results not included in the study of dispersion maps and pulse widths presented in Chapter 3.

These simulations were carried out using the "VPI Transmission Maker" simulation tool. The amplified spontaneous emission (ASE) noise was sampled and included in the signal band. Detailed simulation parameters are presented in Table A.1.

In Chapter 3, the simulation results were presented as maximum 3 dB limit versus signal power for various combinations of dispersion compensating fibres and pulse widths. In this Appendix, additional simulation results are presented. Figures A.1, A.3, A.5 and A.7 presents the power penalty versus span input power for different span lengths, for IDF×1, IDF×2, IDF×3 and conventional dispersion compensating fibre (DCF), respectively. Figures A.2, A.4, A.6 and A.8 show the power penalty versus distance at the optimum power level,[1] for IDF×1, IDF×2, IDF×3 and conventional DCF, respectively.

[1]Note that as the optimum power level changes with distance, the points in these figures are for different power levels.

Parameter	Value
Laser frequency	193.1 THz
Laser linewidth	0 Hz
MZ extinction ratio	30.0 dB
Rise-time of electrical signal	25 ps
EDFA noise figure	5.0 dB
Splice loss	0.25 dB
Optical filter shape	2^{nd}-order Gaussian
Optical filter 3 db bandwidth	100.0 GHz
Photodiode dark current	0 A
Photodiode responsitivity	1 A/W
Photodiode thermal noise	10 pA/$\sqrt{\text{Hz}}$
Low-pass filter shape	4^{th}-order Bessel
Low-pass filter cut-off frequency	7.5 GHz
Simulated bits	1024 bits
PRBS length	$2^{10} - 1$ bits
NLSE step	max 1000 m or 0.05 rad
Samplerate – NRZ	32 samples/bit
Samplerate – RZ 50%	32 samples/bit
Samplerate – RZ 10%	128 samples/bit
Samplerate – RZ 5%	256 samples/bit

Table A.1: Simulation parameters for 10 Gbit/s simulations presented in Chapter 3.

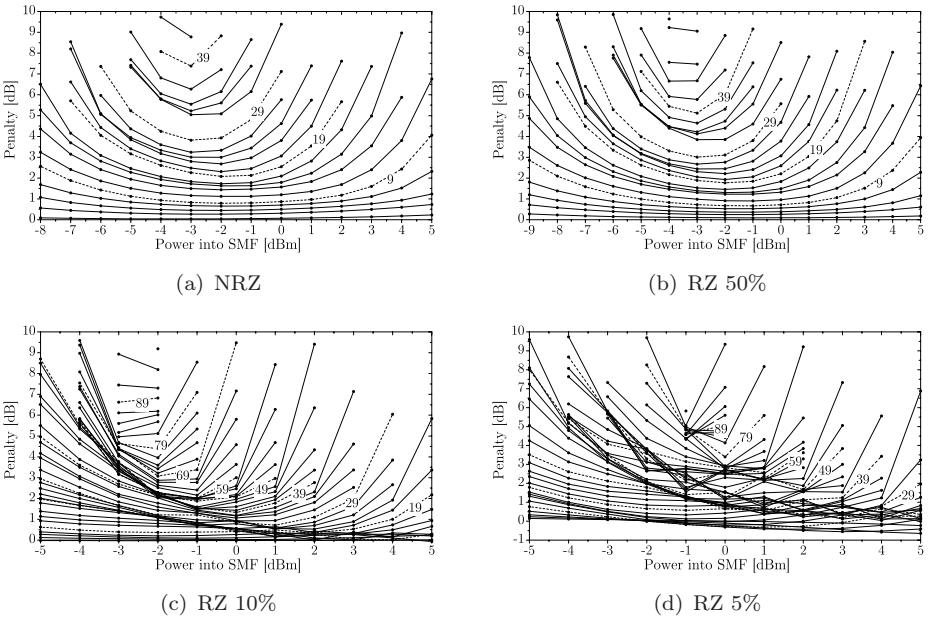

(a) NRZ (b) RZ 50%

(c) RZ 10% (d) RZ 5%

Figure A.1: Penalty versus power of 10 Gbit/s NRZ, RZ 50%, RZ 10% and RZ 5% signals after transmission over 80 km SMF+IDF×1 spans. Lines represent different transmission distances. Results after every second span are shown.

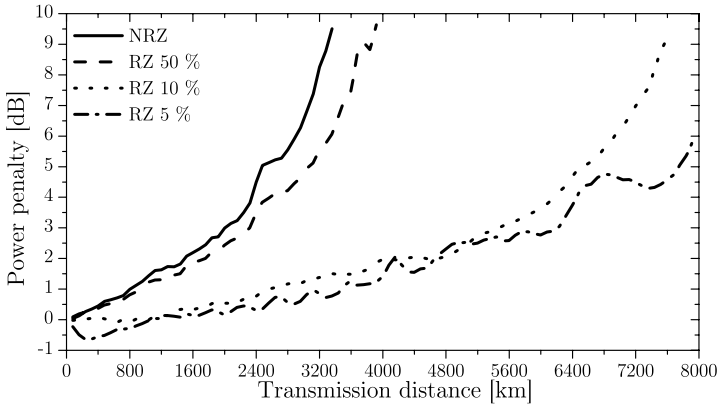

Figure A.2: Penalty versus distance of 10 Gbit/s NRZ, RZ 50%, RZ 10% and RZ 5% signals after transmission over 80 km SMF+IDF×1 spans. Each point corresponds to the power penalty for the optimum power level at that distance.

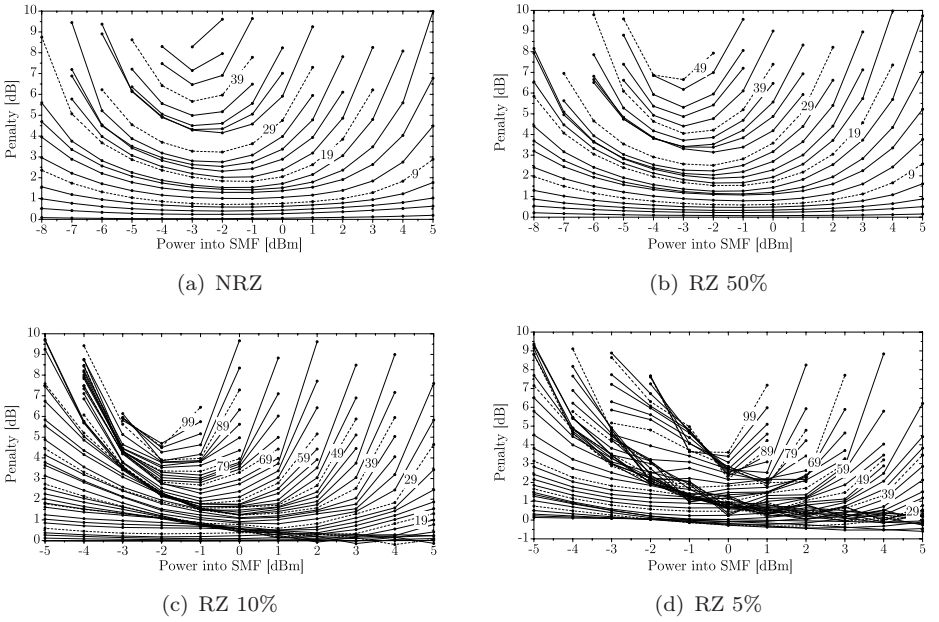

Figure A.3: Penalty versus power of 10 Gbit/s NRZ, RZ 50%, RZ 10% and RZ 5% signals after transmission over 80 km SMF+IDF×2 spans. Lines represent different transmission distances. Results after every second span are shown.

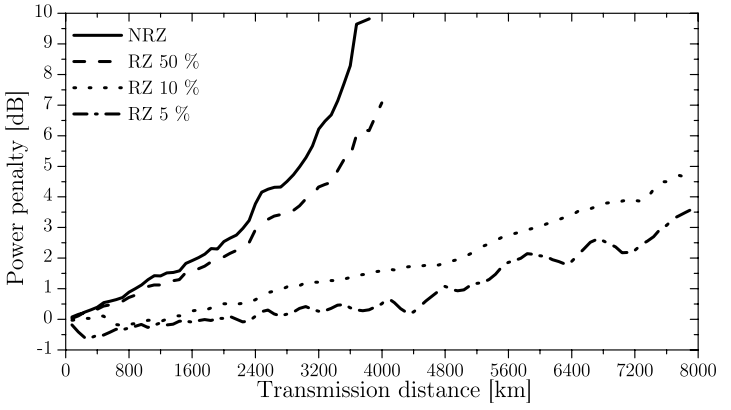

Figure A.4: Penalty versus distance of 10 Gbit/s NRZ, RZ 50%, RZ 10% and RZ 5% signals after transmission over 80 km SMF+IDF×2 spans. Each point corresponds to the power penalty for the optimum power level at that distance.

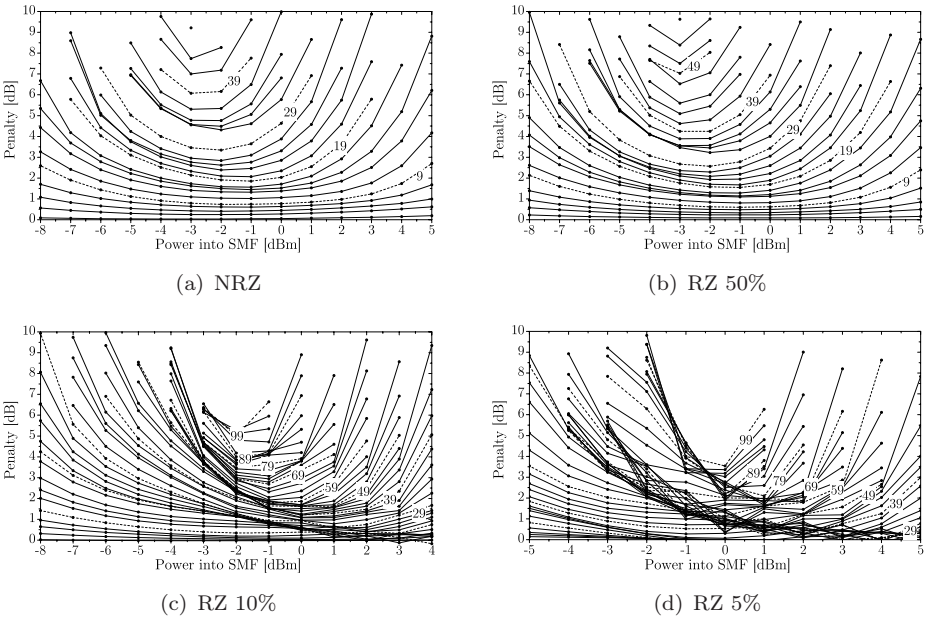

Figure A.5: Penalty versus power of 10 Gbit/s NRZ, RZ 50%, RZ 10% and RZ 5%signals after transmission over 80 km SMF+IDF×3 spans. Lines represent different transmission distances. Results after every second span are shown.

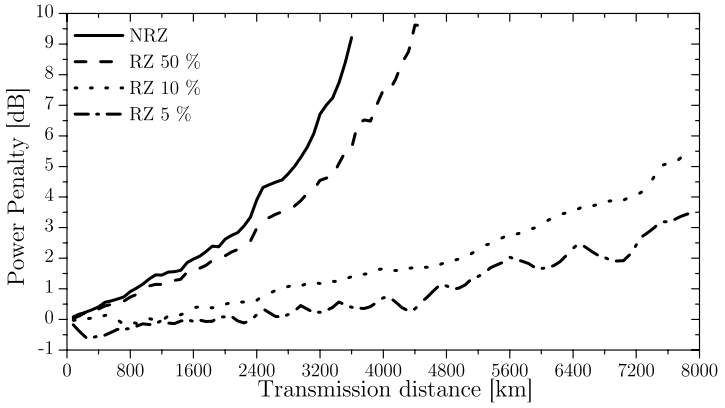

Figure A.6: Penalty versus distance of 10 Gbit/s NRZ, RZ 50%, RZ 10% and RZ 5% signals after transmission over 80 km SMF+IDF×3 spans. Each point corresponds to the power penalty for the optimum power level at that distance.

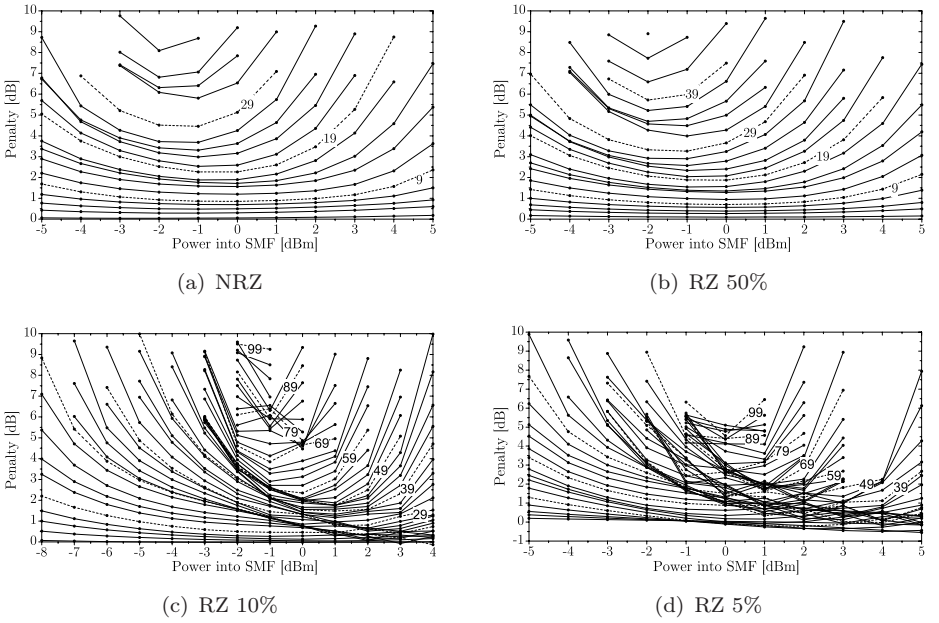

(a) NRZ (b) RZ 50%

(c) RZ 10% (d) RZ 5%

Figure A.7: Penalty versus power of 10 Gbit/s NRZ, RZ 50%, RZ 10% and RZ 5% after transmission over 80 km SMF+DCF spans. Lines represent different transmission distances. Results after every second span are shown.

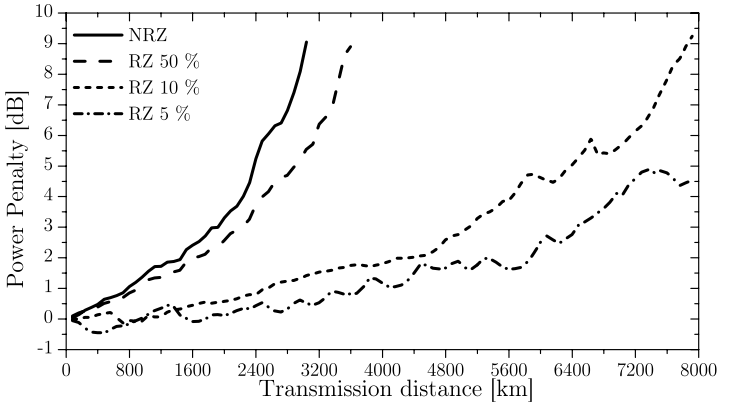

Figure A.8: Penalty versus distance of 10 Gbit/s NRZ, RZ 50%, RZ 10% and RZ 5% after transmission over 80 km SMF+DCF spans. Each point corresponds to the power penalty for the optimum power level at that distance.

Appendix B

Details from Chapter 4

This Appendix presents detailed list of parameters and additional results not included in the discussion of novel modulation formats presented in Chapter 4.

These simulations were carried out using the "VPI Transmission Maker" simulation tool. Noise from amplified spontaneous emission (ASE) was sampled and included in the signal band.

Detailed fibre parameters are listed in Figure 4.3 in Chapter 4. The fibre input power were adjusted by changing the gain of the erbium doped fibre amplifier (EDFA) amplifiers. In some special combinations of the input power to the single mode fibre (SMF) and dispersion compensating fibre (DCF), the EDFA was replaced by an attenuator. For example, in the case with 12 dBm SMF input power and −14 dBm DCF input power, an attenuation of 11.6 dB was needed.[1] Table B.1 lists detailed simulation parameters used to calculate the results presented in Chapter 4.

In Chapter 4, the power penalty versus distance for a single-channel system using SMF + DCF when disregarding optical noise was shown in Figure 4.16. For completeness the corresponding figure using SMF + IDF×2 is shown in Figure B.1. And in Figure B.2, the noise-free results from the wavelength division multiplexing (WDM) system using SMF + IDF×2 are presented.

Before starting the simulations on the WDM system, an investigation to find the required number of bits was performed. An 8×40 Gbit/s

[1] 12 dBm SMF input power leads to −2.4 dBm SMF output power, thus 11.6 dB attenuation is needed to reach −14 dBm DCF input power.

Parameter	Value
Laser frequency	193.1 THz
Laser linewidth	0 Hz
Rise-time of electrical signal	5 ps
MZ modulator extinction ratio	infinite
Duobinary low-pass filter shape	4^{th}-order Bessel
Duobinary low-pass filter cut-off frequency	11.2 GHz
EDFA noise figure	5.0 dB
Splice loss	0 dB
Optical filter shape	2^{nd}-order Gaussian
Optical filter 3 dB bandwidth	100.0 GHz
Photodiode dark current	0 A
Photodiode responsitivity	1 A/W
Photodiode thermal noise	10 pA/$\sqrt{\text{Hz}}$
Receiver low-pass filter shape	4^{th}-order Bessel
Receiver low-pass filter cut-off frequency	30.0 GHz
Simulation bits	1024 bits
PRBS length	$2^{10} - 1$ bits
NLSE step	max 1000 m or 0.05 rad
Samplerate	32 samples/bit

Table B.1: Simulation parameters for the 40 Gbit/s modulation formats comparison presented in Chapter 4.

return-to-zero (RZ) 50% WDM system with 80 km SMF + DCF spans was investigated using different number of bits. Figure B.3 presents the power penalty versus distance for this system, showing several different noise realisations. It is seen that there is very large variance of the results based on 129 and 1024 bits. By setting the threshold at 0.5 dB variance at 3 dB power penalty, we found that 16384 bits were required for this WDM simulation study.

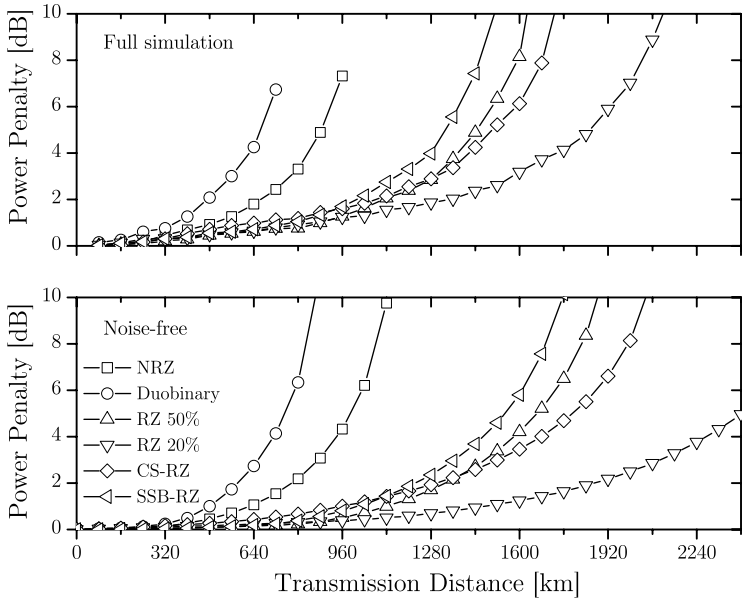

Figure B.1: Power penalty versus distance for single-channel simulation with both noise and nonlinearities (top), without noise (centre) and without nonlinearities (bottom), using the SMF + IDF×2 fibre span. Span input powers were −1 dBm to the SMF and −7 dBm to the IDF×2.

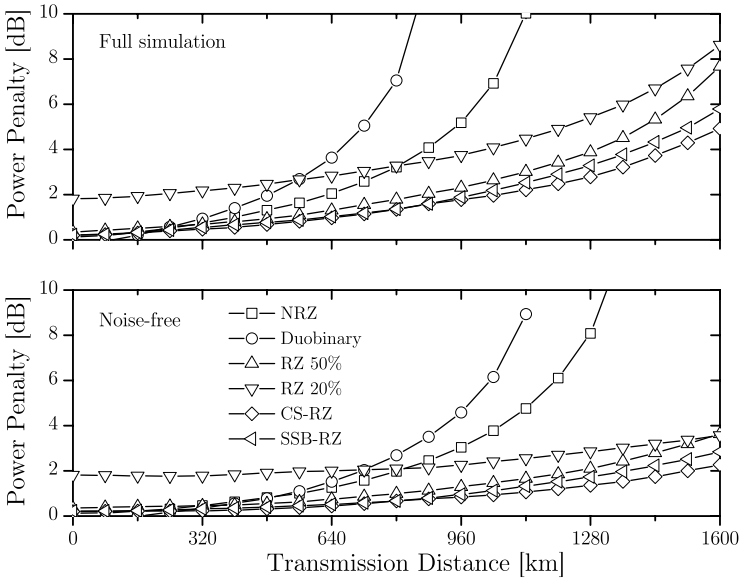

Figure B.2: Power penalty (for the worst channel) versus distance for simulation of the WDM system when disregarding the optical noise, after transmission over SMF+IDF×2 spans. The per channel span input powers were −1 dBm to the SMF and −7 dBm to the IDF×2.

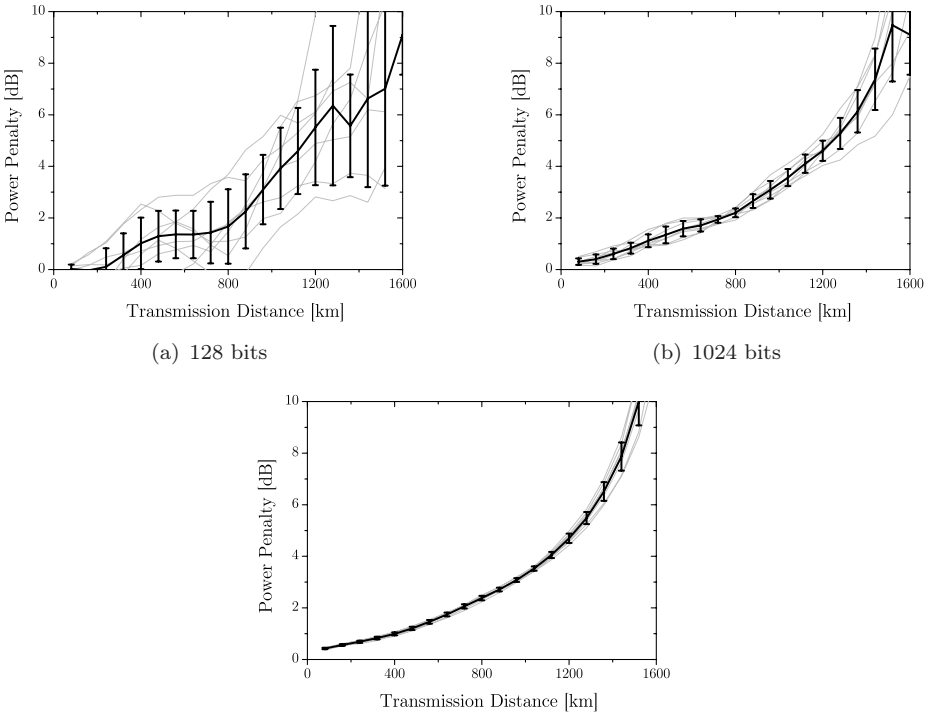

(a) 128 bits

(b) 1024 bits

(c) 16384 bits

Figure B.3: Power penalty versus distance for 40 Gbit/s RZ 50% after transmission over 80 km SMF + DCF fibre spans when simulating 128 bits (a), 1024 bits (b) and 16384 bits (c).

Appendix C

Details from Chapter 6

This appendix presents additional information not included in the differential quadrature phase shift keying (DQPSK) study presented in Chapter 6.

The pre-coding, encoding and decoding of a DQPSK system using a dual-MZ transmitter is illustrated in Table C.1. A corresponding table for a system with dual-Mach-Zehnder (MZ) generated DQPSK system is shown in Table 6.1 in Chapter 6.

The signals in a DQPSK receiver were illustrated in Figure 6.7 for signals generated with a dual-MZ modulator. For completeness, the sig-

u_k	0	0	1	1	0	1	1	1	1	0	0
v_k	0	1	0	0	0	1	0	1	0	1	1
I_k	0	1	0	0	0	1	0	1	1	1	0
Q_k	0	1	0	1	1	1	0	0	1	0	1
P_k	$\frac{E_0^2}{2}$	$\frac{E_0^2}{2}$	$\frac{E_0^2}{2}$	$\frac{E_0^2}{2}$	$\frac{E_0^2}{2}$	$\frac{E_0^2}{2}$	$\frac{E_0^2}{2}$	$\frac{E_0^2}{2}$	$\frac{E_0^2}{2}$	$\frac{E_0^2}{2}$	$\frac{E_0^2}{2}$
ϕ_k	0	$\frac{3\pi}{2}$	0	$\frac{\pi}{2}$	$\frac{\pi}{2}$	$\frac{3\pi}{2}$	0	π	$\frac{3\pi}{2}$	π	$\frac{\pi}{2}$
$\Delta\phi_k$	-	$\frac{3\pi}{2}$	$\frac{\pi}{2}$	$\frac{\pi}{2}$	0	π	$\frac{\pi}{2}$	π	$\frac{\pi}{2}$	$-\frac{\pi}{2}$	$-\frac{\pi}{2}$
r_k	-	0	1	1	0	1	1	1	1	0	0
s_k	-	1	0	0	0	1	0	1	0	1	1

Table C.1: Input data, pre-coded data, encoded data and received data at time $t = t_k$ for a DQPSK system with PM or MZ-PM generation.

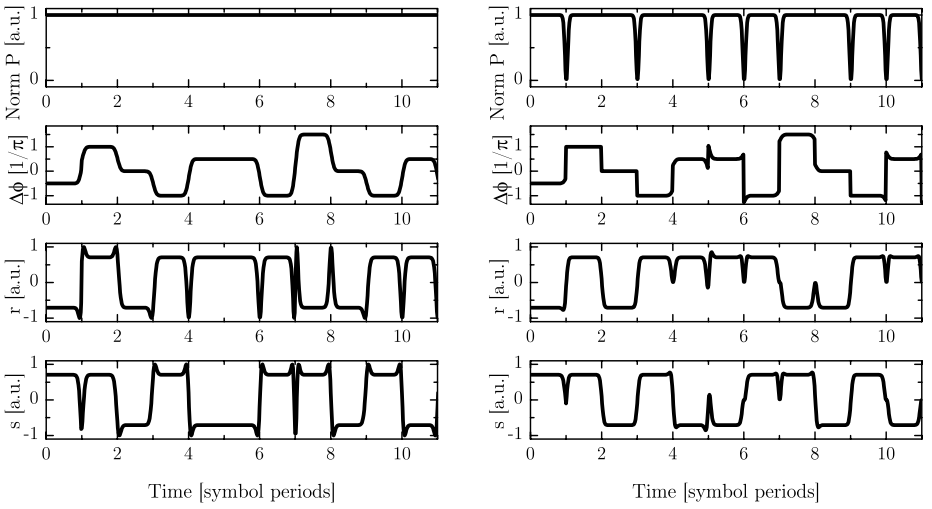

(a) PM (b) MZPM

Figure C.1: Illustration of the signals in a DQPSK receiver for a signal generated with the PM (a) and MZ-PM (b) generation option. The dual-MZ generation method is depicted in Figure 6.7 in Chapter 6.

nals in the receiver when using the PM or MZ-PM generation method are presented in Figure C.1.

In the transmission experiment presented in Chapter 6, half of the channels were 12.5 Gbit/s return-to-zero differential quadrature phase shift keying (RZ-DQPSK), and the other half were 6.25 Gbit/s return-to-zero on-off keying (RZ-OOK). It was argued that as the pulse shape and optical power spectrum is indistinguishable, this simplification of the setup did not affect the cross-talk between neighbouring channels. Figure C.2 presents an comparison of the calculated optical power spectra of 12.5 Gbit/s RZ-DQPSK and 6.25 Gbit/s return-to-zero differential binary phase shift keying (RZ-DBPSK), and no difference between them can be seen.

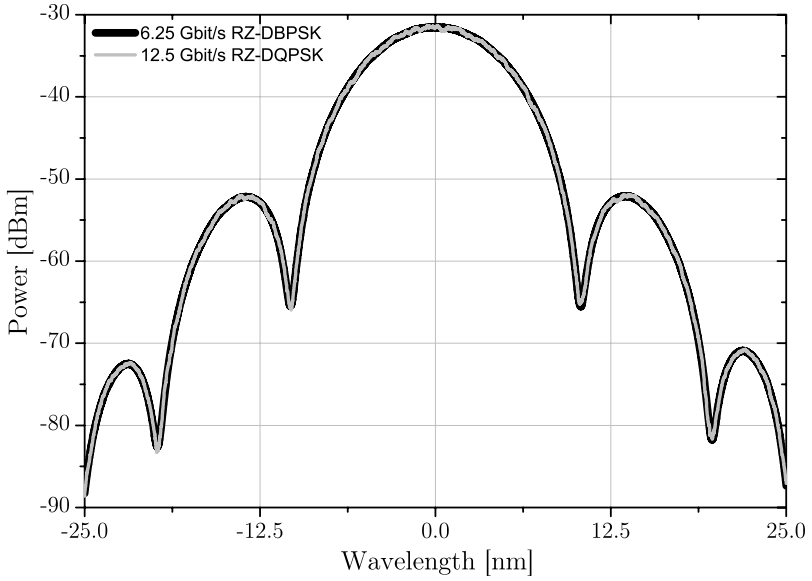

Figure C.2: Comparison of calculated spectral shape of 6.25 Gbit/s RZ-DBPSK and 12.5 Gbit/s RZ-DQPSK signals.